https://doi.org/10.5194/essd-2026-287
Preprint. Discussion started: 23 April 2026

Open Access Earth System Science Data Discussions

Indicators of Global Climate Change 2025: annual update of key indicators of the state of the climate system and human influence

Piers M. Forster[1], Tristram Walsh[2,3], Chris Smith[3], William F. Lamb[1,4], Robin Lamboll[5], Christophe Cassou[6], Mathias Hauser[7], Zeke Hausfather[8,9], June-Yi Lee[10,11], Matthew D. Palmer[12,13], Karina von Schuckmann[14], Aimée B. A. Slangen[15,52], Sophie Szopa[16], Blair Trewin[17], Jeongeun Yun[10], Nathan P. Gillett[18], Stuart Jenkins[2], H. Damon Matthews[19], Krishnan Raghavan[20], Aurélien Ribes[21], Joeri Rogelj[3,5,22], Debbie Rosen[1], Xuebin Zhang[23], Myles Allen[2,24], Robbie M. Andrew[25], Chris Atkinson[12], Richard A. Betts[12,26], Antonio Bombelli[27], Samantha N. Burgess[28], Lijing Cheng[29], Helen E. Claxton[1], Pierre Friedlingstein[6,26], Thomas L. Frölicher[30,31], Catia M. Domingues[32], Thomas Gasser[3], Catherine H. Gregory[30,31], Rachel M. Hoesly[33], Daniel Huppmann[3], Masayoshi Ishii[34], Christopher Kadow[35], Alexia Karwat[10], John Kennedy[27], Rachel E. Killick[12], Mahesh V. M. Kovilakam[37], Paul B. Krummel[38], Xin Lan[39,40], Jean-François Lamarque[41], Aurélien Liné[14], Belén Martín-Míguez[27], Didier P. Monselesan[42], Colin Morice[12], Jens Mühle[43], Pino Mussak[3], Glen P. Peters[25], Anna Pirani[44], Julia Pongratz[45], Matthew Rigby[46], Robert Rohde[8], Abhishek Savita[47,48], Sonia I. Seneviratne[7], Steven J. Smith[33], Ghassan Taha[49,50], Caterina Tassone[27], Peter Thorne[52], Christopher Wells[1], Luke M. Western[53], Guido R. van der Werf[54], Susan E. Wijffels[42,55], Marco Zecchetto[3], Junting Zhong[56], Xiao-ye Zhang[56], Valérie Masson-Delmotte[16], Panmao Zhai[56]

Affiliations:

1 Priestley Centre for Climate Futures, University of Leeds, Leeds, United Kingdom
2 Environmental Change Institute, University of Oxford, Oxford, United Kingdom
3 International Institute for Applied Systems Analysis (IIASA), Laxenburg, Austria
4 Potsdam Institute for Climate Impact Research (PIK), Potsdam, Germany
5 Centre for Environmental Policy, Imperial College London, London, United Kingdom
6 Laboratoire de Météorologie Dynamique, Institut Pierre-Simon Laplace, Paris, France
7 Institute for Atmospheric and Climate Science, ETH Zurich, Zurich, Switzerland
8 Berkeley Earth, Berkeley, CA, United States of America
9 Stripe Inc., South San Francisco, CA, United States of America
10 Research Center for Climate Sciences, Pusan National University, Busan, Republic of Korea
11 Center for Climate Physics, Institute for Basic Science, Busan, Republic of Korea

https://doi.org/10.5194/essd-2026-287
Preprint. Discussion started: 23 April 2026

Open Access Earth System Science Data Discussions

12 Met Office Hadley Centre, Exeter, United Kingdom

13 School of Earth Sciences, University of Bristol, Bristol, United Kingdom

14 Mercator Ocean International, Toulouse, France

15 Royal Netherlands Institute for Sea Research (NIOZ), Yerseke, the Netherlands

16 Laboratoire des Sciences du Climat et de l'Environnement (LSCE), Université Paris-Saclay, Gif-sur-Yvette, France

17 Bureau of Meteorology, Melbourne, Australia

18 Canadian Centre for Climate Modelling and Analysis, Environment and Climate Change Canada, Victoria, BC, Canada

19 Concordia University, Montreal, QC, Canada

20 Indian Institute of Tropical Meteorology, Pune, India

21 CNRM, Météo-France, CNRS, Université de Toulouse, Toulouse, France

22 Grantham Institute for Climate Change and Environment, Imperial College London, London, United Kingdom

23 Pacific Climate Impacts Consortium, University of Victoria, Victoria, BC, Canada

24 Atmospheric, Oceanic and Planetary Physics, University of Oxford, Oxford, United Kingdom

25 CICERO Center for International Climate Research, Oslo, Norway

26 Faculty of Environment, Science and Economy, University of Exeter, Exeter, United Kingdom

27 Global Climate Observing System, World Meteorological Organization, Geneva, Switzerland

28 European Centre for Medium-Range Weather Forecasts (ECMWF), Reading, United Kingdom

29 State Key Laboratory of Earth System Numerical Modeling, Chinese Academy of Sciences, Beijing, China

30 Climate and Environmental Physics, University of Bern, Bern, Switzerland

31 Oeschger Centre for Climate Change Research, University of Bern, Bern, Switzerland

32 National Oceanography Centre, Southampton, United Kingdom

33 Joint Global Change Research Institute, Pacific Northwest National Laboratory, College Park, MD, United States of America

34 Meteorological Research Institute, Tsukuba, Japan

35 German Climate Computing Center (DKRZ), Hamburg, Germany

37 Morgan State University, Baltimore, MD, United States of America

38 CSIRO Environment, Environmental Business Unit, Hobart, Australia

https://doi.org/10.5194/essd-2026-287
Preprint. Discussion started: 23 April 2026

Open Access Earth System Science Data Discussions

39 Cooperative Institute for Research in Environmental Sciences (CIRES), University of Colorado Boulder, Boulder, CO, United States of America

40 Global Monitoring Laboratory, National Oceanic and Atmospheric Administration (NOAA), Boulder, CO, United States of America

41 Three Cairns Group, New York, NY, United States of America

42 CSIRO Environment, Climate Intelligence, Hobart, Australia

43 Scripps Institution of Oceanography, University of California San Diego, La Jolla, CA, United States of America

44 Euro-Mediterranean Center on Climate Change (CMCC), Venice, Italy

45 Ludwig-Maximilians-Universität München, Munich, Germany

46 School of Chemistry, University of Bristol, Bristol, UK

47 Indian Institute of Technology Delhi, New Delhi, India

48 Rosenstiel School of Marine, Atmospheric and Earth Science, University of Miami, Miami, FL, United States of America

49 NASA Goddard Space Flight Center, Greenbelt, MD, United States of America

50 Langley Research Center, NASA, Hampton, VA, United States of America

52 ICARUS Climate Research Centre, Maynooth University, Maynooth, Ireland

53 Center for Sustainability Science and Strategy, Massachusetts Institute of Technology, Cambridge, MA, United States of America

54 Wageningen University & Research, Wageningen, the Netherlands

55 Woods Hole Oceanographic Institution, Woods Hole, MA, United States of America

56 Chinese Academy of Meteorological Sciences, Beijing, China

Correspondence to: Piers. M. Forster (p.m.forster@leeds.ac.uk)

Abstract

In a rapidly changing climate, evidence-based decision-making benefits from up-to-date and timely information. We track twelve key sets of indicators of the state of the climate system, closely following Intergovernmental Panel on Climate Change (IPCC) Sixth Assessment report (AR6) methods, to produce our fourth annual publication. One of the indicators, the Earth's energy imbalance (EEI) provides a crucial integrative measure of the pace of climate change – this has more than doubled since the 1976-1995 period. A newly updated indicator of temperature extremes, the number of days experiencing marine heatwaves, has more than tripled between 1991 and 2025.

https://doi.org/10.5194/essd-2026-287
Preprint. Discussion started: 23 April 2026

For the 2016–2025 decade average, observed warming relative to 1850-1900 was 1.26 [1.13 to 1.36] °C, of which 1.24 [1.0 to 1.5] °C was human-induced. Human-induced warming reached 1.37 °C relative to 1850-1900 in the year 2025, increasing at a rate of 0.27 [0.2 - 0.4] °C per decade over 2016-2025. This high rate of warming, which matches the all-time high seen last year in the instrumental record, was caused by a combination of greenhouse gas emissions being at an all-time high of 54.6 ± 5.5 $GtCO_2e$ per year over the last decade (2015-2024), as well as reductions in the strength of aerosol cooling. Despite this, there is evidence that CO_2 emission growth is slowing. The continuation of these annual updates could track decreases or increases in the rate of human influence and climatic changes presented here, reflecting the outcomes of societal choices during the critical 2020s decade.

In total, we employ analysis from over 40 global datasets (https://doi.org/10.5281/ZENODO.7883757 Smith et al., 2026a) These data are threatened by geopolitical and public funding decisions that are cutting support for key satellite and in-situ observing programs critical for the monitoring of the atmosphere, ocean, cryosphere and land surface, including long-term data preservation and provision that is key to understanding our changing climate for today and for future generations. Overall, the Global Climate Observing System (GCOS) framework, which supports much of our international capability, is under threat. Our ability to monitor effectively many of the indicators presented herein is not guaranteed without concerted international action to ensure the continuity of observation programs and coordination mechanisms, including the GCOS program, that enable their effective integration and use.

1 Introduction

IPCC AR6 provided an assessment of human influence on key indicators of the state of the climate grounded in available data at the time of publication. The preparation for the next IPCC report, the Seventh Assessment Report (AR7), has started, and the assessment is due in around two years. Given the speed of recent change and the need for updated climate knowledge to inform evidence-based decision-making, the Indicators of Global Climate Change (IGCC) was initiated in 2023 to provide policymakers with annual updates of the latest scientific understanding on the state of selected critical indicators of the climate system and, where possible, of the quantified human influence upon these.

IGCC complements other annual updates, most notably, the BAMS State of the Climate Report (Blunden and Regan, 2025) and the WMO State of the Global Climate (World Meteorological Organisation [WMO], 2026). The main difference is that this work goes beyond the observations to make process level estimates of effective radiative forcing and attributed human-induced response, including the remaining carbon budget, using methods rigorously assessed in AR6, modified where necessary to account for new or revised datasets and other key innovations.

This fourth annual update follows broadly the format of last year (Forster et al., 2025) and extends the indicators through 2025. The work focuses on indicators related to heating of the climate system, building from greenhouse gas

https://doi.org/10.5194/essd-2026-287
Preprint. Discussion started: 23 April 2026

125 emissions towards estimates of human-induced warming and the remaining carbon budget for 1.5 °C and other policy-
126 relevant temperature thresholds. New in this year's update are the inclusion of a marine heatwave indicator and an
127 updated interpretation of the exceptional warmth observed during 2023-2025. Fig. 1 presents an overview of the
128 aspects assessed and their interlinkages from cause (emissions) through effect (changes in physical indicators) to
129 climatic impact drivers. It also provides a visual roadmap as to the structure of remaining sections in this paper to
130 guide the reader.

https://doi.org/10.5194/essd-2026-287
Preprint. Discussion started: 23 April 2026

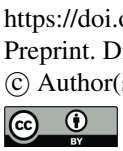

Open Access Earth System Science Data Discussions

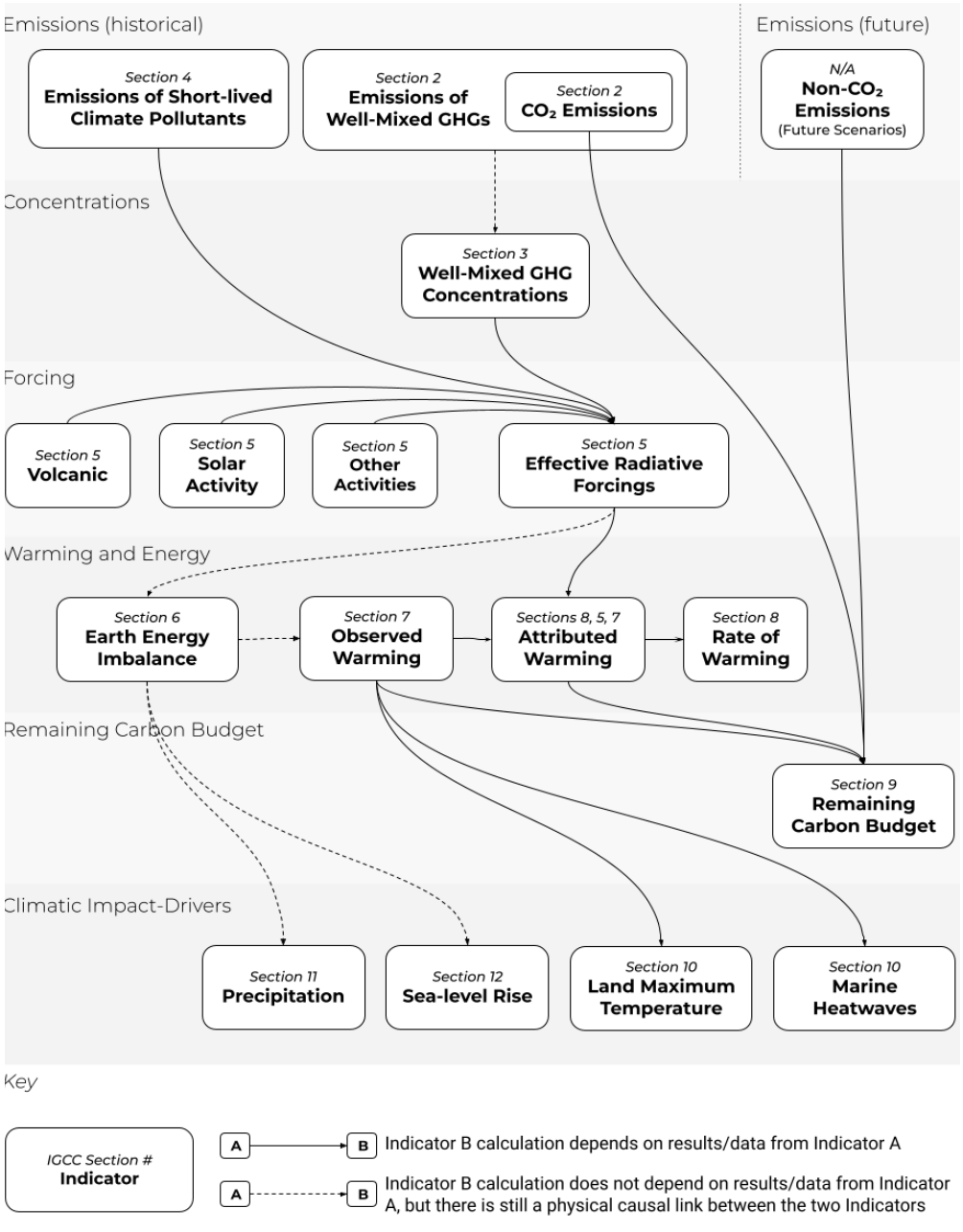

131

https://doi.org/10.5194/essd-2026-287
Preprint. Discussion started: 23 April 2026

Figure 1 The flow chart of data production from emissions to human induced warming, the remaining carbon budget, and changes to Climatic Impact-Drivers, illustrating both the rationale and workflow within this manuscript.

The update is based on methodologies assessed by the IPCC Sixth Assessment Report (AR6) of the physical science basis of climate change (Working Group One (WGI) report; IPCC, 2021a) as well as Chap. 2 of the WGIII report (Dhakal et al., 2022) and is aligned with the efforts initiated in AR6 to implement FAIR (Findable, Accessible, Interoperable, Reusable) principles for reproducibility and reusability (Pirani et al., 2022; Iturbide et al., 2022). IPCC reports make a much wider assessment of the science and methodologies – we do not attempt to reproduce the comprehensive nature of these IPCC assessments here. We also do not consider adopting fundamentally different approaches to AR6. Rather, our aim is to rigorously track both climate system change and evolving methodological improvements between IPCC report cycles, thereby increasing transparency and consistency in between successive reports.

This annual update is organised as follows: greenhouse gas (GHG) emissions (Sect. 2), greenhouse gas concentrations (Sect. 3) and emissions of short-lived climate forcers (Sect. 4) are used to develop updated estimates of effective radiative forcing (Sect. 5). The Earth energy imbalance (Sect. 6) and observations of global surface temperature change (Sect. 7) are key global indicators of a warming world. The contributions to global surface temperature change from human and natural influences are formally attributed in Sect. 8, which tracks the level and rate of human-induced warming. Sect. 9 updates the remaining carbon budget for policy-relevant temperature thresholds. Sect. 10 gives an example of global-scale indicators associated with climate extremes of maximum land surface temperatures and, a new addition to this year's update, the number of marine heatwave days. Sect. 11 shows land-surface precipitation trends and Sect. 12 presents updated estimates of global mean sea-level rise. Code and data availability are described in Sect. 13, and conclusions are presented in Sect. 14. Data are available at https://doi.org/10.5281/ZENODO.7883757 (Smith et al., 2026a).

2 Greenhouse gas emissions

Historic GHG emissions from human activity were assessed in both AR6 WGI and WGIII. Chapter 5 of WGI assessed CO_2 and CH_4 emissions in the context of the carbon cycle (Canadell et al., 2021). Chapter 2 of WGIII, published one year later (Dhakal et al., 2022), assessed the sectoral sources of emissions and gave the most up-to-date understanding of the current level of emissions. This section bases its methods and data on those employed in the WGIII chapter.

2.1 Methods of estimating greenhouse gas emissions changes

Like in AR6 WGIII, net GHG emissions in this paper refer to releases of GHGs from anthropogenic sources minus removals by anthropogenic sinks, for the set of GHGs outlined in the United Nations Framework Convention on

https://doi.org/10.5194/essd-2026-287
Preprint. Discussion started: 23 April 2026

Climate Change (UNFCCC). These include: CO_2 emissions from fossil fuels and industry (CO_2-FFI); net CO_2 emissions from land use, land-use change and forestry (CO_2-LULUCF); CH_4 emissions; N_2O emissions; and fluorinated gas (F-gas) emissions comprising hydrofluorocarbons (HFCs), perfluorocarbons (PFCs), sulphur hexafluoride (SF_6) and nitrogen trifluoride (NF_3) - hereafter the "UNFCCC F-gases".

The IPCC AR6 WGIII calculated total net GHG emissions as the sum of CO_2-FFI, CH_4, N_2O and UNFCCC F-gases from the Emissions Database for Global Atmospheric Research ("EDGAR" version 6, with a fast-track methodology applied for the final year of data - 2019), and net CO_2-LULUCF emissions from the Global Carbon Budget ("GCB"; the 2020 version; Friedlingstein et al., 2020). Net CO_2-LULUCF emissions followed the GCB convention and were derived from the average of three bookkeeping models (Hansis et al., 2015; Houghton and Nassikas, 2017; Gasser et al., 2020).

The analysis presented here continues to provide an "WGIII update" estimate that tracks the same system boundary and compilation of GHGs as in AR6 WGIII, albeit with one difference in the selected data sources: for CO_2-FFI we use GCB (Friedlingstein et al., 2025) instead of EDGAR, in order to report the year-1 projection which is only available for GCB at this point in the reporting cycle. Otherwise, we continue to use EDGAR (Crippa et al., 2025) for non-CO_2 emissions (N_2O, CH_4 and F-gases), and GCB for CO_2-LULUCF. The latter has now been updated to account for historical changes in biomass and soil carbon densities (primarily due to CO_2 fertilisation) based on the average of three bookkeeping models that can represent time-varying carbon densities (BLUE by Hansis et al., 2015; OSCAR by Gasser et al., 2020; LUCE by Qin et al., 2024, see Friedlingstein et al., 2025 and supplement). We follow the same approach for estimating uncertainties and CO_2-equivalent emissions as in AR6, as described in the Supplement. We contextualise the selected data sources by reporting emissions at the level of gases (e.g. CO_2-FFI, CO_2-LULUCF, CH_4, N_2O and F-gases) from other major databases, including the PRIMAP-hist database (Gütschow et al., 2025)[1]; the Community Emissions Data System (CEDS; Hoesly et al,. 2025); the LULUCF Data Hub (Melo et al,. 2025); the Food and Agriculture Organisation of the UN (FAOSTAT) Greenhouse Gas Emissions dataset (FAO, 2025); and the Global Fire Emissions Database (GFED; van der Werf et al., 2025).

In addition to the WGIII update, we provide two further estimates of total GHG emissions that provide clarity and comparison to other existing assessment approaches. This reflects the fact that other decision criteria for tracking emissions are possible (for further detail, see supplement and Lamb et al., 2026). First, in cases where assessments prioritise calculating the best estimate of fluxes to the atmosphere, it would be important to include Ozone Depleting Substances (ODS F-gases), the cement carbonation sink and all non-CO_2 biomass fire emissions, including those from

[1] PRIMAP is a synthetic dataset that includes two time-series: PRIMAP Hist-TP, which is compiled from other underlying products such as EDGAR; and PRIMAP Hist-CR, which prioritises data from national inventories but gap-fills these where necessary.

https://doi.org/10.5194/essd-2026-287
Preprint. Discussion started: 23 April 2026

wildfires. Indeed, these are included in this article in subsequent assessments of concentration change (including compounds formed in the atmosphere as ozone), effective radiative forcing, human-induced warming, carbon budgets and climate impacts, in line with the WGI assessment. We therefore provide an "IPCC update + additional sources and sinks" estimate that shows the change implied by including these three components in the global total. Second, we provide an "inventory-aligned" estimate that is consistent with national reporting and assessments of the Nationally Determined Contributions (NDCs). This explicitly follows the inventory approach to accounting for LULUCF emissions (based on the processed inventory data from the LULUCF Data Hub), while also integrating the latest national inventory data from the Common Reporting Tables (based on PRIMAP Hist-CR). The data sources associated with these additional estimates are detailed in Table S1 in the Supplement.

We expect to see differences between the three estimates, most notably between the "WGIII update" and "inventory-aligned" estimates, primarily because they differ conceptually in their treatment of the LULUCF sector. Whereas the WGIII update excludes "indirect anthropogenic effects" on terrestrial carbon fluxes when they do not coincide with land-use changes (i.e., in the GCB fluxes such as enhanced forest growth in response to increased atmospheric CO_2 levels are treated as part of the natural land sink), these fluxes are included in inventory-aligned estimates where they occur on managed land, effectively summing to a significant sink. Further, national inventory reporting can also differ from third-party datasets in terms of underlying methods: in some countries, investments into statistical infrastructures have enabled the use of more precise emissions factors in inventories to estimate fluxes according to local or national conditions, while in others this may not be the case. In contrast, third-party datasets often use globally consistent emissions factors. Notably, the PRIMAP Hist-CR dataset, which is here used to represent national inventories, has significantly lower total CH_4 emissions relative to other datasets reported herein, as well as the global atmospheric inversion estimates evaluated in this paper. A substantive body of recent literature has consistently found that, on average, national inventories tend to underestimate emissions compared to inversions (Deng et al., 2022; Tibrewal et al., 2024; Janardanan et al., 2024; Scarpelli et al., 2022; Song et al., 2026).

2.2 Updated greenhouse gas emissions

Updated GHG emission estimates following the WGIII assessment are presented in Fig. 2 and Table 1. Total global GHG emissions were 56.8 ± 5.5 $GtCO_2e$ in 2024. Of this total, CO_2-FFI contributed 38.6 ± 3.1 $GtCO_2$, CO_2-LULUCF contributed 4.6 ± 3.2 $GtCO_2$, CH_4 contributed 9.3 ± 2.8 $GtCO_2e$, N_2O contributed 2.6 ± 1.6 $GtCO_2e$ and F-gas emissions contributed 1.7 ± 0.5 $GtCO_2e$.

Note the recent history of emissions in these datasets are continually revised, so there are small differences between each annual update in emission estimates over the recent past. Initial projections for 2025 indicate that CO_2 emissions from fossil fuels and industry increased to 38.9 ± 3.1, and CO_2 emissions from land-use change decreased to 4.1 ± 2.9 $GtCO_2$ (Friedlingstein et al., 2025).

https://doi.org/10.5194/essd-2026-287
Preprint. Discussion started: 23 April 2026

Average annual GHG emissions for the decade 2015–2024 were 54.6 ± 5.5 $GtCO_2e$. Average decadal GHG emissions have increased steadily since the 1970s across all major groups of GHGs, driven primarily by increasing CO_2 emissions from fossil fuel and industry but also rising emissions of CH_4 and N_2O. Emissions of UNFCCC F-gases have grown more rapidly than other GHG, but from low levels. Both the magnitude and trend of CO_2 emissions from land-use change remain highly uncertain, with the latest data indicating an average net flux between 4–6 $GtCO_2\ yr^{-1}$ for the past few decades.

The fossil fuel share of global GHG emissions was approximately 73% in 2024 (GWP100 weighted) (UNEP 2025), based on the EDGAR v2025 dataset (Crippa et al., 2025) and net land-use CO_2 emissions from the Global Carbon Budget (Friedlingstein et al., 2025). The remaining share of non-fossil fuel emissions are mostly from land-use change, agriculture, cement production, waste and F-gas emissions.

Different emissions assessment approaches are shown in Fig. 3. Compared to the WGIII update estimate in 2023 (56.3 ± 5.5 $GtCO2e\ yr^{-1}$), including ODS F-gases, cement carbonation, and CH_4 and N_2O from biomass burning increases emissions to 57.9 ± 5.6 $GtCO2e\ yr^{-1}$, or a total change of +1.5 $GtCO2e\ yr^{-1}$. ODS F-gas emissions have declined substantially since the 1990s under the Montreal Protocol and its amendments, reaching 1.4 $GtCO2e\ yr^{-1}$ in 2024, with a stalling rate of reduction in the past decade. The cement carbonation sink has steadily increased alongside cement production to reach -0.8 $GtCO2e\ yr^{-1}$ in 2024. Biomass fire emissions have a more variable trend and 2024 was a relatively extreme year at 1 $GtCO2e\ yr^{-1}$, compared to an average of 0.8 $GtCO2e\ yr^{-1}$ in the preceding decade.

Emissions according to national inventories were 45.7 ± 5.2 $GtCO2e\ yr^{-1}$ in 2023, or 10.6 $GtCO2e\ yr^{-1}$ lower than the WGIII update (Fig. 3). The main reason is due to diverging estimates of net LULUCF emissions, which according to inventory accounts was a 3.8 $GtCO_2$ sink over the past decade, while it is a 5 $GtCO_2$ source in the WGIII update. This 8.9 $GtCO_2$ difference is primarily due to the inclusion of indirect anthropogenic effects such as CO_2 fertilisation on vegetation growth on "managed land" in the inventory estimate. Additional differences result from a lower estimate of Energy, Industrial Process, Agriculture and Waste emissions in inventories (-1.6 $GtCO_2e\ yr^{-1}$).

Literature published after AR6 shows that increases in atmospheric CH_4 concentrations are also being driven by methane emissions from wetland changes resulting from climate change and variability. For example, Zhang et al. (2025) found an average increase of 6–7 Tg $CH_4\ yr^{-1}$ (0.16-0.20 $GtCO2e\ yr^{-1}$) in wetland emissions in 2010–2019 compared to the average for 2000–2009, attributable mostly to temperature-driven climate change. Changes to these wetland emissions are not captured in the WGIII estimate of anthropogenic emissions as they are not a direct emission

https://doi.org/10.5194/essd-2026-287
Preprint. Discussion started: 23 April 2026

Open Access Earth System Science Data Discussions

263 from human activity, but rather a feedback induced by a changing climate, yet they will contribute to GHG
264 concentration rise, forcing and energy budget changes discussed in the next sections.

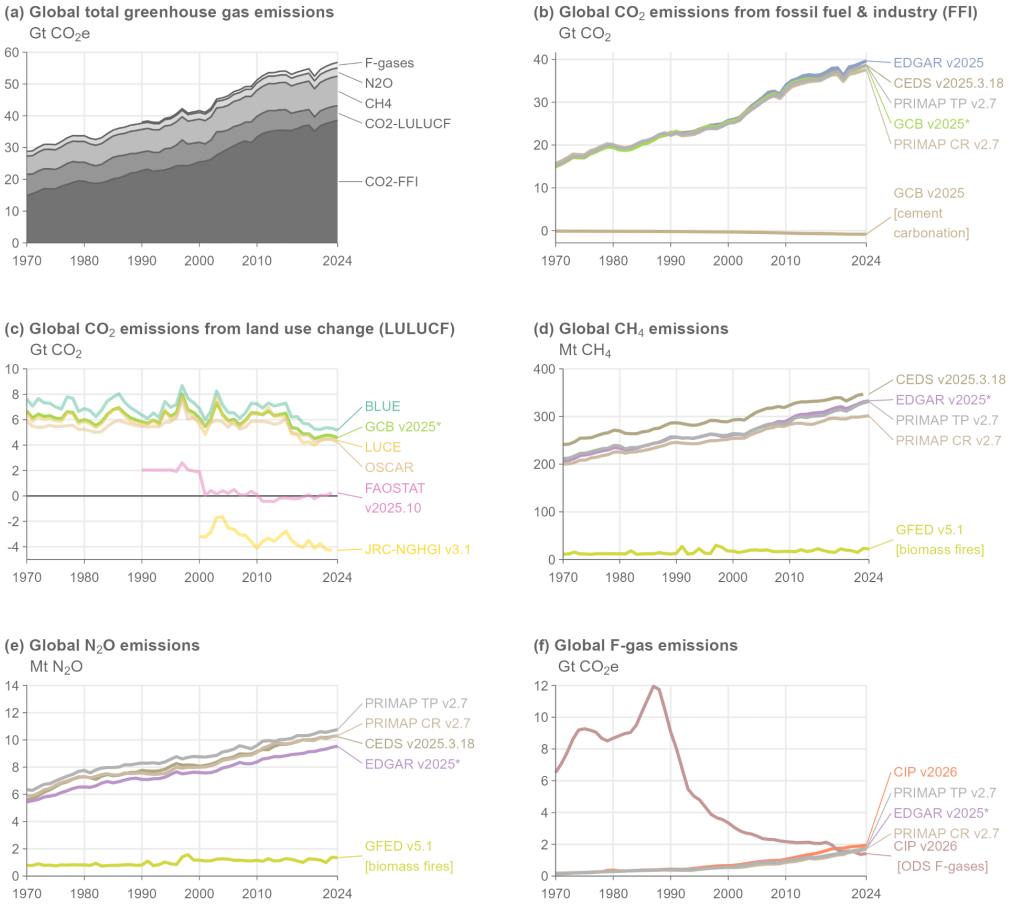

265

266 **Figure 2 Annual global anthropogenic GHG emissions by source, 1970–2024. Refer to Sect. 2.1 and Table S1 for a list of**
267 **datasets. Datasets with an asterisk (*) indicate the sources used to compile global total greenhouse gas emissions following**
268 **the WGIII assessment in (a). CO_2-equivalent emissions in (a) and (f) are calculated using GWP100 from the AR6 WGI**
269 **Chap. 7 (Forster et al., 2021). F-gas emissions in (a) comprise only UNFCCC F-gas emissions (see Sect. 2.1 for a list of**
270 **species). F-gas emissions in (f) refer to UNFCCC F-gases, except for "CIP v2026 [ODS F-gases]". Some of the major depicted**
271 **differences between datasets (e.g. between GCB v2025 and JRC-NGHGI v3.1 in panel c) are due to varying system**
272 **boundaries, rather than underlying uncertainties in activity levels or emissions factors.**

273

https://doi.org/10.5194/essd-2026-287
Preprint. Discussion started: 23 April 2026

Open Access Earth System Science Data Discussions

Table 1 Global anthropogenic greenhouse gas emissions by source and decade following the WGIII assessment. All numbers refer to decadal averages, except for annual estimates in 2023 and 2024. CO_2-equivalent emissions are calculated using GWP100 from AR6 WGI Chap. 7 (Forster et al., 2021). Projections for CO_2 emissions in 2025 are from the Global Carbon Project. Projections of non-CO_2 GHG emissions in 2025 remain unavailable at the time of publication. Uncertainties are ±8 % for CO_2-FFI, ±70 % for CO_2-LULUCF, ±30 % for CH_4 and F-gases, and ±60 % for N_2O, corresponding to a 90 % confidence interval. "GHG" in row one is the sum of the other rows.

Units: $GtCO_2e$	1970-1979	1980-1989	1990-1999	2000-2009	2010-2019	2015-2024	2024	2025 (projection)
GHG	31.3±5.1	34.9±5.2	39.6±5.5	45.6±5.6	53.5±5.8	54.6±5.5	56.8±5.5	
CO_2-FFI	17.2±1.4	20.1±1.6	23.5±1.9	28.9±2.3	35.4±2.8	36.7±2.9	38.6±3.1	38.9±3.1
CO_2-LULUCF	6.3±4.4	6.2±4.3	6.4±4.5	6.2±4.3	5.9±4.2	5±3.5	4.6±3.2	4.1±2.9
CH_4	6.1±1.8	6.7±2	7.2±2.2	7.7±2.3	8.6±2.6	8.9±2.7	9.3±2.8	
N_2O	1.6±1	1.9±1.1	2±1.2	2.2±1.3	2.4±1.4	2.5±1.5	2.6±1.6	
UNFCCC F-gases			0.4±0.1	0.8±0.2	1.2±0.4	1.4±0.4	1.7±0.5	

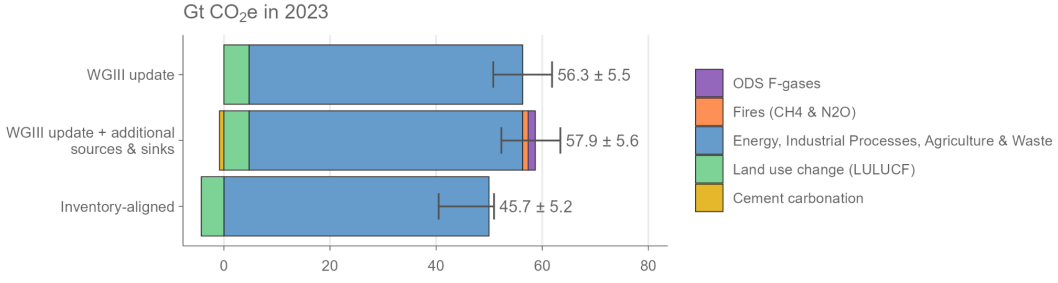

Figure 3 Annual global anthropogenic greenhouse gas emissions by assessment convention in 2023. Refer to Table 1 for a list of underlying datasets. Differences between conventions are primarily due to differences in system boundaries (Lamb et al., 2026). Uncertainties are ±8 % for CO_2-FFI, ±70 % for CO_2-LULUCF, ±30 % for CH_4 and F-gases, and ±60 % for N_2O, corresponding to a 90 % confidence interval.

https://doi.org/10.5194/essd-2026-287
Preprint. Discussion started: 23 April 2026

3 Well-mixed greenhouse gas concentrations

As in Forster et al. (2025), we report best-estimate global mean concentrations for 52 well-mixed GHGs. These concentrations are updated to 2025. CO_2 mixing ratios were taken from the NOAA Global Monitoring Laboratory (GML) and are updated here through 2024 (Lan et al., 2025). As in past IGCC publications, CO_2 is reported on the WMO-CO_2-X2019 scale, which differs from the WMO-CO_2-X2007 scale used in AR6 with WMO-CO_2-X2019 being around 0.18 ppm higher than WMO-CO_2-X2007 in recent years. For consistency with WMO-CO_2-X2019, the AR6 CO_2 concentrations that make up the 1750 to 1978 period in the IGCC dataset (before recent NOAA updates) have been converted to the WMO-CO_2-X2019 scale. Other GHG records were compiled from NOAA and AGAGE global networks or extrapolated from literature. An average of NOAA and AGAGE data, updated through 2025, were used for N_2O, CH_4, CFC-11, CFC-12, CCl_4, HCFC-22, HFC-134a, and HFC-125 (Lan et al., 2025; Dutton et al., 2024; Prinn et al., 2018), which, along with CO_2, account for over 97% of the ERF from well-mixed GHGs. Several other species also use means from the NOAA and AGAGE networks, where the NOAA data is updated to 2025 and AGAGE data is also updated until 2025 (Western et al., 2025, 2026; Prinn et al., 2025). In cases where no updated information is available, global estimates were extrapolated from Vimont et al. (2022), Western et al. (2023, 2024, 2025, 2026), or other literature and scaled to be consistent with those reported in AR6. Some extrapolations of minor GHG concentrations are based on data from the mid-2010s (Droste et al., 2020; Laube et al., 2014; Simmonds et al., 2017; Vollmer et al., 2018), but have an imperceptible effect on the total ERF assessed in Sect. 5, and are included to maintain consistency with AR6. Mixing ratio uncertainties for 2025 are assumed to be like 2019, and we adopt the same uncertainties as assessed in AR6 WGI.

Fig. 4 shows recent GHG concentrations and their changes. Table S2 in the Supplement shows specific updated concentrations for all the GHGs considered. The global surface mean concentrations of CO_2, CH_4 and N_2O in 2025 were 425.6 [±0.4] parts per million (ppm), 1935.9 [±3.3] parts per billion (ppb) and 339.4 [±0.4] ppb, respectively. Concentrations of all three major GHGs have increased since 2019, with CO_2 increasing by 15.6 ppm, CH_4 by 69.8 ppb, and N_2O by 7.2 ppb. Increases since 2019 are consistent with those from the CSIRO network (Francey et al., 1999). With few exceptions, concentrations of ozone-depleting substances, such as CFC-11 and CFC-12, continue to decline, while those of replacement compounds (HFCs) have increased. HFC-134a, for example, has increased 30% since 2019 from 107.6 to 140.3 parts per trillion (ppt). Aggregated across all gases, PFCs have increased from 109.7 to an estimated 118.9 ppt CF_4-eq from 2019 to 2025, HFCs from 237 to 338 ppt HFC-134a-eq, while ozone depleting gases have declined from 1032 to 989 ppt CFC-12-eq. Mixing ratio equivalents are determined by the radiative efficiencies of each GHG from Hodnebrog et al. (2020).

https://doi.org/10.5194/essd-2026-287
Preprint. Discussion started: 23 April 2026

Open Access Earth System Science Data Discussions

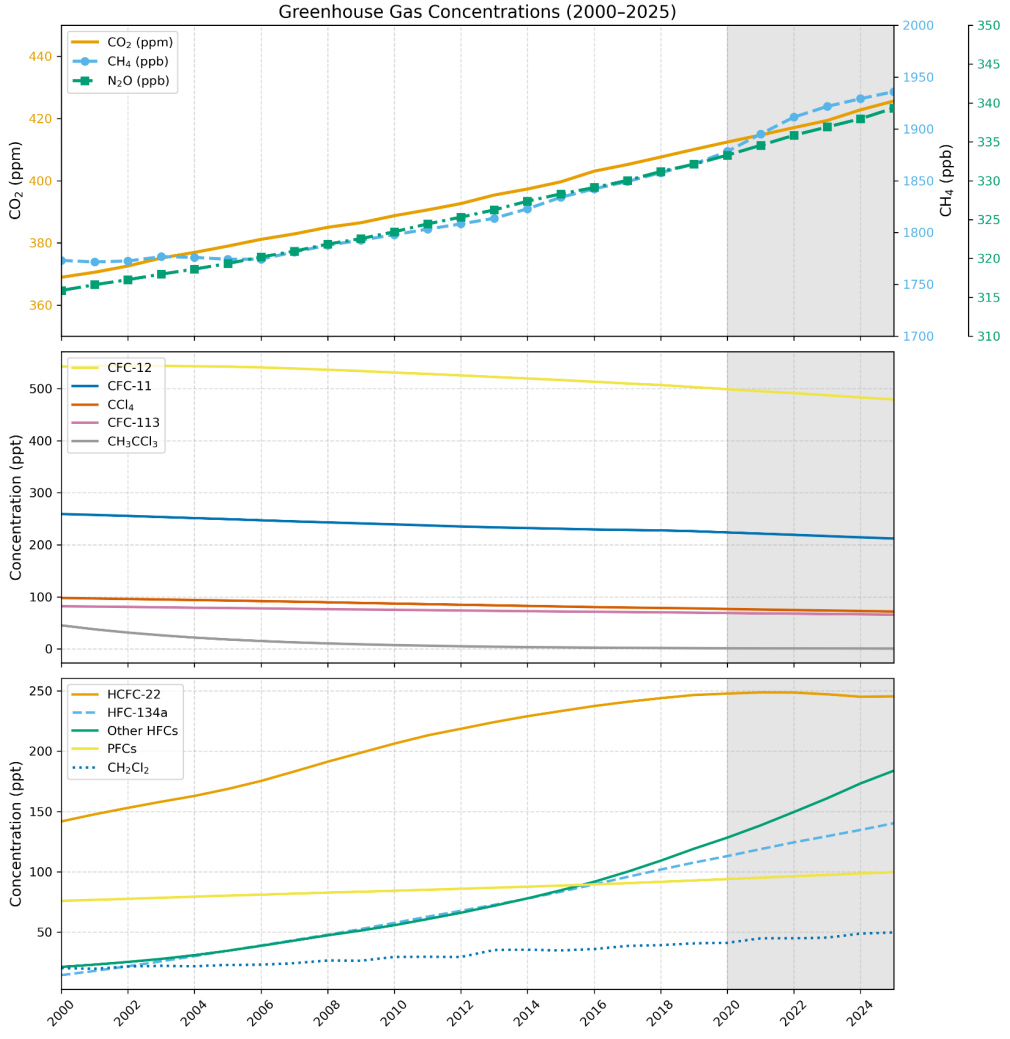

318

319 **Figure 4 Atmospheric concentrations of a set of well mixed greenhouse gases over 2000-2025. The grey shaded region**
320 **represents continuing changes since AR6. Note the different vertical scales.**

321

https://doi.org/10.5194/essd-2026-287
Preprint. Discussion started: 23 April 2026

Ozone and other non-methane SLCFs are not well-mixed in the atmosphere and are thus discussed separately (in Section 4). For this reason, the warming impact of ozone, the third most important GHG (in terms of current contribution to warming) is not included in the contribution of well-mixed GHGs to observed warming, consistently with AR6.

4 Non-methane short-lived climate forcers

Chapter 6 of WGI assessed emissions in the context of understanding the climate and air quality impacts of SLCFs (Szopa et al., 2021). Methane is a SLCF but also a well mixed GHG and is discussed in Sections 2 and 3. Trends in SLCF emissions are spatially heterogeneous (Szopa et al., 2021), with strong shifts in the locations of reductions and increases over the decade 2010–2019 (Hodnebrog et al., 2024). Concentrations of non-methane SLCFs are heterogeneously distributed in the atmosphere and the observation networks are too sparse to report globally averaged concentrations. Typically, a combination of satellite data, where available, and global models and reanalyses are relied upon for estimating global-scale distributions. In the case of models, production of near-real time information relies upon the availability of near-real time updates to SLCF emissions which are still challenging. Little information, whether from observations from local monitoring networks, satellite data or from global model reanalysis, is released in near-real time.

In addition to GHG emissions, we provide an update of anthropogenic emissions of non-methane SLCFs (SO_2, black carbon (BC), organic carbon (OC), NOx, volatile organic compounds (VOCs), CO and NH_3). Data are presented in Table 2 and the evolution of SLCF emission estimates from the AR6 to this study is presented in Sect. S4 of the Supplement. Consistency between emission trends and concentrations is considered whenever feasible. HFCs, whatever their lifetimes, were considered in Sect. 2.2.

Sectoral emissions of SLCFs are derived from two sources: CEDS, which was used in the AR6 and in CMIP6 to assess historical evolution of atmospheric composition and that has been updated since then, and the Copernicus Atmosphere Monitoring Service (CAMS). The most recent release of the CEDS anthropogenic emissions dataset (Hoesly et al., 2025) covers the 1750-2023 period (Hoesly et al., 2018; Hoesly and Smith, 2024). Since 2023, CAMS has released regular updates of their global emission dataset (Soulie et al., 2023). For the years 2024 and 2025, we apply, for each compound, the trend in emission from the CAMS dataset to the 2023 CEDS emission. The CAMS dataset is essentially based on the EDGARv6/v7 emissions as well as on CEDS, so CEDS and CAMS are not entirely independent. The temporal extension is based on evolution of drivers of emissions (energy consumption, production rates) and trends in technologies that affect the emissions factors (e.g. fleet renewal and abatement systems) (Denier van der Gon et al., 2023).

https://doi.org/10.5194/essd-2026-287
Preprint. Discussion started: 23 April 2026

The CAMS v6.2 emission dataset (ECCAD, 2026) indicates a decrease in global anthropogenic emissions of the primary SLCFs (NOx, CO, NMVOCs, SO_2, BC and OC), since the COVID hiatus in emissions, except for NH_3, whose emissions are steadily increasing. Note that the trend in emissions for NMVOCs and OC is very weak. SLCF emissions from biomass burning are taken from GFED (van der Werf et al., 2017) with small fires (GFED4.1s) updated to 2025 (following AR6 WGIII (Dhakal et al., 2022)). Estimates from GFED for 2017 to 2025 are provisional. GFED5 re-evaluations will lead to systematically higher emissions estimates for most species (van der Werf et al., 2025). The estimate of global carbon emissions due to wildfires in 2025 is significantly lower than in 2023 and 2024 which were both higher than the average over the last ten years.

The decrease of global NOx emissions, despite very heterogeneous regional trends (Szopa et al., 2021), is confirmed by global NO_2 satellite observations from OMI (tropospheric NO_2 column from OMI visualised through the Giovanni system, Acker and Leptoukh, 2007). The trends in global CO concentration are less clear due to significant interannual variability. Surface data from MOPITT and AIRS, via the Giovanni system, show a slight increase over the 2022-2024 period followed by a slight decrease in 2025 (according to AIRS since MOPITT stopped mid-2025). Increases in CO concentration results from CO anthropogenic emissions as well as variable biomass burning emissions. CO is also influenced by NMVOC emissions, including methane oxidation, which can help explain differences in trends between emissions and concentrations. Multi-instrumental analysis of satellite observations do not reveal clear trends in aerosol optical depth at the global scale between 2002 and 2024, despite large positive trends over India and negative trends over Europe, Eastern China, Eastern US consistent among the datasets for the 2012-2024 period (Sawyer et al. 2025). Fire related peaks in AOD are observed more frequently in some regions like Brazil or Western Canada but the record is not long enough to conclude to a positive trend (Sawyer et al. 2025). Study of ozone trends requires multi-instruments datasets which are not yet available after 2022 (Szopa et al., 2026). Analysis of multi-instrument satellite data over the 2005-2022 period indicates no trend for the tropospheric column (Hubert et al. 2026, Szopa et al., 2026).

Overall, the trends in SLCF emissions were similar (see Supplement Sect. S4) over the 2020-23 period in the most recent CEDS dataset to our previous estimate (Forster et al., 2024) but with a lower post COVID rebound for NOx and SO_2. Regarding SO_2, the CEDS datasets (v2024_04_01 used in Forster et al., 2024 and v2025_03_18 since Forster et al., 2025) account for the introduction of strict fuel sulphur controls brought in by the International Maritime Organization in January 2020. Total SO_2 emissions in 2019 were 80.9 $TgSO_2$ (Table 2). The SO_2 emissions from international shipping declined by 8.4 $TgSO_2$ from 10.4 $TgSO_2$ in 2019 to 2.0 $TgSO_2$ in 2020, which is close to the expected 8.5 $TgSO_2$ reduction estimated by the International Maritime Organization. This decrease was estimated at 7.4 $TgSO_2$ in the previous CEDS version used in Forster et al. (2024). More generally, the reduction pace of the global SO_2 emission over the last ten years corresponds to that of the first ten years of the SSP scenarios assuming strong air pollution control (SSP1 and SSP5).

https://doi.org/10.5194/essd-2026-287
Preprint. Discussion started: 23 April 2026

In the combined estimate of GFED and CEDS (with a 2024-2025 extrapolation based on CAMS), emissions of all SLCFs were reduced in 2022 relative to 2019, but rebounded in 2023 and then slightly decreased in 2024 and 2025 (relative to 2023) for all compounds except NOx which increased in 2024 partly due to biomass burning emissions (Table 2 and Supplement Sect. S4). 2023 was a record year for emissions of organic carbon (driven again by a very active biomass burning season) and ammonia (driven by a steady background increase in agricultural sources, plus a contribution from biomass burning)., OC emissions from biomass burning remained high in 2024 before reverting back to recent trends in 2025. Fires can be worsened by climate change, because of increased fire prone weather conditions (Burton et al., 2024, Oliveira et al. 2026). Strictly speaking, such fires could be considered as climate feedbacks and not be included in anthropogenic forcings, though cleanly separating forced and climate driven components could prove difficult. However, we choose to include fires in our tracking, as historical biomass burning emissions inventories have previously been consistently treated as an anthropogenic forcing (for example in the CMIP6 and CMIP7 emissions datasets used to run Earth System Models), though this assumption may need to be revisited in the future. This differs from the treatment of CO_2 and CH_4 emissions at present (Sect. 2), where we do not include natural emissions in the inventories. As described in Sect. 5, this treatment of all biomass burning emissions as a forcing has implications for several categories of anthropogenic radiative forcing.

Table 2 Emissions of the major SLCFs in 1750, 2019, 2023, 2024 and 2025 from a combination of CEDS and GFED (trends in anthropogenic emissions for 2024 and 2025 from CAMS). Emissions of SO_2+SO_4 use SO_2 molecular weights. Emissions of NO_x use NO_2 molecular weights. VOCs are for the total mass. Note that estimates for 2019 to 2024 were updated in Forster et al., 2025. WGI 2019 estimates from Smith et al. (2021).

Compound	SLCF emissions (Tg yr^{-1})					
	1750	2019 (WGI for ERF estimates)	2019	2023	2024	2025
Sulphur dioxide (SO_2) + sulfate (SO_4^{2-})	2.8	83.7	80.9	72.7	71.2	69.1
Black carbon (BC)	2.1	7.8	7.3	7.6	7.5	6.7
Organic carbon (OC)	15.5	29.8	33.0	41.0	36.1	28.9
Ammonia (NH_3)	6.6	64.9	66.3	72.7	70.6	68.9

https://doi.org/10.5194/essd-2026-287
Preprint. Discussion started: 23 April 2026

Oxides of nitrogen (NO_x)	19.4	135.3	133.6	128.4	130.4	120.4
Volatile organic compounds (VOCs)	60.9	209.1	204.8	224.1	212.7	184.0
Carbon monoxide (CO)	348.4	855.0	816.1	896.0	845.3	693.2

412
413
414 Uncertainties associated with these emission estimates are difficult to quantify. From the non-biomass-burning sectors
415 they are estimated to be smallest for SO_2 (±14 %), largest for black carbon (BC) (a factor of 2) and intermediate for
416 other species (Smith et al., 2011; Bond et al., 2013; Hoesly et al., 2018). Relative uncertainties are also likely to
417 increase both backwards in time (Hoesly et al., 2018) and again in the most recent years. Future updates of CEDS are
418 expected to include uncertainties (Hoesly et al., 2018).
419

420 **5 Effective radiative forcing (ERF)**

421 ERFs were principally assessed in Chap. 7 of AR6 WGI (Forster et al., 2021), which focussed on assessing ERF from
422 changes in atmospheric concentrations; it also supported estimates of ERF in Chap. 6 that attributed forcing to specific
423 precursor emissions (Szopa et al., 2021) and generated the time history of ERF shown in AR6 WGI Fig. 2.10 and
424 discussed in Chap. 2 (Gulev et al., 2021).
425
426 The ERF calculation follows the methodology used in Forster et al. (2025) which was based on AR6 WGI methods
427 (Smith et al., 2021). Compared to AR6, there as some minor methodological changes as detailed in Forster et al.
428 (2025) and described in the Supplement Sect. S5).
429
430 The summary results for the anthropogenic constituents of ERF and solar irradiance in 2025 relative to 1750 are shown
431 in Fig. 5a. In Table 3 these are summarised alongside the equivalent ERFs from AR6 (1750–2019) and last year's
432 Climate Indicators update (1750-2024). Fig. 5b shows the time evolution of ERF from 1750 to 2025.

https://doi.org/10.5194/essd-2026-287
Preprint. Discussion started: 23 April 2026

433

434 **Table 3 Contributions to anthropogenic effective radiative forcing (ERF) for 1750–2025 assessed in this section. Data is for**
435 **single year estimates unless specified. All values are in watts per square metre (W m^{-2}), and 5 %–95 % ranges are in square**
436 **brackets. As a comparison, the equivalent assessments from AR6 (1750–2019) and last year's Climate Indicators (1750-**
437 **2024) are shown. Solar ERF is included and unchanged from AR6, based on the most recent solar cycle (2009–2019), thus**
438 **differing from the single-year estimate in Fig. 5a. Volcanic ERF is excluded due to the sporadic nature of eruptions.**

Forcer	1750-2019 [W m^{-2}] (AR6)	1750-2024 [W m^{-2}] (Forster et al., 2025)	1750-2025 [W m^{-2}]	Reason for change since last year
CO_2	2.16 [1.90 to 2.41]	2.33 [2.05 to 2.61]	2.37 [2.09 to 2.65]	Increases in GHG concentrations resulting from ongoing high emissions
CH_4	0.54 [0.43 to 0.65]	0.57 [0.45 to 0.68]	0.57 [0.45 to 0.68]	
N_2O	0.21 [0.18 to 0.24]	0.23 [0.20 to 0.26]	0.23 [0.20 to 0.26]	
Halogenated GHGs	0.41 [0.33 to 0.49]	0.41 [0.34 to 0.49]	0.41 [0.34 to 0.49]	
Ozone	0.47 [0.24 to 0.71]	0.50 [0.25 to 0.75]	0.48 [0.24 to 0.72]	
Stratospheric water vapour	0.05 [0.00 to 0.10]	0.05 [0.00 to 0.11]	0.05 [0.00 to 0.11]	
Aerosol-radiation interactions	-0.22 [-0.47 to +0.04]	-0.22 [-0.44 to +0.01]	-0.20 [-0.40 to +0.00]	Decrease in most aerosol and aerosol precursor emissions (Table 2)
Aerosol-cloud interactions	-0.84 [-1.45 to -0.25]	-0.85 [-1.65 to -0.25]	-0.76 [-1.37 to -0.23]	
Land use (surface albedo changes and effects of irrigation)	-0.20 [-0.30 to -0.10]	-0.19 [-0.30 to -0.05]	-0.19 [-0.30 to -0.05]	
Light-absorbing particles on snow and ice	0.08 [0.00 to 0.18]	0.08 [0.00 to 0.19]	0.07 [0.00 to 0.16]	
Contrails and contrail-induced cirrus	0.06 [0.02 to 0.10]	0.06 [0.02 to 0.11]	0.07 [0.02 to 0.12]	
Total anthropogenic	2.72 [1.96 to 3.48]	2.97 [2.05 to 3.77]	3.10 [2.35 to 3.83]	Increasing positive GHG forcing and decreasing negative aerosol forcing
Solar irradiance	0.01 [-0.06 to 0.08]	0.01 [-0.06 to 0.08]	0.01 [-0.06 to 0.08]	Not reassessed

https://doi.org/10.5194/essd-2026-287
Preprint. Discussion started: 23 April 2026

Open Access Earth System Science Data Discussions

439

440

441

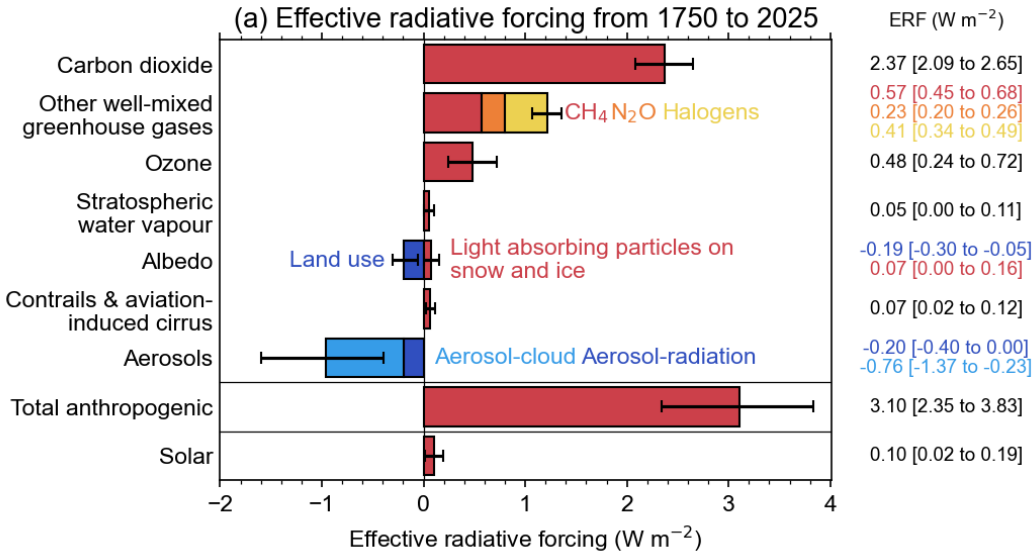

442

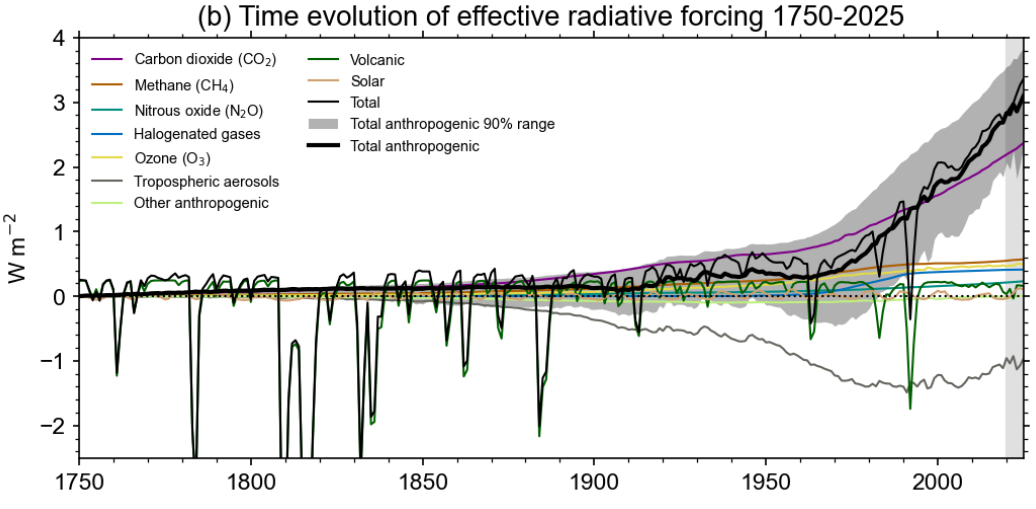

443

https://doi.org/10.5194/essd-2026-287
Preprint. Discussion started: 23 April 2026

Figure 5 Effective radiative forcing (ERF) from 1750–2025. (a) 1750–2025 change in ERF, showing best estimates (bars) and 5 %–95 % uncertainty ranges (lines) from major anthropogenic components to ERF, total anthropogenic ERF and solar forcing. Note that solar forcing in 2025 is a single-year estimate and hence differs from Table 3. (b) Time evolution of ERF from 1750 to 2025. Best estimates from major anthropogenic categories are shown along with solar and volcanic forcing (thin coloured lines),total (thin black line), and anthropogenic total (thick black line). The 5 %–95 % uncertainty in the anthropogenic forcing is shown by grey shading.

Total anthropogenic ERF has increased to 3.10 [2.35 to 3.83] W m^{-2} in 2025 relative to 1750, compared to 2.72 [1.96 to 3.48] W m^{-2} for 2019 relative to 1750 in AR6. The ERF has increased considerably from the 2024 estimate of 2.97 [2.35 to 3.83] W m^{-2}. Sulphur emissions have declined since 2019, weakening the aerosol ERF and adding around +0.1 W m^{-2} over 2020 to 2025 (see Sect. 7.2 and Supplement Sects. S5 and S7). However, the large reduction in biomass burning aerosol from 2024 to 2025 is the primary driver of this single year increase, contributing +0.11 W m^{-2} of the total +0.13 m^{-2} change from 2024 to 2025. The approach of including all biomass burning aerosols, while potentially aliasing some of a climate feedback into the forcing as discussed in the previous section, is consistent with reporting ERF based on concentration increase of GHGs independent of whether CO_2 and CH_4 are caused by anthropogenic emissions or a smaller part is caused by any feedbacks such as from biomass burning fires or wetlands. Changes in mineral dust and sea salt are not easily relatable to human activity and are not included in the ERF of aerosols.

The ERF from well-mixed GHGs is 3.58 [3.27 to 3.91] W m^{-2} for 1750–2025, of which 2.37 W m^{-2} is from CO_2, 0.57 W m^{-2} from CH_4, 0.23 W m^{-2} from N_2O and 0.41 W m^{-2} from halogenated gases. This is an increase of around 7% from 3.32 [3.03 to 3.61] W m^{-2} for 1750–2019 in AR6. ERFs from CO_2, CH_4 and N_2O have all increased since the AR6 WG1 assessment for 1750–2019, owing to increases in atmospheric concentrations.

The total aerosol ERF (sum of the ERF from aerosol–radiation interactions (ERFari) and aerosol–cloud interactions (ERFaci)) for 1750–2025 is −0.96 [−1.58 to −0.40] W m^{-2} for 1750–2025 compared to −1.07 [−1.90 to −0.43] W m^{-2} for 1750–2024 (Forster et al., 2024) and −1.06 [−1.71 to −0.41] W m^{-2} assessed for 1750–2019 in AR6 WGI. Attributing year-to-year trends to aerosol forcing is problematic due to the variability in biomass burning emissions, and can result in relatively larges single-year increases in net anthropogenic ERF (as in 2024 to 2025), or even single-year decreases (such as 2022 to 2023; Forster et al., 2024)..

Ozone ERF is determined to be 0.48 [0.24 to 0.72] W m^{-2} for 1750–2025, about the same as the AR6 assessment of 0.47 [0.24 to 0.71] W m^{-2} for 1750–2019. Stratospheric water vapour from methane oxidation is unchanged (to two decimal places) since AR6. ERF from light-absorbing particles on snow and ice is 0.08 [0.00 to 0.19] W m^{-2} for

https://doi.org/10.5194/essd-2026-287
Preprint. Discussion started: 23 April 2026

1750–2024, unchanged from AR6. For the first time since 2019, we determine from provisional data that aviation activity exceeded pre-COVID levels in 2025 (IATA, 2025), which is used as one indicator of ERF from contrails and contrail-induced cirrus (Supplementary Material Section S5.5) We estimate ERF from contrails and contrail-induced cirrus to be 0.07 [0.02 to 0.12] W m^{-2} in 2025. The methodology to determine land-use ERF has been updated (Sect. S5.4) but this forcing has a similar best estimate to 2023 and AR6, with a wider uncertainty range that accounts for the separate assessment of irrigation forcing.

The headline assessment of solar ERF has not been re-assessed, at 0.01 [−0.06 to +0.08] W m^{-2} from pre-industrial to the 2009–2019 solar cycle mean (Table 3). Separate to the assessment of solar forcing over complete solar cycles, we provide a single-year solar ERF for 2025 of +0.10 [+0.02 to +0.19] W m^{-2} (Fig. 5a). This is higher than the single-year estimate of solar ERF for 2019 (a solar minimum) of −0.02 [−0.08 to 0.06] W m^{-2}.

Volcanic ERF is included in the overall time series (Fig. 5b) but following IPCC convention we do not provide a single-year estimate for 2025 given the sporadic nature of volcanoes. Alongside the time series of stratospheric aerosol optical depth derived from proxies and satellite products, for 2022–2025 we include the stratospheric water vapour contribution from the Hunga Tonga-Hunga Ha'apai (HTHH) eruption derived from Microwave Limb Sounder (MLS) data. We note that the elevated stratospheric water vapour from HTHH persists into 2025. We estimate a net positive (positive forcing from stratospheric water vapour more than outweighing negative forcing from stratospheric aerosols) forcing from HTHH through 2025 (Supplementary Material Sect. S5), though note that other studies find the net HTHH forcing to be negative (Gupta et al., 2025) or close to zero (Schoeberl et al., 2024). The stratospheric aerosol input from HTHH has, by 2025, virtually decayed away, leaving the water vapour contribution (Zhu et al., 2025). We do not separately account for indirect effects, such as stratospheric ozone depletion or other chemical or dynamical adjustments that could affect the net ERF from HTHH (Zhang et al., 2024a).

In addition to the concentration-based ERF estimates in Table 3 and Fig. 5, we present an updated analog of AR6 WG1 Figure 6.12 (Szopa et al., 2021) that decomposes ERF and global surface air temperature (GSAT) change by emitted compound, including secondary effects on other forcing agents (Fig. 6). While the original AR6 figure attributed assessed ERF to emitted compounds using radiative efficiencies and passed the resulting time series through an impulse-response function, here we adopt an emissions-driven counterfactual approach using FaIR v2.2 (Leach et al., 2021) with the v1.4.5 calibrated constrained parameterization (Smith et al., 2024). For each emitted compound, a counterfactual scenario is run with that compound's emissions set to zero from 1750 to 2025 while all other emissions remain at historical levels. The difference in forcing and temperature between the baseline and counterfactual simulations gives the contribution of each compound, decomposed across forcing agents (e.g. greenhouse gas forcing,

https://doi.org/10.5194/essd-2026-287
Preprint. Discussion started: 23 April 2026

ozone, aerosol-radiation and aerosol-cloud interactions). Methodological differences between this and the original AR6 figure are discussed in more depth in the Supplement Sect S5.

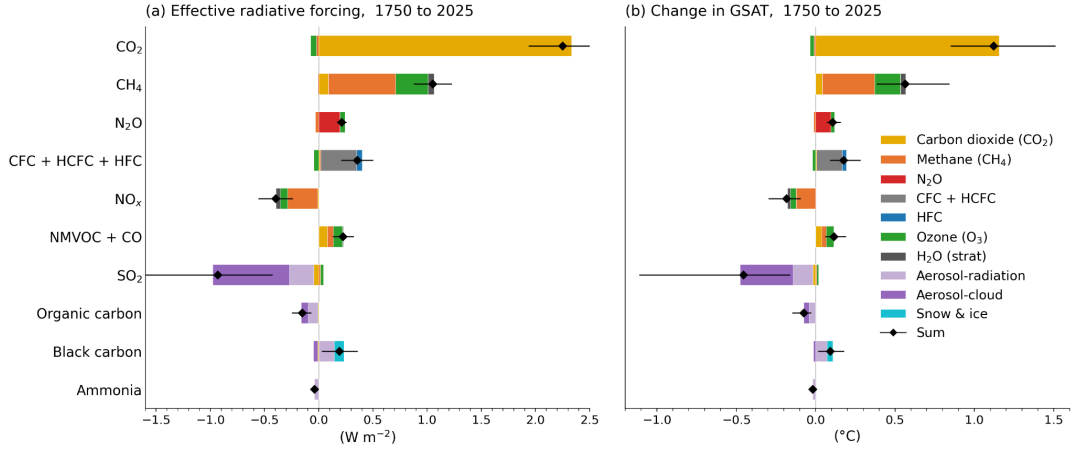

Figure 6 Effective radiative forcing (ERF) and global surface air temperature (GSAT) response between 1750 and 2025 by individual emitted species, including secondary effects. Update to the IPCC AR6 WG1 Figure 6.12 using FaIR emissions-driven runs with each species individually excluded. Uncertainty ranges (5%-95%) are shown as whiskers on the total (diamond) markers and are derived from the constrained ensemble, with sub-bar segments determined by averaging per-agent ERF values across ensemble members falling within a narrow band around the target percentile to ensure exact additivity. Note that the resulting species-specific ERF and GSAT responses are not fully independent and cannot be directly summed.

6 Earth energy imbalance (EEI)

EEI, assessed in Chap. 7 of AR6 WGI (Forster et al., 2021), measures the surplus energy accumulating in the climate system and is hence an essential global climate indicator for monitoring the current and future state of global warming. It represents the difference between the radiative forcing acting to warm the climate and Earth's radiative response, which acts to oppose that warming. Under stable climate conditions, for example, in the absence of anthropogenic climate forcing, this imbalance would average close to zero over interdecadal time scales (Forster et al., 2021). Since at least 1970, however, a persistent positive imbalance in the Earth's energy flows has led to continued heat uptake by the climate system (Church et al., 2011a, 2013; Rhein et al., 2013; von Schuckmann et al., 2020; Forster et al., 2021).

On annual and longer timescales, changes in Earth heat inventory associated with the positive EEI are dominated by the changes in global ocean heat content (OHC), which has accounted for about 90 % of excess heat uptake since the 1970s (Rhein et al., 2013; von Schuckmann et al., 2020; Forster et al., 2021). The remainder is partitioned among land

https://doi.org/10.5194/essd-2026-287
Preprint. Discussion started: 23 April 2026

warming, atmospheric warming, and cryospheric melt (Rhein et al., 2013; von Schuckmann et al., 2023). This planetary heat accumulation drives widespread changes across the Earth system, including sea-level rise, ocean warming, ice loss, warming and moistening of the atmosphere, changes in ocean and atmospheric circulation, continental warming and permafrost thaw (e.g. Cheng et al., 2022; Cuesta-Valero et al., 2023; von Schuckmann et al., 2023a), with adverse impacts on ecosystems and human systems (Douville et al., 2021; IPCC, 2022; UNEP, 2025).

On decadal timescales, changes in global surface temperatures (Sect. 7) can become decoupled from EEI by ocean heat redistribution processes (e.g. Palmer and McNeall, 2014; Allison et al., 2020). The increase in the Earth heat inventory therefore provides a more robust indicator of the rate of global change on interannual-to-decadal timescales (Cheng et al., 2019; Forster et al., 2021; von Schuckmann et al., 2023a). Since AR5 WGI, confidence in the assessment of changes in the Earth heat inventory has increased, owing to observational advances and improved closure of both the Earth's energy and global mean sea level budgets (Church et al., 2013; Rhein et al., 2013; Forster et al., 2021; Fox-Kemper et al., 2021).

AR6 estimated that EEI increased from 0.50 [0.32–0.69] $\mathrm{W\,m^{-2}}$ over 1971–2006 to 0.79 [0.52–1.06] $\mathrm{W\,m^{-2}}$ over 2006–2018 (Forster et al., 2021). Over 1971–2018, about91 % of excess heat uptake was stored in the full-depth ocean, 5 % in land, 3 % the the cryosphere and 1 % in the atmosphere (Forster et al., 2021). Since AR6, the annual IGCC updates have extended this assessment using the same underlying Earth heat inventory framework while progressively incorporating updated observations (Forster et al., 2023, 2024, 2025). Recent studies have shown that since 1960, the rate of warming of the world ocean is accelerating at a relatively consistent pace of 0.15 ± 0.05 $\mathrm{W\,m^{-2}}$ per decade (Minière et al., 2023; Storto and Yang, 2024; Merchant et al., 2025), while the combined rate of warming for the land, cryosphere, and atmosphere has been accelerating at a rate of 0.013 ± 0.003 $\mathrm{W\,m^{-2}}$ per decade (Minière et al., 2023; Cuesta-Valero et al., 2025). An increase in EEI over recent decades (Fig. 7) has also been reported by Cheng et al. (2019), von Schuckmann et al. (2020, 2023a), Loeb et al. (2021), Hakuba et al. (2021), Kramer et al. (2021), Raghuraman et al. (2021) and Minère et al. (2023), with studies further strengthening confidence in both its magnitude and acceleration.

In particular, recent studies indicate that Earth's energy imbalance has more than doubled in recent decades, highlighting a faster-than-expected increase and reinforcing its central role as an integrative metric of ongoing climate change (Loeb et al., 2024; Maurtisen et al., 2025). The observed increase in EEI over the most recent period (i.e., past 2 decades) is contributing to exceptionally warm conditions (Sect. 7; Minobe et al., 2025), with short-term variability—such as the recent transition from La Niña to El Niño—superimposed on the long-term forced trend (Tsuchida et al., 2026). The recent increase in EEI has been interpreted in several ways in the literature. It has been linked to rising concentrations of well-mixed GHGs and recent reductions in aerosol emissions (Sect. 5; Raghuraman et al., 2021; Kramer et al., 2021; Hansen et al., 2023; Myhre et al., 2025). It can be also be viewed in terms of increased

https://doi.org/10.5194/essd-2026-287
Preprint. Discussion started: 23 April 2026

absorbed solar radiation associated with decreased reflection by clouds and sea-ice and a decrease in outgoing longwave radiation (OLR) arising from increases in greenhouse gases and atmospheric water vapor (Loeb et al., 2021; Goesling et al., 2025; Allan and Merchant, 2025). A recent study further identified a decline in low-cloud cover as an important contributor to increased solar absorption and the recent increase in EEI (Ceppi et al., 2026). Consistent with these radiative changes, continued and accelerating ocean heat uptake together with increasing penetration of warming into the deep ocean, provides an integrative constraint on EEI trends (Pan et al., 2026; Cazenave et al., 2026). At the same time, there is growing concern regarding the continuity of the observing system underpinning EEI estimates, as the ability to directly monitor the top-of-atmosphere radiation budget is threatened by the progressive decommissioning of satellite missions while in situ monitoring faces pressures from observing gaps, reduced support and maintenance, despite the fundamental importance of these observations for tracking climate change (von Schuckmann et al., 2023; Mauritsen et al., 2025).

Here we update the AR6 estimate of changes in the Earth heat inventory for 1971-2020 based on updated observational time series (Table 4 and Fig. 7). Time series of heating associated with loss of ice, and warming of the atmosphere and continental land surface are obtained from the recent Global Climate Observing System (GCOS) initiative (von Schuckmann et al., 2023b; Adusumilli et al., 2022; Cuesta-Valero et al., 2023; Vanderkelen and Thiery, 2022; Nitzbon et al., 2022; Kirchengast et al., 2022). We update the AR6 ensemble OHC time series for the period 1971–2025 based on the most recent versions of the underlying datasets (see Supplement Sect. S6 for further details). The AR6 heating rates and uncertainties for the ocean below 2000 m are assumed to be constant throughout the period. The time evolution of the Earth heat inventory is determined as a simple summation of time series of atmospheric heating; continental land heating; heating of the cryosphere; and heating of the ocean over three depth layers: 0–700, 700–2000 and below 2000 m (Fig. 7a). Although von Schuckmann et al. (2023a) also quantified heat taken up by permafrost and inland lakes and reservoirs, these terms are small and excluded here for consistency with AR6 (Forster et al., 2021). Because the GCOS estimates of heat uptake by the atmosphere, cryosphere and land are currently only available up to 2020, we use total OHC change as a proxy for Earth system heat uptake for 2021-2025, scaling values upward on the basis that the ocean accounts for 91% of the total (Forster et al., 2021). Updated GCOS estimates following the approach of von Schuckmann et al. (2023) are currently in preparation and are expected to become available in the near future.

https://doi.org/10.5194/essd-2026-287
Preprint. Discussion started: 23 April 2026

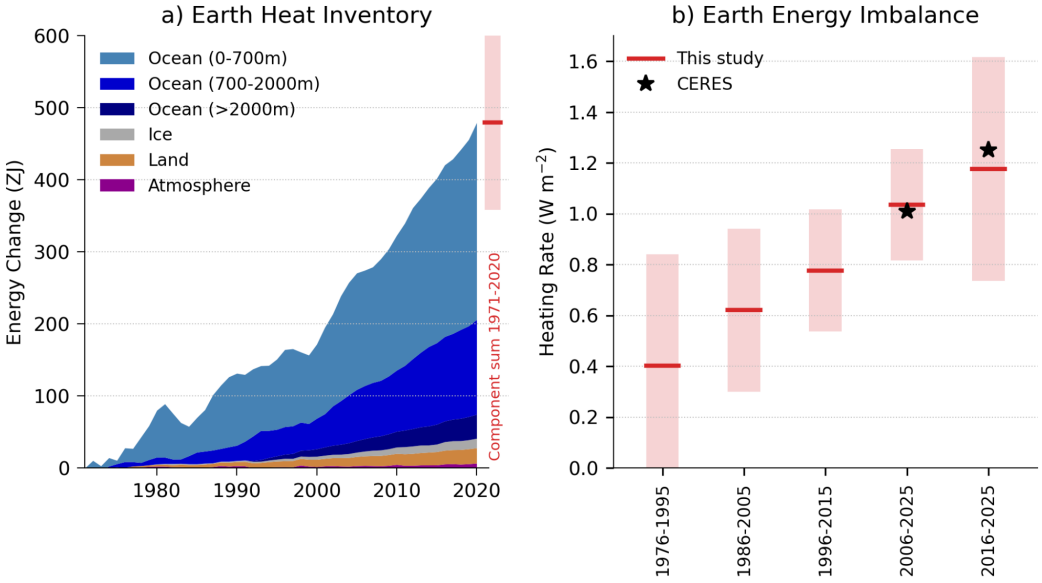

Figure 7 (a) Observed changes in the Earth heat inventory for the period 1971–2020, with component contributions as indicated in the figure legend. (b) Estimates of the Earth energy imbalance for successive overlapping 20-year periods and the most recent decade. Shaded regions indicate the *very likely* range (90 % to 100 % probability). The CERES EBAF-TOA Ed4.2.1 estimates for the two most recent periods are shown for comparison (Loeb et al, 2024). Data use and approach are based on the AR6 methods and further described in Supplement Sect. S6. .

Our updated analysis show successive increases in EEI for each 20-year period since 1976, from 0.40 [-0.03 to 0.84] W m^{-2} during 1976–1995 to 1.04 [0.82 to 1.25] W m^{-2} during 2006–2025 (Fig. 7b). There is also evidence that the warming signal is propagating into the deeper ocean over time, as indicated by a robust increase in warming within the 700-2000m depth layer since the 1990s (von Schuckmann et al., 2020; 2023; Cheng et al., 2019, 2022). Model simulations qualitatively agree with this observational evidence (e.g. Gleckler et al., 2016; Cheng et al., 2019), further suggesting that more than half of the OHC increase since the late 1800s occurred after the 1990s. Our EEI estimates also agree with the NASA Clouds and the Earth's Radiant Energy System (CERES) observations, which use a different estimate of ocean heat uptake to "anchor" their timeseries of net top-of-atmosphere radiative fluxes (Loeb et al, 2024). However, the CERES-based estimates indicate a larger increase in EEI between 2006-2025 and 2016-2025 of about 0.25 Wm^{-2} compared with about 0.15 Wm^{-2} in our estimate, although both are within the bounds of observational uncertainty (Fig. 7b).

Updating the AR6 assessment periods to end in 2025 results in systematic larger EEI values: 0.72 W m^{-2} during 1978–2025 compared with 0.58 W m^{-2} during 1971–2018, and 1.12 W m^{-2} during 2013–2025 compared with 0.87 W m^{-2}

https://doi.org/10.5194/essd-2026-287
Preprint. Discussion started: 23 April 2026

620 during 2006–2018 (Table 4). The trend and interannual variability of EEI can largely be explained by a combination
621 of radiative forcing and surface temperature changes and (Hodnebrog et al., 2024). However, there was a rapid increase
622 in 2023 and 2024 which is still being investigated (see Sect. 7.2), and is also discussed in the context of recent
623 exceptional climate extremes (Minobe et al., 2025).
624

625 **Table 4 Estimates of the Earth energy imbalance (EEI) for AR6 and the present study.**

Time Period	Earth energy imbalance (W m^{-2}). Square brackets [show 90% confidence intervals].	
	IPCC AR6	**This Study**
1971-2018	0.57 [0.43 to 0.72]	0.58 [0.43 to 0.74]
1971-2006	0.50 [0.32 to 0.69]	0.49 [0.28 to 0.69]
2006-2018	0.79 [0.52 to 1.06]	0.87 [0.62 to 1.12]
1978-2025	-	0.72 [0.55 to 0.90]
2013-2025	-	1.12 [0.78 to 1.46]

626

627 **7 Observed surface temperature change**

628 **7.1 Change since 1850-1900**

629 AR6 WGI Chap. 2 assessed the 2011–2020 globally averaged surface temperature change above an 1850–1900
630 baseline to be 1.09 [0.95 to 1.20] °C (Gulev et al., 2021). Updated estimates to 2013-2022 of 1.15 [1.00–1.25] °C were
631 given in AR6 SYR (Lee et al., 2023), matching the estimate in Forster et al. (2023).
632
633 There are choices around the methods used to aggregate surface temperatures into a global average, how to correct for
634 systematic errors in measurements, methods of infilling missing data, and whether surface measurements or
635 atmospheric temperatures just above the surface are used. These choices, and others, affect temperature change
636 estimates and contribute to their uncertainty (AR6 WGI Chap. 2, Cross Chap. Box 2.3, Gulev et al., 2021). The
637 methods chosen here closely follow AR6 WGI and are presented in the Supplement Sect. S7. Confidence intervals are
638 taken from AR6 as only one of the employed datasets regularly updates ensembles (see Supplement Sect. S7).

https://doi.org/10.5194/essd-2026-287
Preprint. Discussion started: 23 April 2026

639

640 Based on the updates available as of March 2026, the change in global surface temperature from 1850–1900 to 2016–
641 2025 is presented in Fig. 8. These data, using the same underlying datasets (with some version changes: see
642 Supplement Sect. S7) and methodology as AR6, estimate 1.26 [1.13–1.36] °C of warming, an increase of 0.17 °C
643 within five years from the 2011–2020 value reported in AR6 WGI (Table 5), or 0.18 °C from the 2011–2020 value in
644 the most recent dataset version. The decade 2016-2025 was 0.32 °C warmer than the previous decade (2006–2015).
645 These changes, although amplified somewhat by the exceptionally warm years in 2023 and 2024, are larger than
646 typical warming rates over the last few decades, which were assessed in AR6 as 0.19 °C per decade over the 1980–
647 2020 period (Gulev et al., 2021). They are also broadly consistent with projected warming rates from 2001–2020 to
648 2021–2040 reported in AR6, which had a very likely range between 0.016 °C per year and 0.036 °C per year under
649 SSP2-4.5 (Lee et al., 2021, their Table 4.5), and with human-induced warming rates discussed in Sect. 8.2. GMST in
650 2025 was 1.39 +/- 0.13 °C warmer than the 1850–1900 baseline, which is cooler than 2024 (1.51 +/- 0.13 °C) but
651 warmer than any year prior to 2023.
652
653 Natural drivers and internal variability are expected to modulate human-caused warming at interannual-to-decadal
654 timescales. Observed global surface temperature in 2024 is assessed to be 0.15 ºC higher than the updated human-
655 induced value while 2022 was 0.06 ºC lower. The 2025 observed value corresponds exactly to the mean expected
656 anomalies of human-induced warming. The probability to get such an observed value at current human-induced
657 warming levels, conditional to the fact that 2025 was in a weak La Nina state in the Pacific and that the Atlantic
658 Multidecadal Variability (AMV) was in a positive phase, is equal to around 1 chance out of 4 (p=0.26 [0.22-0.30])
659 (see Supplement Sect. S7). 2025 can therefore be treated as a “normal” year, i.e. very much expected at the actual
660 human-caused global warming level when the internal modes of variability are taken into account and when assessed
661 from a very large number of simulations from large ensembles. Forster et al. (2025) and Supplement Sect. S7 has
662 further discussion of the very high global surface temperature observed in 2023 and 2024 and probabilities of
663 outcomes for annual global surface temperature resulting from the modulation of global warming trends by internal
664 variability..
665
666 Land temperatures have increased by 1.81 [1.63-2.07] °C from 1850-1900 to 2016-2025, and ocean temperatures by
667 1.03 [0.83-1.14] °C over the same period. As was the case for the periods reported in AR6, the ratio of observed land
668 to ocean warming is in the vicinity of 1.75, somewhat higher than the ratio of 1.5 [1.4-1.7] projected by the end of the
669 century in CMIP6 models (AR6, their Table 4.2 and Section 4.5.1.1.1). The additional observed warming since 2020
670 in the most recent dataset versions (0.24 °C for land, 0.15 °C for ocean) has a ratio within the CMIP6 projections
671 range.
672

https://doi.org/10.5194/essd-2026-287
Preprint. Discussion started: 23 April 2026

Open Access Earth System Science Data Discussions

673 **Table 5 Estimates of global surface temperature change from 1850–1900 [*very likely* (90 %–100 % probability) ranges] for**
674 **IPCC AR6 and the present study.**

Region	Decadal average temperature change from 1850-1900 (°C)	
	IPCC AR6 (2011-2020, as reported)	This study (2016-2025)
Global	1.09 [0.95 to 1.20]	1.26 [1.13 to 1.36]
Land	1.59 [1.34 to 1.83]	1.81 [1.63 to 2.07]
Ocean	0.88 [0.68 to 1.01]	1.03 [0.83 to 1.14]

675

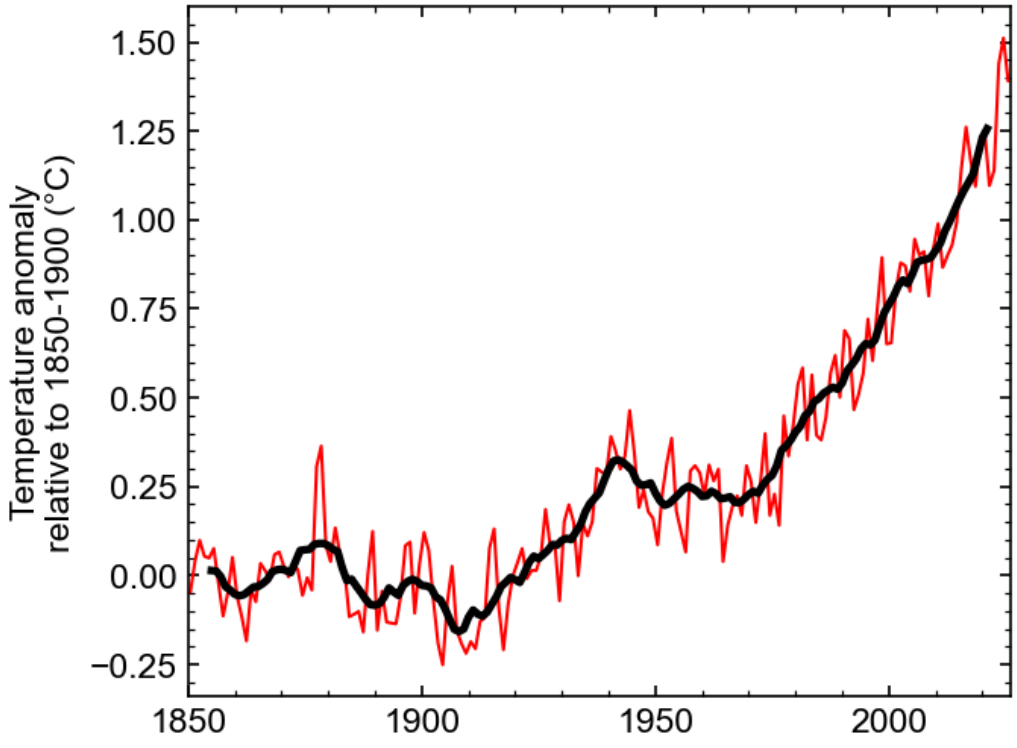

676

https://doi.org/10.5194/essd-2026-287
Preprint. Discussion started: 23 April 2026

Figure 8 Annual (thin line) and decadal (thick line) means of global surface temperature (expressed as a change from the 1850–1900 reference period). Temperatures are based on an average of four datasets following AR6, see Supplement Sect. S7 for details.

8 Human contribution to surface temperature change

Human-induced warming, also known as anthropogenic warming, refers to the component of observed global surface temperature increase attributable to both the direct and indirect effects of human activities, which are typically grouped as follows: well-mixed GHGs (consisting of CO_2, CH_4, N_2O and F-gases) and other human forcings (consisting of aerosol–radiation interaction, aerosol–cloud interaction, black carbon on snow, contrails, ozone, stratospheric H_2O and land use) (Eyring et al., 2021). The remaining contributors to total warming are natural, consisting of both natural forcings (such as solar and volcanic activity) and internal variability of the climate system (such as variability related to El Niño/La Nina events).

An assessment of human-induced warming was provided in two reports within the IPCC's Sixth Assessment cycle: first in SR1.5 in 2018 [Chap. 1 Sect. 1.2.1.3 and Fig. 1.2 (Allen et al., 2018), summarised in the Summary for Policymakers (SPM) Sect. A.1 and Fig. SPM.1 (IPCC, 2018)] and second in AR6 in 2021 [WGI Chap. 3 Sect. 3.3.1.1.2 and Fig. 3.8 (Eyring et al., 2021), summarised in the WGI Summary for Policymakers (SPM) Sect. A.1.3 and Fig. SPM.2 (IPCC, 2021b)], and quoted again without any updates in SYR [Sect. 2.1.1 and Fig. 2.1 (IPCC,2023a) and SYR Summary for Policymakers (SPM) Sect. A.1.2. (IPCC 2023b)].

Temperature increases are defined relative to a baseline; IPCC assessments typically use the 1850–1900 average temperature as a proxy for the climate in pre-industrial times, even though a small amount of warming likely occurred over 1750-1850 (see AR6 WGI Cross Chapter Box 1.2). Temperatures in the IPCC were reported as either GMST or GSAT, see Supplement Sect. 8.1 for details. Tracking progress towards the long-term global goal to limit warming, in line with the Paris Agreement, requires the assessment of both what the current level of global surface temperatures are and whether a level of global warming, such as 1.5 °C, is being reached (Betts et al., 2023, Thorne et al., 2026). Definitions for these were not specified in the Paris Agreement, and several ways of tracking levels of global warming are in use. When determining whether warming thresholds have been passed, both AR6 and SR1.5 adopted definitions that depend on future warming; in practice, levels of current warming were therefore reported in AR6 and SR1.5 using additional definitions that circumvented the need to wait for observations of the future climate, as described in Supplement Sect. S8.1.1 and Fig. S12.

https://doi.org/10.5194/essd-2026-287
Preprint. Discussion started: 23 April 2026

8.1 Updated assessment approach of human-induced warming to date

This paper provides an update of the AR6 and SR1.5 human-induced warming assessments, including, for completeness, all the three definitions: (i) the lagged decade mean value as used in AR6, (ii) the trend based value for a single-year as used in SR1.5, and (iii) the annual mean value for a single year as also used in SR1.5 (see Supplement Sect. S 8.1.1). The two latter definitions have produced identical or almost identical results in recent years, hence they are sometimes used interchangeably; where they differ we prioritise the SR1.5 trend-based definition which reduces the effects of any internal variability in the annual mean estimates, while acknowledging that there is increasing confidence in the robustness of the simpler annual mean (Ribes et al., 2025). The 2025 updates in this paper follow the same methods and process as Forster et al. (2023, 2024, 2025). Global mean surface temperature (GMST) is adopted as the definition of global surface temperature (see Supplement Sect. S8.1.2). The three attribution methods used in AR6 are retained: the Global Warming Index (GWI) (building on Haustein et al., 2017), regularised optimal fingerprinting (ROF) (as in Gillett et al., 2021) and kriging for climate change (KCC) (Ribes et al., 2021). Details of each method, their different uses in SR1.5 and AR6, and any methodological changes, are provided in Supplement Sect. S8.2; method-specific results are also provided in Supplement Sect. S8.3. The overall estimate of attributed global warming for each definition (decade-average, trend-based, and annual-mean), is based on a multi-method assessment of the three attribution methods (GWI, KCC, ROF); the best estimate is given as the 0.01 °C-precision mean of the 50th percentiles from each method, and the *likely* range is given as the smallest 0.1 °C-precision range that envelops the 5th to 95th percentile ranges of each method. This assessment approach is directly traceable to and fully consistent with the assessment approach in AR6, though it has been lightly extended for these annual updates in ways that are explained in Supplement Sect. S8.4.

Results are summarised in Table 6 and Fig. 9. Method-specific contributions to the assessment results, along with time series, are given in the Supplement, Sect. S8.3. Where results reported in GSAT differ from those reported in GMST (see Supplement Sect. S8.1), the additional GSAT results are given in Supplement Sect. S8.3.

https://doi.org/10.5194/essd-2026-287
Preprint. Discussion started: 23 April 2026

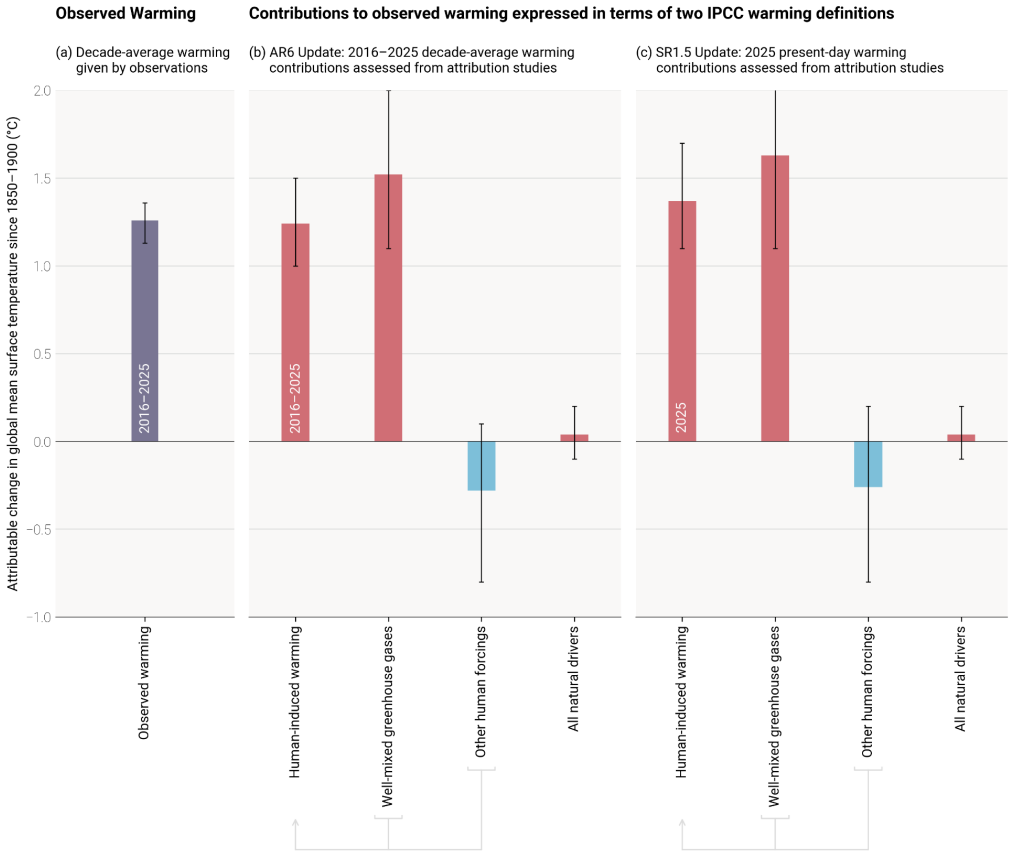

734

https://doi.org/10.5194/essd-2026-287
Preprint. Discussion started: 23 April 2026

Open Access Earth System Science Data Discussions

Figure 9 Updated assessed contributions to observed warming relative to 1850–1900; see AR6 WGI SPM.2. Results for all time periods in this figure are calculated using updated datasets and methods. The 2016–2025 average and 2025 results are this year's updated assessments of the attributable warming reported in AR6 and SR1.5, respectively. Panel (a) shows updated observed global warming from Sect. 7, expressed as total global mean surface temperature (GMST), due to both anthropogenic and natural influences. Whiskers give the "*very likely*" range. Panels (b) and (c) show updated assessed contributions to warming, expressed as global mean surface temperature (GMST), from natural forcings and total human-induced forcings, which in turn consist of contributions from well-mixed GHGs and other human forcings. Whiskers give the "*likely*" range. Changes to warming levels since the IPCC sixth assessment cycle are depicted in Supplement Fig. S11.

Table 6 Updates to assessments in the IPCC 6th assessment cycle of warming attributable to multiple influences. Estimates of warming attributable to multiple influences, in °C, relative to the 1850–1900 baseline period. Results are given as best estimates, with the *likely* range in brackets, and reported as global mean surface temperature (GMST). Results from the IPCC 6th assessment cycle, for both AR6 and SR1.5, are quoted in columns labelled (i) and are compared with repeat calculations in columns labelled (ii) for the same period using the updated methods and datasets, including new observations up to 2025, to see how methodological and dataset updates alone would change previous assessments. Assessments for the updated periods are reported in columns labelled (iii). * Updated GMST observations, quoted from Sect. 7 of this update, are marked with an asterisk, with "*very likely*" ranges given in brackets. ** In AR6 WGI, best-estimate values were not provided for warming attributable to well-mixed GHGs, other human forcings and natural forcings (though a "*likely*" range was assessed); for comparison, best estimates (marked with two asterisks) have been retrospectively calculated in an identical way to the best estimate that AR6 provided for anthropogenic warming (see discussion in Supplement Sect. S8.4.1). * The SR1.5 assessment drew only on GWI rounded to 0.1°C precision, whereas the repeat and updated calculations use the updated multi-method assessment approach.**

Estimates of warming attributable to multiple influences, in °C, relative to the 1850–1900 baseline period
Results are given as best estimates, with the *likely* range in brackets, and reported as Global Mean Surface Temperature (GMST).

Definition ➡	**(a) IPCC AR6 Attributable Warming Update**			**(b) IPCC SR1.5 Attributable Warming Update**		
	Value for decade (average of previous 10-year period)			*Value for single year (30-year mean centred on current year)*		
Period ➡	**(i) 2010-2019** *Quoted from AR6 Chapter 3 Sect. 3.3.1.1.2 Table 3.1 for attributed warming, and Cross-chapter Box 2.3 Table 1 for observed warming*	**(ii) 2010-2019** *Repeat calculation using the updated methods and datasets*	**(iii) 2016-2025** *Updated value using updated methods and datasets*	**(i) 2017** *Quoted from SR1.5 Chapter 1 Sect. 1.2.1.3*	**(ii) 2017** *Repeat calculation using the updated methods and datasets*	**(iii) 2025** *Updated value using updated methods and datasets*
Component ⬇️						
Observed	1.06 [0.92 to 1.17]	1.06 [0.89 to 1.22] *	1.26 [1.13 to 1.36] *	-	-	1.39 [1.26 to 1.52]
Anthropogenic	1.07 [0.8 to 1.3]	1.07 [0.9 to 1.3]	1.24 [1.0 to 1.5]	1.0 [0.8 to 1.2] ***	1.12 [0.9 to 1.3]	1.37 [1.1 to 1.7]
Well-mixed GHGs	1.40** [1.0 to 2.0]	1.39 [1.0 to 1.8]	1.52 [1.1 to 2.0]	N/A	1.44 [1.0 to 1.9]	1.63 [1.1 to 2.1]

https://doi.org/10.5194/essd-2026-287
Preprint. Discussion started: 23 April 2026

Other human forcings	-0.32** [-0.8 to 0.0]	-0.31 [-0.8 to 0.1]	-0.28 [-0.8 to 0.1]	N/A	-0.31 [-0.8 to 0.1]	-0.26 [-0.8 to 0.2]
Natural forcings	0.03** [-0.1 to 0.1]	0.05 [-0.1 to 0.2]	0.04 [-0.1to 0.2]	N/A	0.05 [-0.1 to 0.2]	0.04 [-0.1 to 0.2]

The repeat calculations for attributable warming in 2010–2019 exhibit good correspondence with the results in AR6 WGI for the same period (see also Supplement, Sect. S8). The repeat calculation for the level of attributable anthropogenic warming in 2017 is about 0.1 °C larger than the estimate provided in SR1.5 for the same period, resulting from changes in methods and observational data (see AR6 WGI Chapter 2 Box 2.3). The updated results for warming contributions in 2025 are higher than in 2017 due also to 8 additional years of increasing anthropogenic forcing. Note also that the SR1.5 assessment only used the GWI method, whereas these annual updates apply the full AR6 multi-method assessment (see Supplement Sect. S8.4 for details and rationale).

In this 2026 update, we assess the 2016–2025 decade average human-induced warming at 1.24 [1.0 to 1.5] °C, which is 0.17°C above the AR6 assessment for 2010–2019. The single year average human-induced warming is assessed to be 1.37 [1.1 to 1.7] °C in 2025 relative to 1850–1900. In general, these forced warming levels have evolved steadily and predictably in line with the current warming rate within uncertainty. Note that the interannual increase in assessed human-induced warming since last year's assessment is smaller than the assessed rate of human-induced warming, due in part to the change from HadCRUT 5.0.2 to 5.1.0, which contributed to a small downward revision of historical warming compared to Forster et al. (2025). Even with the slight downward historical revision, the central estimate for well-mixed greenhouse gases lies above 1.5°C for the 2016–2025 average and above 1.6°C by 2025, which is masked by the net cooling contribution from all other human forcings.

AR6 assessed that, averaged for the 2010–2019 period, essentially all observed global surface temperature change was human-induced, with solar and volcanic drivers and internal climate variability making a negligible contribution. For both 2016–2025 and 2025 the observed warming again is only 0.02°C different than the assessed level of human-induced warming; indeed for all three attribution methods, observed warming in 2025 was extremely close to the total forced warming, indicating that 2025 was a typical year for the current level of forced warming, with only a minimal contribution from internal variability (see Sect .7). This conclusion remains the same for the 2016–2025 period. Generally, whatever methodology is used, on a global scale, the best estimate of the current level of human-induced warming is (within uncertainty) similar to the observed global surface temperature change (Table 6).

https://doi.org/10.5194/essd-2026-287
Preprint. Discussion started: 23 April 2026

784 **8.2 Rate of human-induced global warming**

785 Estimates of the human-induced warming rate follow the same methodology as in previous years (a rolling 10-year
786 linear trend in attributed anthropogenic warming). A description of the approach can be found in the Supplement (Sect.
787 S8.5). Our assessed rate of attributed anthropogenic warming over time is distinct from the rate of increase in the
788 observed global surface temperature, discussed in section 7, which is also affected by internal variability (see Sect.
789 7.2). In this section we isolate the rate of *anthropogenic* warming driven by the rate of change of anthropogenic ERF
790 (Sect. 5), with variations in the climate forcing trend over time correlating with variations in the rate of attributed
791 warming (Fig. 10).
792

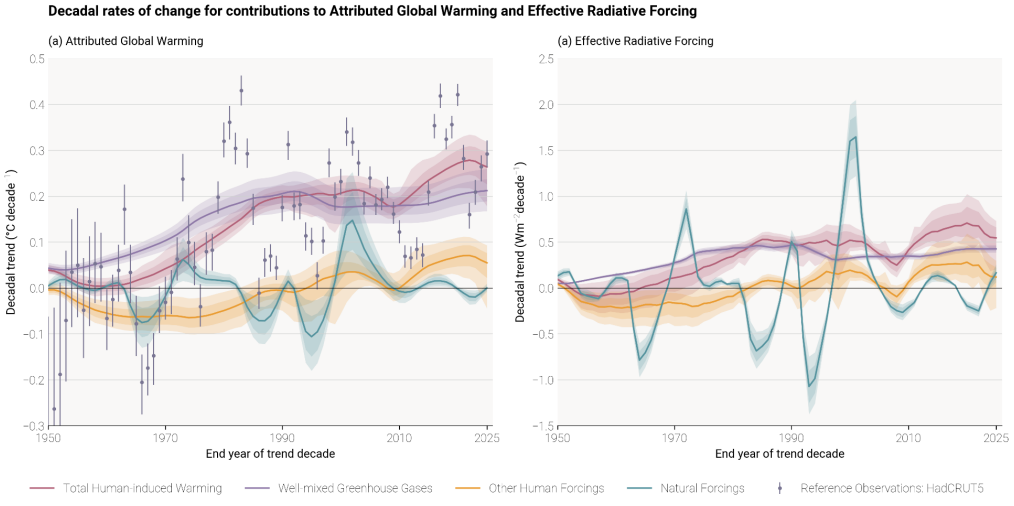

793
794

795 **Figure 10 Rates of (a) attributable warming (global mean surface temperature (GMST)) and (b) effective radiative forcing.**
796 **The attributable warming rate time-series are calculated using the Global Warming Index method with full ensemble**
797 **uncertainty. The observed GMST rates included for reference are also calculated with uncertainty from the HadCRUT5**
798 **ensemble, and, for consistency with the attributed warming rates, do not include standard regression error, which, for**
799 **observed warming, would increase the size of the error bars. The effective radiative forcing rates are calculated using a**
800 **representative 1000-member ensemble of the forcings provided in Sect. 5 of this paper. The depicted rates are the decadal**
801 **rates, with the end year of the decade in question being the value given on the time axis. See Fig. S14 in the supplement for**
802 **a breakdown of these aggregate rates into their components.**

803

804 A combined estimate for the trend derived using the three warming attribution methodologies is presented in Table 7,
805 with results for individual methods shown in Supplement Table S7. As in previous assessments, the GWI (based on
806 observed warming and forcing) and KCC (based on observed warming and CMIP simulations) methodologies are in
807 close agreement, while estimates derived with the ROF method (also based on observed warming and CMIP

https://doi.org/10.5194/essd-2026-287
Preprint. Discussion started: 23 April 2026

simulations) imply higher warming rates. The ROF results are more strongly influenced by residual internal variability that remains in the anthropogenic warming signal due to the limitations in size of the available CMIP ensemble.

The assessed attributed rate of human-induced warming is unchanged on the previous year's assessment (0.27°C/decade for the decade 2016–2025). The spread of rates across the three attribution methods remains similar to their spread in AR6, and previous updates of this work, and hence does not support a decrease in the headline uncertainty range overall, which we maintain at 0.2–0.4°C/decade overall (see discussion in SI; reflecting the agreement of the 5% floors and the larger spread in the 95% ceilings of the three methods, and higher rate from the ROF method).

The overall assessed rate of human-induced warming (0.27 (0.2–0.4) °C/decade agrees with the decadal trend in observed warming of 0.30 °C per decade (also calculated as a linear trend through 10-year periods – see Table 7). Last year we noted that internal variability leads to the decadal rates of observed warming being far less stable than for anthropogenic warming, and the continued close correspondence between the two this year is, again, somewhat coincidental (see Fig. 10). This year we diagnose a slightly lower decadal human-induced warming rate compared to the last couple of years. This slight revision is due to a decrease in the attributed warming rate from aerosol emissions (with aerosol forcing trends peaking and declining in recent years, see Fig. S13). Aerosols have been the predominant driver of the acceleration in anthropogenic warming since the decade 2000–2009 due to their emission rate falling. A slowing in the rate at which aerosol emissions are falling (i.e. a deceleration) are contributing a slight reduction in anthropogenic warming rates (i.e. a net deceleration) over the last three years, though we note that wildfire emissions, which were particularly high in 2023 and 2024, are included in the aerosol emissions underlying this calculation (Section 4). Carbon-dioxide-induced warming remains the dominant contribution to the anthropogenic warming rate, and, having consistently increased over the assessed historical period, reached a new historical high over the decade 2016–2025 (individually-attributed warming rates using the GWI methodology are shown in Supplement Fig. S13). The contributions from internal variability were small for the 2016–2025 period, though the decadal rate from internal variability fluctuates strongly year-on-year (see Fig. S13). Finally, we note that, based on the current assessed level and rate of warming, human-induced warming will reach 1.5°C around the year 2030.

https://doi.org/10.5194/essd-2026-287
Preprint. Discussion started: 23 April 2026

836 **Table 7 Updates to the IPCC AR6 rate of human-induced warming. Results for each method are given in the Supplement**
837 **Table S6; assessment results are given as a best estimate with *likely* range in brackets. Results from AR6 WGI (Ch.3 Sect.**
838 **3.3.1.1.2 Table 3.1) are quoted in column (i), and compared with a repeat calculation using the updated methods and**
839 **datasets in column (ii), and finally updated for the 2016-2025 period in column (iii). The AR6 assessment result was identical**
840 **to the SR1.5 assessment result, though the latter was based on a different set of studies and timeframes. * Note that for**
841 **clarity and ease of comparison with this year's updated assessment, the assessed rate in column (i) both quotes the**
842 **assessment from AR6 and retrospectively applies the median approach adopted in this paper. The observed rates are**
843 **calculated using the multi-dataset observed temperature dataset from Sect. 7; no ensemble is available for this, hence the**
844 **absence of an uncertainty range.**

Estimates of anthropogenic warming rate, in °C per decade Results are given as best estimates, with brackets giving the *likely* range for the assessments, and 5-95% uncertainty for the individual methods			
Definition ➡	**IPCC AR6 Anthropogenic Warming Rate Update** *Linear trend in anthropogenic warming over the trailing 10-year period*		
Period ➡	**(i) 2010-2019** *Quoted from AR6 Chapter 3 Sect. 3.3.1.1.2 Table 3.1*	**(ii) 2010-2019** *Repeat calculation using the updated methods and datasets*	**(iii) 2016-2025** *Updated value using updated methods and datasets*
Anthropogenic Warming Rate Assessment	Quoted from AR6: 0.2 [0.1 to 0.3] Using the median approach: 0.23 [0.1 to 0.3] *	0.26 [0.2 to 0.4]	0.27 [0.2 to 0.4]
Observed		0.37	0.30

845
846

847 9 Remaining Carbon Budget

848 Long-term global surface temperature increase caused by CO_2 emissions is close to linearly proportional to the total
849 amount of cumulative CO_2 emissions (IPCC, 2013; Collins et al., 2013), an assessment reaffirmed by AR6 (Canadell
850 et al., 2021). This near-linear relationship implies that for keeping global warming below a specified temperature
851 level, one can estimate the total amount of CO_2 that can ever be emitted. When expressed relative to a recent reference
852 period, this is referred to as the remaining carbon budget (Rogelj et al., 2018).
853
854 AR6 WGI assessed the remaining carbon budget (RCB) for warming levels ranging from 1.3 to 2.4 °C relative to the
855 1850-1900 period (see Table 5.8 in Canadell et al., 2021). A selection of these (1.5, 1.7, and 2 °C) were also reported
856 in its Summary for Policymakers (Table SPM.2, IPCC, 2021b). These RCB values are updated in this section using
857 the same method as previously (Forster et al., 2024, 2025).
858
859 The RCB is estimated by application of the WGI AR6 method described in Rogelj et al. (2019), which involves the
860 combination of the assessment of five factors: (i) the amount of human-induced warming for the most recent decade

https://doi.org/10.5194/essd-2026-287
Preprint. Discussion started: 23 April 2026

(given in Sect. 8), (ii) the transient climate response to cumulative emissions of CO_2 (TCRE), which quantifies the linear proportionality between cumulative CO_2 emissions and CO_2-induced warming (iii) the zero emissions commitment (ZEC), representing the expected amount of additional (at present unrealized) warming caused by past CO_2 emissions (iv) the temperature contribution of future non-CO_2 emissions and (v) an adjustment term for Earth system feedbacks that are otherwise not captured through the other factors. AR6 WGI reassessed all five terms (Canadell et al., 2021). Lamboll et al. (2023) further considered the temperature contribution of non-CO_2 emissions and integrated different uncertainties, while Rogelj and Lamboll (2024) clarified the reductions in non-CO_2 emissions that are assumed in the RCB estimation.

The RCB is re-assessed based on the most recent available data. Estimated RCBs for 0.1°C increments in global warming between 1.5°C and 2°C are reported in Table 8. They start from 2026 and are based on the 2016–2025 human-induced warming update (Sect. 8). Several robustness cases are included in the Supplement Sect. S9 - values for the calculation using observed rather than anthropogenic warming, as well as versions using both MAGICC and FaIR results for the emulators and including ZEC uncertainty in the distribution. Based on the variation in non-CO_2 emissions across the scenarios in AR6 WGIII scenario database, the estimated RCB values can be higher or lower by around 200 $GtCO_2$ depending on how successful non-CO_2 emissions reductions are (Lamboll et al., 2023; Rogelj and Lamboll, 2024). Notably, RCB estimates consider the subset of non-CO_2 emission scenarios in the AR6 WGIII database that are aligned with a global transition to net zero CO_2 emissions (Lamboll et al., 2023; Rogelj and Lamboll, 2024). These estimates assume median reductions in non-CO_2 emissions between 2020–2050 of CH_4 (about 50 %), N_2O (about 20 %) and SO_2 (about 80 %) (see Supplement, Sect. S9 and Table S11 and (Rogelj and Lamboll, 2024)). If these non-CO_2 GHG emission reductions are not achieved, the RCB for all temperature targets would be smaller than the values reported here in Table 8 (see Lamboll et al., 2023, Rogelj and Lamboll, 2024).

Compared to RCB values reported in AR6, our estimates here are smaller owing to several factors. First, AR6 budgets were expressed from 2020 onwards, and approximately 250 $GtCO_2$ have been emitted between 2020 and 2025 (Friedlingstein et al., 2025), so the expected budget is smaller. Second, we use updated physical models of non-CO_2 forcing which lead to an increased estimate of the importance of aerosols that are expected to decline with time in low emissions pathways (Rogelj et al., 2014; Rogelj and Lamboll, 2024). This decreased negative forcing from aerosols is expected to cause additional net non-CO_2 warming because more non-CO_2 GHG warming is being unmasked and this decreases the RCB (Lamboll et al., 2023) by around100 $GtCO_2$. There was also a small reduction in the budget (about 10 $GtCO_2$) from using the newer AR6 scenario set compared to the SR1.5 scenario set on which AR6 WGI still had to rely. Finally, the updated warming estimate reported in Sect. 8 is slightly increased compared to central estimates at the time of AR6 due to the higher than expected recent warming in the last few years, which resulted in a further reduction of the budget by a few tens of $GtCO_2$. This gives a total reduction in RCB values estimated from the beginning of 2026 of ~370 $GtCO_2$ compared to the values from 2020 reported in AR6. Note that both the

https://doi.org/10.5194/essd-2026-287
Preprint. Discussion started: 23 April 2026

anthropogenic warming and the RCBs changed by less than expected from linear extrapolation in the last year, although this largely offset the unexpectedly large change in these values the year before. The 1.5 °C 50% RCB is approximately the same as that given last year, see Forster et al. (2025), due in part to including some non-anthropogenic warming in last year's estimate.

Table 8 Estimates of the remaining carbon budget for 1.5 - 2.0 °C temperature increase, for five levels of likelihood, considering only uncertainty in TCRE. Estimates are expressed relative to the start of 2026. The probability includes only the uncertainty in how the Earth immediately responds to CO_2 emissions (TCRE), not long-term committed warming or uncertainty in the climate response to other non-CO_2 emissions. All values are rounded to the nearest 10 $GtCO_2$. Additional values can be found in the Supplementary Tables S9 and S9, and the corresponding time to net zero based on a linear pathway are presented in Supplementary Tables S10.

Temperature change (°C)	Estimated remaining carbon budgets from the beginning of 2026 base year ($GtCO_2$)						
Avoidance probability (TCRE uncertainty only):	10%	17%	33%	50%	67%	83%	90%
1.5	480	340	210	130	80	30	10
1.6	840	630	430	320	240	170	130
1.7	1210	930	650	500	390	300	250
1.8	1570	1220	870	680	550	430	370
1.9	1940	1510	1090	860	700	560	480
2	2300	1800	1310	1050	860	690	600

This year's update of the 1.5 °C budget uses the historical warming level for the 2016-2025 period of 1.24 °C, with a 0.10 °C future contribution of non-CO_2 warming. Assuming a median TCRE estimate of 0.45 °C per 1000 $GtCO_2$ this gives around 360 $GtCO_2$ from the midpoint of the period, from which we subtract around 220 $GtCO_2$ (consisting of 213 $GtCO_2$ that were already emitted from the middle until the end of the 2016-2025 period, and 7 $GtCO_2$ that represents the median estimate of the impact of Earth systems feedbacks such as permafrost feedback that would otherwise not be covered). The same method is used to calculate budgets for the other warming levels.

The values in Table 8 are all greater than zero, implying that we have not yet emitted the amount of CO_2 that would commit us to these levels of warming for these ranges of probability. However, including the uncertainty in ZEC (as

https://doi.org/10.5194/essd-2026-287
Preprint. Discussion started: 23 April 2026

in the Supplementary Table S9), non-CO_2 emission and forcing uncertainty, and underrepresented Earth-system feedbacks results in negative RCB estimates for limiting warming to low temperature limits with high likelihood. A negative RCB for a specific temperature limit would mean that the world is already committed to this amount of warming, even if CO_2 emissions ceased now, and that net negative CO_2 emissions would be required to return to the temperature limit after a period of overshoot. The assumption behind such a calculation is that we can treat the warming impact of positive and negative net emissions as approximately symmetric. While the claim of symmetry is likely valid for small levels of carbon budget overconsumption, some model studies have shown that it holds less well for reversal of larger emissions (Canadell et al., 2021, Zickfeld et al., 2021, Vakilifard et al., 2022) As such, larger exceedances of the RCB for a particular temperature target would decrease the likelihood that the temperature target could still be achieved by an equivalent amount of net negative emissions.

Note that the RCB estimate of 130 $GtCO_2$ (50% likelihood) would be exhausted in a little more than 3 years if global CO_2 emissions remain at 2025 levels (42 $GtCO_2$/yr, see Table 1). This is not expected to correspond exactly to the time that 1.5 °C of global warming is reached due to uncertainty associated with committed warming from past CO_2 emissions (the ZEC) as well as ongoing warming and cooling contributions from non-CO_2 emissions. For comparison, our estimate of 2025 anthropogenic warming (1.37 °C) and the recent rate of increase (0.27 °C/decade) would suggest that continued emissions at current levels would cause human-induced global warming to reach 1.5°C around the year 2030.

10 Indicators of climate and weather extremes: land average maximum temperatures and number of marine heat waves days

Changes in climate and weather extremes are among the most visible effects of human-induced climate change. Within AR6 WGI, a full chapter was dedicated to the assessment of past and projected changes in extremes on continents (Seneviratne et al., 2021). The AR6 WGI chapter on ocean, cryosphere and sea level changes (Fox-Kemper et al., 2021) also provided assessments on changes in marine heatwaves .

10.1 Land average maximum temperature

The presented climate indicator for changes in temperature extremes consists of land average maximum temperatures for any single day in a year (TXx) (excluding Antarctica). Fig. 11 updates the land mean TXx shown in Forster et al. (2023, 2024, 2025), originally based on Fig. 11.2 from Seneviratne et al. (2021). Three datasets are analyzed: HadEX3 (Dunn et al., 2020), Berkeley Earth Surface Temperature (building off Rohde et al., 2013), and the fifth-generation ECMWF atmospheric reanalysis of the global climate (ERA5; Hersbach et al., 2020). HadEX3 is static and has not received any updates. Berkeley Earth intends to release an extended and updated dataset in May 2026, which we plan to include in the revision of this paper. Currently, Berkeley Earth only extends to 2023 and is the same as in Forster

https://doi.org/10.5194/essd-2026-287
Preprint. Discussion started: 23 April 2026

et al. (2025). Of the three datasets, only ERA5 covers the whole of 2025 at the present time. TXx is calculated by averaging the annual maximum temperature over all available land grid points (excluding Antarctica) and then converted to anomalies with respect to a base period of 1961–1990. To express the TXx as anomalies with respect to 1850–1900, we add an offset of 0.51 °C to all three datasets. See Supplement Sect. S10 for details on the data selection, averaging and offset computation. Note that the updated Berkeley Earth dataset will likely lead to changed TXx and offset estimates.

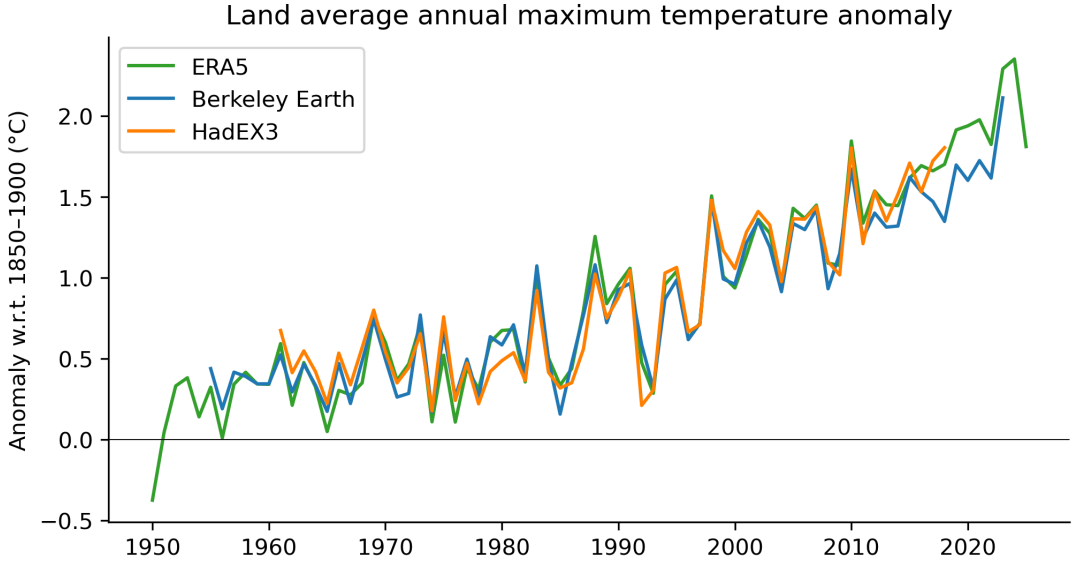

Figure 11 Time series of observed temperature anomalies for land average annual maximum temperature (TXx) for ERA5 (1950–2025), Berkeley Earth (1955–2023) and HadEX3 (1961–2018), with respect to 1850–1900. The datasets have different spatial coverage and are not coverage-matched. All anomalies are calculated relative to 1961–1990, and an offset of 0.51 °C is added to obtain TXx values relative to 1850–1900. Note that while the HadEX3 numbers are the same as shown in Seneviratne et al. (2021) Fig. 11.2, these numbers were not specifically assessed.

Our climate has warmed rapidly in the last few decades (Sect. 7), which also manifests in changes in the occurrence and intensity of climate and weather extremes. From about 1980 onwards, all datasets point to a strong TXx increase, which coincides with the transition from global dimming, associated with aerosol increases, to brightening, associated with aerosol decreases (Wild et al., 2005, Sect. 4). The ERA5 based TXx warming estimate w.r.t. 1850–1900 for 2025 is at 1.81 °C; a decrease of 0.54°C compared to 2024, on par with the anomaly in 2022. On longer time scales, land average TXx has warmed 0.49 °C in the past 10 years (comparing the decades 2016–2025 to 2006–2015) and 1.92 °C with respect to pre-industrial conditions (Table 9). Since the offset relative to our pre-industrial baseline period is calculated over 1961–1990, temperature anomalies align by construction over this period but can diverge afterwards.

https://doi.org/10.5194/essd-2026-287
Preprint. Discussion started: 23 April 2026

Table 9 Anomalies of land average annual maximum temperature (TXx) for recent decades based on HadEX3, Berkeley Earth, and ERA5, with respect to 1850–1900. All anomalies are calculated relative to 1961–1990, and an offset of 0.51 °C is added to obtain TXx values relative to 1850–1900.

	HadEX3	Berkeley Earth	ERA5
2000–2009	1.23	1.18	1.21
2006–2015	1.40	1.34	1.42
2009–2018	1.52	1.41	1.54
2014–2023	-	1.60	1.81
2015–2024	-	-	1.90
2016–2025	-	-	1.92

10.2 Marine heatwave days

We include, for the first time, an updated assessment of global marine heatwaves (MHWs) since AR6. MHWs can have detrimental impacts on marine ecosystems and socio-economic systems (Hughes et al., 2017; Frölicher and Laufkötter 2018; Smale et al., 2019; Smith et al., 2021; Cheung et al., 2021; Smith et al., 2023; Wernberg et al., 2025), influence air-sea carbon exchange (Li et al., 2024; Müller et al., 2025), impact marine biological productivity, acidity and oxygen levels (Le Grix et al., 2021; Burger et al., 2022; Gruber et al., 2021), and influence extreme weather over land (Hu 2021; Berthou et al., 2024).

The SROCC reported with *high confidence* that MHW days approximately doubled between 1982 and 2016 (Collins et al,. 2019; Frölicher et al., 2018). Over the same period, MHW intensity increased by about 0.04 °C per decade and the spatial extent of MHW conditions increased by about 19% per decade (Frölicher et al. 2018). The number of annual MHW days also increased by 54% during 1987–2016 relative to 1925–1954 (Oliver et al., 2018). With further evidence, the AR6 assessed with *high confidence* that MHWs have increased in frequency over the 20th century, with an approximate doubling from 1982 to 2016, and *medium confidence* that they have become more intense and longer since the 1980s (Fox-Kemper et al., 2021).

Based on the AR6 and SROCC approach, MHWs here are defined as days when the deseasonalized SST exceeds the daily 99th percentile within an 11-day moving window relative to a climatological baseline (i.e., 1985-2014) (Fox-Kemper et al., 2021; Collins et al., 2019). We consider MHWs only between 60 ºS and 60 ºN, as their identification in polar regions is more challenging than at lower latitudes due to seasonal-to-interannual variability in sea-ice cover,

https://doi.org/10.5194/essd-2026-287
Preprint. Discussion started: 23 April 2026

which hampers the calculation of consistent climatologies and percentile-based thresholds. Four datasets spanning up to 2025 were analysed: NOAA's Optimum Interpolation SST (OISST; Huang et al., 2021), the Operational SST and Sea Ice Analysis (OSTIA; Donlon et al., 2012), the fifth-generation ECMWF atmospheric reanalysis (ERA5; Hersbach et al., 2020), and NOAA's Coral Reef Watch daily 5km SST product (CRW; Liu et al., 2014). Spatial maps of the number of MHW days from each of these datasets are included in Supplement Fig. S16.

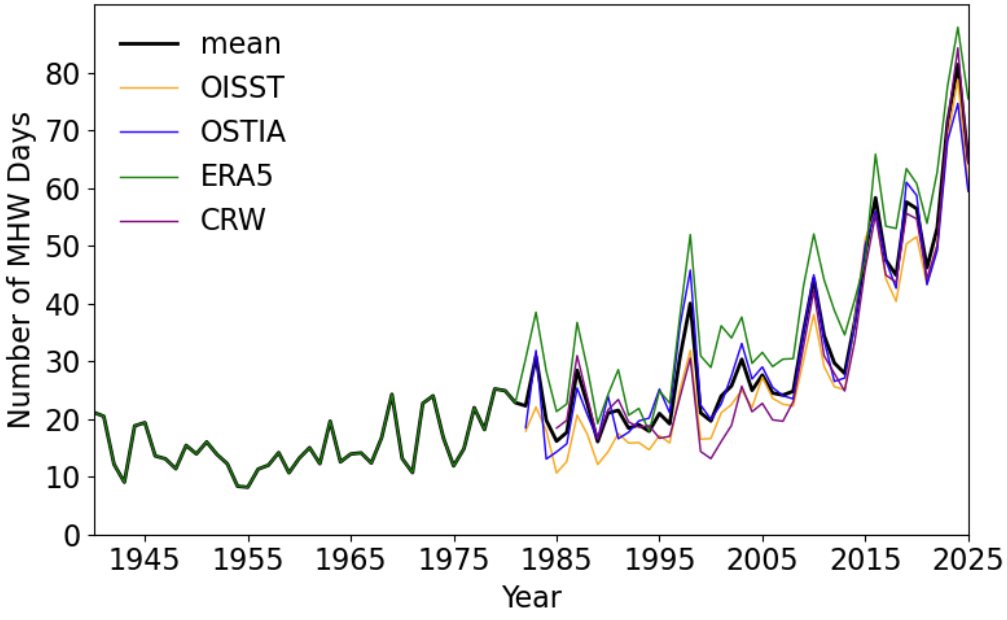

Figure 12 Global mean annual number of marine heatwave (MHW) days from ERA5 (1940-2025), OISST (1982-2025), OSTIA (1982-2025), and CRW (1985-2025), and the mean of these shown in black. MHWs are defined as days exceeding the 99th percentile of deseasonalized SST anomalies, calculated using an 11-day moving window and a 1985-2014 climatology. An offset relative to the 1850-1900 baseline (using ERSST v6 (Huang et al., 2025)) was added to data to scale the results to the preindustrial level (see Supplement Fig. S15).

All four datasets show a consistent and pronounced increase in the number of MHW days beginning in the early 1980s, coincident with strong ocean warming (Figure 12). The satellite-based products (OISST, OSTIA, and CRW) start in the early 1980s, while the reanalysis product ERA5 extends the record back to the 1940s and exhibits similar variability during the pre-satellite era, when the warming trend was smaller. Interannual peaks are evident throughout the record, with several prominent maxima aligning with strong El Niño events (e.g., 1982-83, 1987–88, 1997–98, 2015–16, and 2023–24), which are known to enhance the occurrence of MHWs (Gregory et al., 2024; Holbrook et al., 2020). The upward trend intensifies in the most recent decade, culminating in a maximum mean of 82 MHW days in 2024. The global mean annual numbers of MHWs increased by approximately 60% during the latest decade 2016–

https://doi.org/10.5194/essd-2026-287
Preprint. Discussion started: 23 April 2026

2025 (58 days) compared with the previous decade 2007–2016 (37 days) (Table 10). The global mean annual numbers of MHWs averaged over all four products were 70, 82, and 65 days in 2023, 2024, and 2025, respectively (Supplement Fig. S15).

In summary, evidence accumulated since the AR6 assessment further indicates that MHWs are becoming more frequent, consistent with the ongoing warming of the ocean surface. Compared to the doubling between 1982 and 2016, MHW days more than tripled between 1991 and 2025 (Supplement Table S12).

Table 10 Global mean annual number of MHW days from OISST, OSTIA, ERA5, CRW, and their mean.

	OISST	OSTIA	ERA5	CRW	Mean
2000–2009	23	27	33	21	26
2007-2016	34	36	43	34	36
2010-2019	40	43	49	41	43
2011–2020*	41	44	50	42	44
2012-2021	42	45	51	43	45
2013–2022	45	47	54	45	48
2014–2023	49	51	58	50	52
2015–2024	54	55	63	55	57
2016–2025	54	56	65	57	58

*latest decade for some indicators in AR6

11 Global land precipitation

As one of the large-scale indicators of climate change with great societal relevance, AR6 assessed that global land precipitation has *likely* increased since the middle of the 20th century with a faster increase since the 1980s with large interannual variability and regional heterogeneity (Gulev et al., 2021; Douville et al., 2021). The observed Northern Hemispheric land summer monsoon precipitation experienced a significant decline during 1901-2014, which has been attributed to the dominant influence of anthropogenic aerosols (Cao et al., 2022).

Figure 13 updates annual global land precipitation anomaly relative to 1991–2020 shown in Forster et al. (2025), originally based on Fig.2.15c in AR6 WGI (Gulev et al., 2021). The datasets used are from GPCC V2020 (Schamm et al., 2014), CRU TS 4.09 (Harris et al., 2020), GPCP V.2.3 (Adler et al., 2018), and GHCN V4 (Menne et al., 2018) observed datasets. There is little consistency among datasets due to differences in input data, completeness of records, periods covered, and the gridding procedures applied (Sun et al., 2018; Nogueira, 2020; Yate and Ren, 2025). Su et

https://doi.org/10.5194/essd-2026-287
Preprint. Discussion started: 23 April 2026

al. (2026) highlighted important gaps in global precipitation monitoring, indicating that only 13.4% of the global land surface meets the World Meteorological Organization requirements for annual precipitation monitoring at present.

While the globally averaged land surface specific humidity has continuously increased (Dunn et al., 2024), global land precipitation has exhibited considerable interannual to interdecadal variability (Fig. 13). Zhang et al. (2024b) suggested that precipitation variability over 75% of land area has already increased over the past century, driven mainly by anthropogenic warming-induced atmospheric moistening. In 2025, all datasets show a larger positive anomaly in global land precipitation than in 2024. Enhanced rainfall is observed over Asia and the Maritime Continent, likely linked to La Niña conditions, as well as over Siberia and southern Africa. The pronounced rainfall deficit over central South America during 2023–2024 was markedly reduced in 2025. In contrast, wet conditions have persisted over the Arctic and much of the Siberian region from 2023 to 2025 (Supplement Fig. S17).

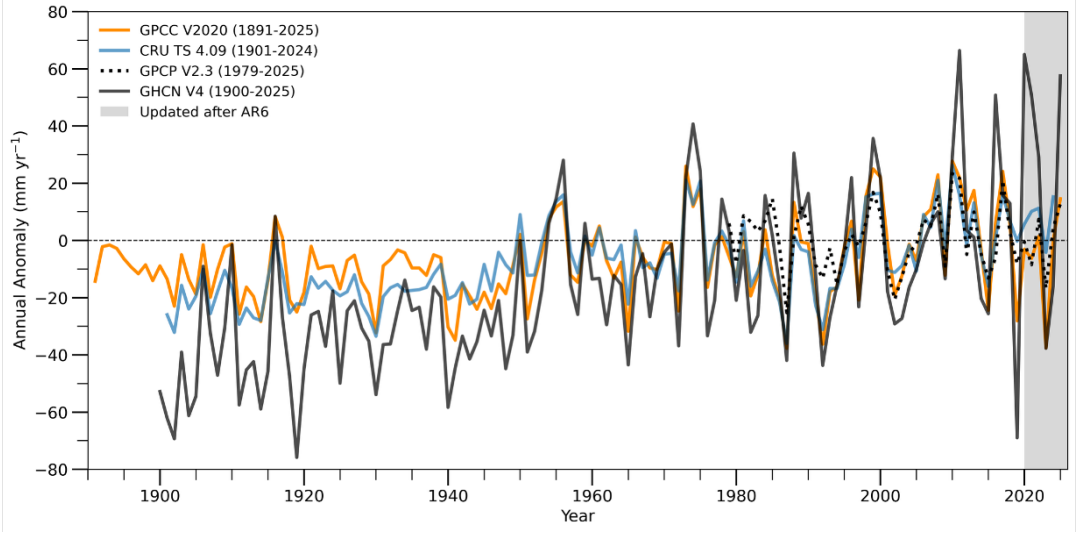

Figure 13 Time series of annual global land precipitation (mm yr^{-1}) from 1891 to date relative to a 1991-2020 climatology obtained from GPCP V2020, CRU TS 4.09, GPCP V2.3, and GHCN V4 (note that different products commence at distinct times). Annual global land precipitation for each observed data is estimated following the AR6 method except the period of climatology and updated from 2020 to 2025. In AR6, the reference period of the climatology was from 1981 to 2010.

https://doi.org/10.5194/essd-2026-287
Preprint. Discussion started: 23 April 2026

12 Global mean sea-level rise

Global mean sea-level (GMSL) rise is primarily driven by: (i) thermal expansion as the ocean warms; and (ii) increases in ocean mass associated with the addition of water or ice from land-based reservoirs, including glaciers and ice sheets (Fox-Kemper et al., 2021). Most of these processes are directly linked to changes in the global Earth energy inventory (Sect. 6). Sea-level rise can have large consequences for coastal ecosystems, safety and management, as it increases the baseline for sea-level extremes arising from short-term phenomena such as storm surges, waves and tides.

The observed total GMSL change was assessed in AR6 WG1, in Chapter 2 (their Section 2.3.3.3, Gulev et al., 2021) and Chapter 9 (their Section 9.6.1 and Cross-Chapter Box 9.1, Fox-Kemper et al., 2021) on the basis of tide gauge reconstructions (up to 1993) and satellite altimeter observations (1993-2018). AR6 concluded that GMSL increased by 0.20 [0.15 to 0.25] m over the period 1901 to 2018, with a rate of 1.73 [1.28 to 2.17] mm yr^{-1} (*high confidence*). Periods closer to the present showed an accelerating GMSL, with a rate of 2.3 [1.6 to 3.1] mm yr^{-1} over the period 1971–2018 increasing to 3.7 [3.2 to 4.2] mm yr^{-1} over the period 2006–2018 (*high confidence*).

Forster et al. (2025) included an extension of the AR6 GMSL time series from 2019 up to the end of 2024 using three out of the six satellite data products from the WCRP estimate used in AR6: NASA (2025), NOAA (2025) and AVISO (2025). This year, we update the GMSL time series to the end of 2025, and replace the entire satellite part of the GMSL time series (from 1993 onwards) using three satellite products that have been updated at the time of writing: AVISO (downloaded 11/02/2026), NASA (downloaded 11/03/2026) and the University of Colorado (downloaded 13/02/2026). By updating the entire satellite altimetry period there is consistency across the altimetry record for the type of corrections that are performed, and this approach ensures that the satellite record represents the state-of-the-art. We use the global mean time series based on the reference missions, with seasonal signals removed and corrected for glacial isostatic adjustment. We first compute annual averages and then an ensemble average time series, which is spliced to the AR6 GMSL TG record ending in 1993. For comparison to the AR6 tide gauge ensemble, we show three new tide gauge reconstructions over the 20th century in Fig.14: Dangendorf et al., 2024, Wang et al., 2024 and Mu et al., 2025.

Over the period 1901 to 2025, we find that GMSL has increased by 229.6 [178.6 to 280.6] mm, with an average rate of 1.85 [1.44 to 2.26] mm yr^{-1} (Table 11, Fig. 14). For the post-AR6 period (2018-2025), the observed rise is 26.9 [21.1 to 32.7] mm with an average rate of 3.84 [3.01 to 4.67] mm yr^{-1}. Compared to Forster et al. (2025), the different satellite ensemble (replacing NOAA by University of Colorado) results in an addition of 0.3 mm to the estimates over 2018-2024. Variations in the year-to-year changes occur throughout the GMSL time series as a result of internal climate variability (Figure 13a). In this case, the small GMSL change of 0.4 mm from 2024 to 2025 has been attributed to last years' transition from El Niño to weak La Niña conditions which affected precipitation patterns (WMO, 2026). To reduce the impact of year-to-year variations on the climatic signal, sea-level trends are typically computed over

https://doi.org/10.5194/essd-2026-287
Preprint. Discussion started: 23 April 2026

longer (at least decadal) periods (Fig. 14b, Table 11). When comparing 20-year averaged rates, GMSL has accelerated from 1.69 ± 1.81 mm yr^{-1} in 1976-1995 to 3.37 ± 2.19 mm/yr in 1996-2015 and to 3.67 ± 2.47 mm/yr in 2006-2025 (Fig. 14b). This finding is in line with the assessments of AR6 (Fox-Kemper et al., 2021), SROCC (Oppenheimer et al., 2019) and AR5 (Church et al., 2013) that sea-level change has been accelerating over the course of the 20th and early 21st centuries, and consistent with the observed acceleration in some components of the Earth heat inventory (see Sect. 6).

Table 11 Observed global mean sea-level rise (GMSLR), comparing the extended time series in this study to IPCC AR6 (Table 9.5, Fox-Kemper et al., 2021) and to Forster et al., 2025. Values are expressed as the total change (Δ) in the annual mean over each period (mm) along with the equivalent rate calculated as the total change divided by the number of years (mm yr^{-1}). Uncertainties represent the *very likely* range.

Observed GMSLR		IPCC AR6	Forster et al (2025)	This study
Start year		**End year 2018**	**End year 2024**	**End year 2025**
1901	Δ(mm)	201.9 [150.3 to 253.5]	228.0 [176.4 to 279.6]	229.6 [178.6 to 280.6]
	mm yr^{-1}	1.73 [1.28 to 2.17]	1.85 [1.43 to 2.27]	1.85 [1.44 to 2.26]
1971	Δ(mm)	109.6 [72.8 to 146.4]	135.8 [99.0 to 172.5]	137.3 [101.4 to 173.3]
	mm yr^{-1}	2.33 [1.55 to 3.12]	2.56 [1.87 to 3.26]	2.54 [1.88 to 3.21]
1993	Δ(mm)	81.2 [72.1 to 90.2]	107.3 [98.2 to 116.4]	108.9 [104.5 to 113.3]
	mm yr^{-1}	3.25 [2.88 to 3.61]	3.46 [3.17 to 3.75]	3.40 [3.26 to 3.54]
2006	Δ(mm)	44.3 [38.6 to 50.0]	70.4 [64.7 to 76.1]	69.7 [65.0 to 74.4]
	mm yr^{-1}	3.69 [3.21 to 4.17]	3.91 [3.59 to 4.23]	3.66 [3.42 to 3.92]

https://doi.org/10.5194/essd-2026-287
Preprint. Discussion started: 23 April 2026

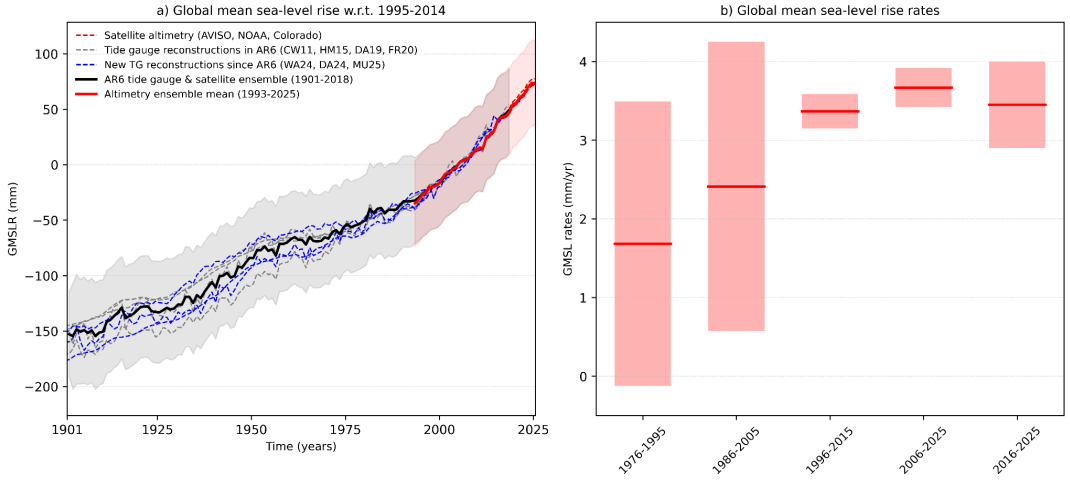

Figure 14 (a) Global mean sea-level rise time series 1901-2025 (mm) w.r.t. 1995-2014. The GMSLR ensemble from AR6 in black; the updated satellite altimetry ensemble in red. Uncertainties represent the 1 sigma range, computed relative to 1901, including estimates of both structural uncertainty and parametric uncertainty (Palmer et al., 2021). Individual time series shown with dashed lines, with reconstructions available for AR6 in grey (Church and White, 2011; Hay et al., 2015; Dangendorf et al., 2019; Frederikse et al., 2020) and new reconstructions in blue (Dangendorf et al., 2024; Wang et al., 2024; Mu et al., 2025). (b) Global mean sea-level rates (mm yr-1) for four successive overlapping 20-year periods and the most recent decade, uncertainties indicating the *very likely* range.

13 Code, data availability and visualisations

IGCC will deliver an operational, annually updated suite of Indicators of Global Climate Change through the Copernicus Climate Data Store (CDS), accompanied by communication and outreach platforms that provide timely, trusted and readily accessible evidence for consumers of climate data.

A main feature will be a new data dashboard, currently in development, designed for broad accessibility, and leveraging the software tools and infrastructure of the CDS to facilitate access to the indicators by a less technical audience. This will ensure that IGCC, and the scientific evidence that it provides, is associated with an established and robust service and that it can reach a wider range of users with free, open-access climate data and tools.

Working within the Copernicus Climate Change Service (C3S) ecosystem, including via the CDS, we aim to consolidate the position of IGCC as a trusted source of authoritative climate information, strengthen its contribution to international policy and assessment processes, and facilitate ways to reach a far wider audience than IGCC can achieve working alone. This includes but is not limited to policymakers involved in UNFCCC negotiations, and decision makers working in climate change mitigation and adaptation.

https://doi.org/10.5194/essd-2026-287
Preprint. Discussion started: 23 April 2026

The carbon budget calculation is available from https://github.com/Rlamboll/AR6CarbonBudgetCalc/tree/RCB2025-v1 (Lamboll and Rogelj, 2026). The code and data used to produce other indicators are available in repositories under https://github.com/ClimateIndicator/data/tree/v2026.04.14 (Smith et al., 2026b). All data are available from https://doi.org/10.5281/ZENODO.7883757 (Smith et al., 2026a). Data are provided under the CC-BY 4.0 License.

HadEX3 [3.0.4] data were obtained from https://catalogue.ceda.ac.uk/uuid/115d5e4ebf7148ec941423ec86fa9f26 (Dunn et al., 2023) on 5 April 2023 and are © British Crown Copyright, Met Office, 2022, provided under an Open Government Licence; http://www.nationalarchives.gov.uk/doc/open-government-licence/version/2/ (last access: 2 June 2023).

Table 12 lists the main global observational and inventory datasets used to produce the indicators.

Table 12 Observations and datasets utilised in producing this year's key indicators of global climate change

Indicator	Section	Key observations and datasets utilised
Greenhouse gas emissions	2	GCB, EDGAR, PRIMAP Hist-CR v2.7, JRC-NGHGI v2024, GFED v4s
Well-mixed greenhouse gas concentrations	3	NOAA GML, AGAGE
Non-methane short-lived climate forcers	4	CEDS, CAMS, GFED
Effective radiative forcing (natural forcing)	5	GloSSAC, OMPS LP
Earth Energy Imbalance	6	IAP, EN4, JMA, NCEI, NOC-CSIRO-WHOI-IIT, GCOS EHI, CERES
Observed surface temperature change	7	HadCRUT5, NOAA GlobalTemp, Kadow, Berkeley Earth, China-MST
Human contribution to surface temperature change	8	HadCRUT5, NOAA GlobalTemp, Kadow, Berkeley Earth, China-MST, Radiative Forcing data, CMIP6 climate models
Land average maximum temperatures	10	HadEX3, Berkeley Earth, ERA5
Marine heatwave days	10	NOAA OISST, ERA5, OSTIA, NOAA CRW, ERSST v6
Global land precipitation	11	GPCC, CRU TS, GPCP, GHCN
Global mean sea level rise	12	AR6 GMSLR time series (tide gauge and satellite altimetry - AVISO/CNES, CSIRO, NASA/GSFC, NOAA, SL_cci/ESA and University of Colorado)

https://doi.org/10.5194/essd-2026-287
Preprint. Discussion started: 23 April 2026

14 Discussion and conclusions

The fourth year of the Indicators of Global Climate Change (IGCC) initiative has built on previous years' efforts to provide a comprehensive update of the climate change indicators required to estimate the human-induced warming and the remaining carbon budget. Table 13 and Fig. 15 present a summary of the headline indicators from each section compared to those given in the AR6 assessment. Table 13 also summarises methodological updates.

Table 13 Summary of headline results and methodological updates from the Indicators of Global Climate Change (IGCC) initiative.

Climate Indicator	AR6 2021 assessment	This 2025 assessment	Explanation of changes	Methodological updates since AR6
GHG emissions **AR6 WGIII Chapter 2: Dhakal et al. (2022); see also Minx et al. (2021)**	**2010-2019 average:** **55.9 ± 6 $GtCO_2e$**	**2010-2019 average:** **53.5±5.8 $GtCO_2e$** **2015-2024 average:** **54.6±5.5 $GtCO_2e$**	**GHG emissions have continued to increase due to the use of fossil fuels, industrial processes, agriculture, land use change (including deforestation) and waste.**	**CO_2-LULUCF emissions now based on bookkeeping models that consider transient carbon densities (see Supplement). Revisions in non-CO2 GHG emissions data to make use of updated activity data and emissions factors since AR6. CO_2 GCB Fossil Fuel and Industry emissions used instead of EDGAR. These changes reduce estimates by around 2 $GtCO_2e$ (Sect. 2).**
GHG concentrations **AR6 WGI Chapter 2: Gulev et al. (2021)**	**2019:** **CO_2, 410.1 [± 0.36] ppm** **CH_4, 1866.3 [± 3.2] ppb** **N_2O, 332.1 [± 0.7] ppb**	**2025:** **CO_2, 425.6 [±0.4] ppm** **CH_4, 1935.9 [±3.3] ppb** **N_2O, 339.4 [±0.4] ppb**	**Increases caused by continued GHG anthropogenic emissions**	**Updates based on NOAA data and AGAGE (Sect. 3)**

https://doi.org/10.5194/essd-2026-287
Preprint. Discussion started: 23 April 2026

SLCF			**Increase in CH_4 concentration (SLCF and ozone precursor Increase in global NH_3 emissions Decrease in SO_2, NOx, CO, black carbon global emissions Weak positive increase in NMVOC and organic carbon emissions**	
Effective radiative forcing change since 1750 **AR6 WGI Chapter 7: Forster et al. (2021)**	**2019:** **2.72 [1.96 to 3.48] W m^{-2}**	**2025:** **3.10 [2.35 to 3.83] W m^{-2}**	**Trend since 2019 is caused by increases in GHG concentrations and reductions in aerosol precursors.**	**Follows AR6 with minor update to aerosol precursor treatment and emissions dataset that revises 2019 ERF estimate relative to 1750 downwards (more negative) by 0.09 W m^{-2}. Added this year is a new method to estimate the ERF from land use surface reflection and irrigation to avoid scaling with cumulative emissions. This does not materially affect the ERF. (Sect. 5)**
Earth's energy imbalance **AR6 WGI Chapter 7: Forster et al. (2021)**	**2006-2018 average:** **0.79 [0.52 to 1.06] W m^{-2}**	**2013-2025 average:** **1.12 [0.78 to 1.46] W m^{-2}**	**A 40% increase in energy imbalance estimated based on increased rate of heat uptake by the climate system.**	**Ocean heat content timeseries updated for 1971 to 2025 using all of the five AR6 datasets. Other heat inventory terms updated following von Schuckmann et al. (2023a) for 1971 to 2020. Ocean heat content uncertainty is used as a proxy for total uncertainty. Further details in Sect. 6.**
Global mean surface temperature change since 1850-1900 **AR6 WGI Chapter 2: Gulev et al. (2021)**	**2011-2020 average:** **1.09 [0.95 to 1.20] °C**	**2016-2025 average:** **1.26 [1.13 to 1.36] °C**	**An increase of 0.17 °C within five years, indicating a high decadal rate of change which may in part be internal variability.**	**Methods match four datasets used in AR6. Individual datasets have updated historical data, but these changes are not materially affecting results. (Sect. 7).**

https://doi.org/10.5194/essd-2026-287
Preprint. Discussion started: 23 April 2026

Human-induced global warming since preindustrial **AR6 WGI Chapter 3: Eyring et al. (2021)** **SR1.5 Chapter 1: Allen et al., (2018)**	**2010-2019 decade average:** **1.07 [0.8 to 1.3] °C** **2017 single year: 1.0 [0.8 to 1.2] °C**	**2016-2025 decade average:** **1.24 [1.0 to 1.5] °C** **2025 single year: 1.37 [1.1 to 1.7] °C**	**The forced change from 2024 to 2025 in this year's assessment increased in line with the rate of human-induced warming, but the increase relative to last year's assessment is slightly smaller, in part due to a small downward revision of historical temperatures in a new dataset version this year.**	**The three methods for the basis of the AR6 assessment are retained, but each has new input data (Sect. 8)**
Remaining carbon budget for 50% likelihood of limiting global warming to 1.5 °C **AR6 WGI Chapter 5: Canadell et al. (2021)**	**From the start of 2020:** **500 $GtCO_2$**	**From the start of 2026:** **130 $GtCO_2$**	**The 1.5 °C budget is roughly the same as last year. The RCB can exhaust before the 1.5 °C threshold is reached due to having to allow for future non-CO_2 warming.**	**Emulator and scenario change has reduced budget since 2020 by 100 $GtCO_2$ (Sect. 9)**
Land average maximum temperature change compared to pre-industrial. **AR6 WGI Chapter 11: Seneviratne et al., (2021)**	**2009-2018 average:** **1.55 °C**	**2016-2025 average:** **1.92 °C**	**Rising at a substantially faster rate compared to global mean surface temperature**	**HadEX3 data used in AR6 replaced with ERA reanalysis data employed in this report which is more updatable going forward. Adds 0.01 °C to estimate (Sect. 10.1)**
Number of marine heatwave days **AR6 WGI Chapter 9: Fox-Kemper et al. (2021)**	**2007-2016 average:** **16 days**	**2016-2025 average:** **58 days**	**Approximate doubling from 1982 to 2016 can be compared to a more than tripling (3.3) from 1991 to 2025**	**First year with update. The NOAA OISST dataset used in AR6 has been extended and three new datasets added (Sect. 10.2)**

https://doi.org/10.5194/essd-2026-287
Preprint. Discussion started: 23 April 2026

Global land precipitation compared to preindustrial **AR6 WGI Chapter 8: Douville et al. (2021)**	**Likely increased since the middle of the 20th century with a faster increase since the 1980s with large interannual variability**	**Large interannual variability associated with El Niño dominates the record in recent years, making long-term trend less clear**	**2025 exhibited a positive anomaly relative to preindustrial due to La Niña conditions**	**The four datasets used in AR6 have been extended (Sect. 11)**
Global mean sea-level rise since 1901 **AR6 WGI Chapters 2 and 9: Gulev et al., (2021); Fox-Kemper et al., (2021)**	**1901 to 2018 change** **201.9 [150.3 to 253.5] mm** **at a rate of** **1.73 [1.28 to 2.17] mm yr^{-1}**	**1901 to 2025 change** **229.6 [178.6 to 280.6] mm** **at a rate of** **1.85 [1.44 to 2.26] mm yr^{-1}**	**Sea-level rise continues to accelerate.**	**AR6 data extended with three of the six datasets from AR6, using latest satellite data (Sect. 12).**

1152

https://doi.org/10.5194/essd-2026-287
Preprint. Discussion started: 23 April 2026

Open Access Earth System Science Data Discussions

1153

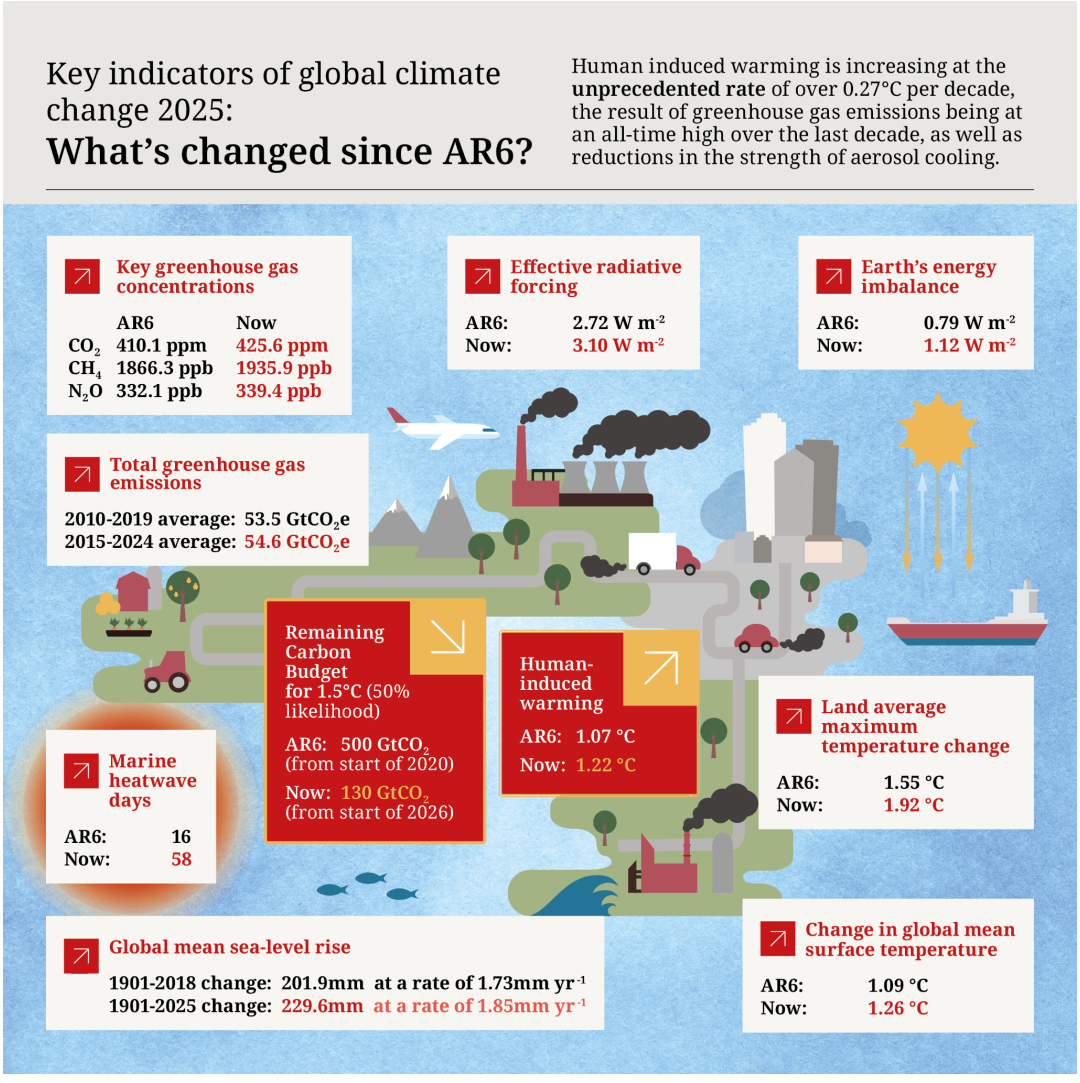

1154

1155 **Figure 15 Infographic for the best estimate of headline indicators assessed in this paper.**

1156 In spite of the increasing deployment of renewable energy, GHG emissions are at an all-time high, reaching
1157 56.8±5.5 $GtCO_2e$ in 2024 (Sect. 2). However, these emissions are no longer rapidly increasing, leading to a steady rise
1158 in the atmospheric concentrations of the major greenhouse gases (Sect. 3). This, combined with a reduction in aerosol
1159 cooling (Sect. 4), has caused a 0.25 Wm^{-2} (10%) increase in the level of radiative forcing since AR6 (Sect. 5, Table
1160 13). This increase in forcing would be expected to increase the Earth's Energy Imbalance (EEI) (Sect. 6). Theory and

https://doi.org/10.5194/essd-2026-287
Preprint. Discussion started: 23 April 2026

physical laws would suggest that as the Earth's temperature has warmed in response to the forcing, the increase in EEI should be less than the increase in radiative forcing. However, the best estimate of the EEI trend is slightly larger: 0.33 [0.0 to 0.65] Wm^{-2}, assuming standard errors. Reasons for this higher than expected trend (a 40% increase in EEI since AR6) is an area of very active research and observational errors, an underestimate of the positive aerosol forcing trend, a higher than expected climate sensitivity or cloud regime changes are all under investigation (Sect. 6).

Although reasons for the magnitude of EEI trend are unexplained, a positive trend is expected and clear signs of accelerated planetary warming, comparing the previous decades with earlier decades. Trends in other indicators from sea-level (Sect. 12) rise and temperature extremes (Sect. 11) support evidence of this acceleration. Marine heatwave days, a new indicator for this update, has tripled since 1991 (Sect. 11.2, Table 13). The pace of human-induced warming remains at its all-time high in the instrumental record (Sect. 8).

Generally, scientists and scientific organisations have an important role as "watchdogs" to critically inform evidence-based decision-making. This annual update and the complimentary updates of the State of the Climate (BAMS) and State of Global Climate (WMO) report critically depend on continued support for high quality global monitoring networks of climate data, and also on open data sources that are regularly updated and easily accessed. In total, we employ analysis from over 40 global datasets (Table 12). These data are increasingly threatened by funding choices and geopolitical decisions. Several envisaged satellite programs are threatened including key U.S missions, and the ESA TRUTHS mission which would have provided an absolutely calibrated mission for key radiances supporting the construction of many climate datasets was recently cancelled. In-situ programs in many countries have diminished, particularly weather balloon data, and much of the ocean observing system relies upon project funding which is highly insecure, imperilling our ability to monitor and understand key diagnostics including EEI. The preservation of historical holdings is also under threat with many data centres being cut either partially or fully. Yet these data are a common good - the cornerstone not just of today's science to advance understanding and inform society but the science that will be undertaken by future generations who need access to the original observational records. The Global Climate Observing System (GCOS) program which directly supports much of our international capability is also under threat. The World Climate Research Programme (WCRP) has also seen its funding approximately halved. The GCOS program is in the process of preparing a report assessing the adequacy of the observing system for climate- that will be delivered in early 2027. The panels have completed initial assessments per Essential Climate Variable (ECVs) which highlight a system under considerable strain. For almost all ECVs at least some components are under threat and for some ECVs they are prone to a single point of failure and / or funding is not secure in the short term (Table 14).

Table 14 Initial expert assessment of the stability of Essential Climate Variables (ECVs) undertaken by the GCOS panels and invited experts. The first column denotes the 55 ECVs, differentiated by domain. The second column considers whether the ECV as a whole is prone to a single point of failure (green=no; yellow=significant component; red= entire ECV). The

https://doi.org/10.5194/essd-2026-287
Preprint. Discussion started: 23 April 2026

third column denotes funding stability foreseen over the next 5 years (green=stable; yellow=concern; red=not secured). The fourth column denotes funding stability compared to 2022 (white=no change; green=better; yellow=slightly degraded; red=worse). The final column considers specific components of the observing system under threat (green=none identified; yellow=important component under threat; red=critical components under threat which will substantively harm our ability to monitor the ECV globally).

https://doi.org/10.5194/essd-2026-287
Preprint. Discussion started: 23 April 2026

Open Access Earth System Science Data Discussions

Essential Climate Variable (ECV)	Single Point of Failure	Funding stability for next 5years	Funding stability vs. 2022	Components under threat
ATMOSPHERE				
Surface pressure				Marine networks
Surface temperature				Marine networks
Surface humidity				Marine networks
Surface winds				Marine networks/scatterometer
Precipitation				Satellite/volunteer rainfall networks
Surface radiation budget		Uncertain regionally		BSRN in the SH, Arctic
Earth Radiation budget	Single agency and single satellite (CERES) in orbit			US observing programme
Clouds				
Lightning				Satellite mission cancelled or uncertain
UA Temperature				Radiosondes
UA humidity				Radiosondes; Limb soundeRadiosondes (humidity UTLS)
UA winds				Radiosondes
Ozone		Uncertain for some comp.		Sondes; Limb sounders, Brewers, Dobsons
Aerosols			Regionally dependent	Limb sounders
GHGs	Calibration standards		Uncertainty in the continuity of key records.	Calibration
Precursors		Similar issues to GHG		Limb sounders
OCEAN				
Sea subsurface temperature	Very dependent on one country			Decrease in observations for in situ networks (e.g. research cruises, moorings, gliders)

https://doi.org/10.5194/essd-2026-287
Preprint. Discussion started: 23 April 2026

Sea subsurface salinity	Very dependent on one country			Decrease in observations for in situ networks (e.g. research cruises, moorings, gliders)
Surface salinity				Lower resolution in the satellite mission
Surface temperature				Decrease in observations for in situ networks (e.g. research cruises, moorings, gliders)
Subsurface current				Tropical moorings arrays very affected
Surface current				New satellite mission not funded
Sea state				Tropical moorings, drifting moorings
Sea level				Tropical mooring arrays very affected
Wind stress				Decrease in observations for in situ networks (in particular ship observations)
Ocean heat flux				Decrease in observations for in situ networks (moorings, ships)
Sea Ice				Cuts in several satellite missions
Biogeochemistry	BGC Argo improves O_2 but rest of BGC ECVs are worse			Research cruises, decreased support
Biology/Ecology	*missing info*			
TERRESTRIAL				
Evaporation from land				In-situ networks (representativeness)
Groundwater		Funding uncertainty		Satellite (same as TWS)
Lakes				In-situ networks coordination
Rivers				Data sharing at national level
Soil Moisture				
Terrestrial Water Storage	Single satellite in orbit			Satellite satellite in orbitfailure
Glaciers				In-situ (partially depending on US)
Ice Sheets and Ice Shelves				RS (ASTER and MODIS sensors)
Permafrost				In-situ monitoring in the Artic
Snow				RS and in-situ (both partially)
Albedo				RS and in-situ (both partially)
FAPAR				in-situ (partially)

https://doi.org/10.5194/essd-2026-287
Preprint. Discussion started: 23 April 2026

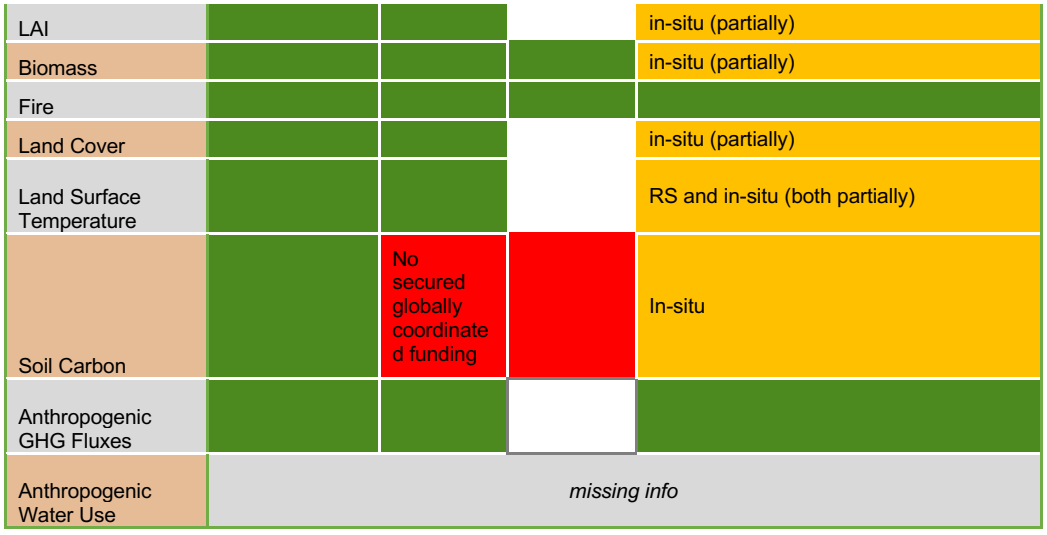

1201

1202

1203 Table 14 provides an initial assessment of the funding stability for monitoring Essential Climate Variables (ECVs)
1204 and components of the observing system under threat. The assessment was undertaken by the GCOS panels and invited
1205 experts at a joint panel meeting in Harwell, UK in February 2026 (see Supplement Table S13). The initial analysis, to
1206 be finalised in a status report to be delivered to the UNFCCC highlights the precarity of many components including
1207 in several components that underpin the monitoring reported in the main analysis sections in this paper.

1208 **Supplement**

1209 The supplement related to this article is available online.

1210 **Author contributions**

1211 PMF, CS, MA, PF, JR and AP developed the concept of an annual update in discussions with the wider IPCC
1212 community over many years. CS led the work of the data repositories with contributions from PM, DH and MZ. VMD,
1213 PZ, SS, CS, SIS, AP, NPG, GPP, BT, MDP, KvS, JR, PF, MA,, XZ, RB, , CC, SB and PT provided important IPCC
1214 and UNFCCC framing. PMF, CS and TW coordinated the production of the manuscript with support from DR and
1215 HC. WFL led Sect. 2 with contributions from PF, GPP, JP and RA. CS led Sect. 3 with inputs from JM, PK, LW,
1216 PMF, MK, XL and MR. SS led Sect. 4 with inputs from CS, SJS, GT, JZ, XYZ and GvdW. CS led Sect. 5 with
1217 contributions from CW, TG, SS, JFL, RMH, SJS, GT, JZ, XYZ, and GvdW. KvS and MDP led Sect. 6 with
1218 contributions from CA, LC, MI,, REK, ABS, CMD, DPM, AL and SEW. BT, CC and ZH led Sect. 7 with contributions

https://doi.org/10.5194/essd-2026-287
Preprint. Discussion started: 23 April 2026

from PT, CM, CK, JK, RB, RR, AL and LC. TW led Sect. 8 with contributions and calculations from AR, CK, NPG, RB, SJ, CS and MA. RL led Sect. 9 with contributions from JR, PF and HDM. Sect. 10 was led by MH, with contributions from SIS, XZ, CHG, TLF, JYL, AK, and VMD. JYL and JEY led Sect. 11 with contributions from KR, VMD, PT, and KvS. AS led Sect. 12 with contributions from MDP, AL, CA, ABS, SEW and CMD. PMF led Sect. 13 with contributions from DR. PMF led Sect. 14 with contributions from AB, CT and BMM. All authors either edited or commented on the manuscript. DR and TW coordinated the data visualisation effort.

Competing interests

The contact author has declared that none of the authors has any competing interests.

Disclaimer

Publisher's note: Copernicus Publications remains neutral with regard to jurisdictional claims in published maps and institutional affiliations.

Acknowledgements

The University of Leeds has been contracted by ECMWF to coordinate the production of these indicators and provide them to Copernicus. Copernicus is the Earth observation component of the European Union's space programme. The European Centre for Medium-Range Weather Forecasts (ECMWF) has been appointed by the European Commission with funding from the EU to operate the Copernicus Atmosphere Monitoring Service and the Copernicus Climate Change Service on its behalf. This research has been supported by the European Union's Horizon Europe research and innovation programme under Grant Agreement Nos. 820829, 101081395, 101081661, 101137656 and 821003, the H2020 European Research Council (grant no. 951542), the Natural Environment Research Council (NE/X00452X/1) and the Engineering and Physical Research Council (EP/V000772/1). Matthew Palmer, Colin Morice, Rachel Killick and Richard Betts were supported by the Met Office Hadley Centre Climate Programme funded by DSIT. Peter Thorne was supported by Co-Centre award number 22/CC/11103. The Co-Centre award is managed by Research Ireland Northern Ireland's Department of Agriculture, Environment and Rural Affairs (DAERA) and UK Research and Innovation (UKRI), and supported via UK's International Science Partnerships Fund (ISPF), and the Irish Government's Shared Island initiative. Analyses and visualizations for concentrations of short-lived climate forcers used in this paper were produced with the Giovanni online data system, developed and maintained by the NASA GES DISC (as available in March 2026). June-Yi Lee, Jeongeun Yun, and Alexia Karwat were supported by the National Research Foundation of Korea (NRF) grant funded by the Korea government (MSIT) (No. RS-2024-00416848). Aimée Slangen was supported by the research programme ENW-Vidi (DARSea, project number VI.Vidi.2023.058)

https://doi.org/10.5194/essd-2026-287
Preprint. Discussion started: 23 April 2026

1249 funded by the Dutch Research Council (NWO). We thank Xin Lan for assistance with compiling the GHG
1250 concentration data.

1251 **References**

1252 Acker, J. G. and Leptoukh, G.: Online analysis enhances use of NASA Earth science data, EoS Transactions, 88, 14–
1253 17, https://doi.org/10.1029/2007EO020003, 2007.
1254 Adler, R. F. and Gu, G.: Global precipitation for the year 2023 and how it relates to longer term variations and trends,
1255 Atmosphere, 15, 535, 2024.

1256 Adler, R. F., Sapiano, M. R. P., Huffman, J., Wang, J.-J., Gu G., Bolvin, D., Chiu, L., Schneider, U., Becker, A.,
1257 Nelkin, E., Xie, P., Ferrarok R., and Shin, D.-B.: The global precipitation climatology project (GPCP) monthly
1258 analysis (new version 2.3) and a review of 2017 global precipitation. Atmosphere, 9, 138,
1259 https://doi.org/10.3390/atmos9040138, 2018.

1260 Allan ,R.P. and Merchant, C.J.: Reconciling Earth's growing energy imbalance with ocean warming, Environ. Res.
1261 Lett, 20 04402, https://doi.org/10.1088/1748-9326/adb448, 2025.

1262 Allen, M. R., O. P. Dube, W. Solecki, F. Aragón-Durand, W. Cramer, S. Humphreys, M. Kainuma, J. Kala, N.
1263 Mahowald, Y. Mulugetta, R. Perez, M. Wairiu, and K. Zickfeld, 2018: Framing and Context. In: Global Warming of
1264 1.5°C. An IPCC Special Report on the impacts of global warming of 1.5°C above pre-industrial levels and related
1265 global greenhouse gas emission pathways, in the context of strengthening the global response to the threat of climate
1266 change, sustainable development, and efforts to eradicate poverty [Masson-Delmotte, V., P. Zhai, H.-O. Pörtner, D.
1267 Roberts, J. Skea, P.R. Shukla, A. Pirani, W. Moufouma-Okia, C. Péan, R. Pidcock, S. Connors, J.B.R. Matthews, Y.
1268 Chen, X. Zhou, M.I. Gomis, E. Lonnoy, T. Maycock, M. Tignor, and T. Waterfield (eds.)], Cambridge University
1269 Press, Cambridge, UK and New York, NY, USA, 49-92, https://doi.org/10.1017/9781009157940.003, 2018.

1270 Allen, M. R., Frame, D. J., Friedlingstein, P., Gillett, N. P., Grassi, G., Gregory, J. M., Hare, W., House, J.,
1271 Huntingford, C., Jenkins, S., Jones, C. D., Knutti, R., Lowe, J. A., Matthews, H. D., Meinshausen, M., Meinshausen,
1272 N., Peters, G. P., Plattner, G.-K., Raper, S., Rogelj, J., Stott, P. A., Solomon, S., Stocker, T. F., Weaver, A. J., and
1273 Zickfeld, K.: Geological Net Zero and the need for disaggregated accounting for carbon sinks, Nature, 638, 343–350,
1274 https://doi.org/10.1038/s41586-024-08326-8, 2025.
1275 Allison, L. C., Palmer, M. D., Allan, R. P., Hermanson, L., Liu, C., and Smith, D. M.: Observations of planetary
1276 heating since the 1980s from multiple independent datasets, Environ. Res. Commun., 2, 101001,
1277 https://doi.org/10.1088/2515-7620/abbb39, 2020.

1278 AVISO: Mean sea-level product, https://www.aviso.altimetry.fr/en/data/products/ocean-indicators-products/mean-
1279 sea-level/data-acces.html, [data set], accessed 19 February 2025, 2025.
1280 Barnes, C., Boulanger, Y., Keeping, T., Gachon, P., Gillett, N., Haas, O., Wang, X., Roberge, F., Kew, S., Heinrich,
1281 D., Singh, R., Vahlberg, M., Van Aalst, M., Otto, F., Kimutai, J., Boucher, J., Kasoar, M., Zachariah, M., and Krikken,

https://doi.org/10.5194/essd-2026-287
Preprint. Discussion started: 23 April 2026

1282 F.: Climate change more than doubled the likelihood of extreme fire weather conditions in Eastern Canada, Imperial
1283 College London, https://doi.org/10.25561/105981, 2023.
1284 Basu, S., Lan, X., Dlugokencky, E., Michel, S., Schwietzke, S., Miller, J. B., Bruhwiler, L., Oh, Y., Tans, P. P.,
1285 Apadula, F., Gatti, L. V., Jordan, A., Necki, J., Sasakawa, M., Morimoto, S., Di Iorio, T., Lee, H., Arduini, J., and
1286 Manca, G.: Estimating emissions of methane consistent with atmospheric measurements of methane and δ 13 C of
1287 methane, Atmos. Chem. Phys., 22, 15351–15377, https://doi.org/10.5194/acp-22-15351-2022, 2022.
1288 Bellouin, N., Davies, W., Shine, K. P., Quaas, J., Mülmenstädt, J., Forster, P. M., Smith, C., Lee, L., Regayre, L.,
1289 Brasseur, G., Sudarchikova, N., Bouarar, I., Boucher, O., and Myhre, G.: Radiative forcing of climate change from
1290 the Copernicus reanalysis of atmospheric composition, Earth Syst. Sci. Data, 12, 1649–1677,
1291 https://doi.org/10.5194/essd-12-1649-2020, 2020.
1292 Berthou, S., Renshaw, R., Smyth, T., Tinker, J., Grist, J. P., Wihsgott, J. U., Jones, S., Inall, M., Nolan, G., Berx, B.,
1293 Arnold, A., Blunn, L. P., Castillo, J. M., Cotterill, D., Daly, E., Dow, G., Gomez, B., Fraser-Leonhardt, V., Hirschi,
1294 J. J.-M., Lewis, H. W., Mahmood, S., and Worsfold, M.: Exceptional atmospheric conditions in June 2023 generated
1295 a northwest European marine heatwave which contributed to breaking land temperature records, Commun. Earth &
1296 Environ., 5, 287, https://doi.org/10.1038/s43247-024-01413-8, 2024.
1297 Betts, R. A., Belcher, S. E., Hermanson, L., Klein Tank, A., Lowe, J. A., Jones, C. D., Morice, C. P., Rayner, N. A.,
1298 Scaife, A. A., and Stott, P. A.: Approaching 1.5 °C: how will we know we've reached this crucial warming mark?,
1299 Nature, 624, 33–35, https://doi.org/10.1038/d41586-023-03775-z, 2023.
1300 Blunden, J. and J. Reagan, Eds.: State of the Climate in 2024. Bull. Amer. Meteor. Soc., 106 (8), Si–S513
1301 https://doi.org/10.1175/2025BAMSStateoftheClimate.1., 2025.
1302 Bond, T. C., Doherty, S. J., Fahey, D. W., Forster, P. M., Berntsen, T., DeAngelo, B. J., Flanner, M. G., Ghan, S.,
1303 Kärcher, B., Koch, D., Kinne, S., Kondo, Y., Quinn, P. K., Sarofim, M. C., Schultz, M. G., Schulz, M., Venkataraman,
1304 C., Zhang, H., Zhang, S., Bellouin, N., Guttikunda, S. K., Hopke, P. K., Jacobson, M. Z., Kaiser, J. W., Klimont, Z.,
1305 Lohmann, U., Schwarz, J. P., Shindell, D., Storelvmo, T., Warren, S. G., and Zender, C. S.: Bounding the role of black
1306 carbon in the climate system: A scientific assessment, J. Geophys. Res.-Atmos., 118, 5380–5552,
1307 https://doi.org/10.1002/jgrd.50171, 2013.
1308 Bun, R., Marland, G., Oda, T., See, L., Puliafito, E., Nahorski, Z., Jonas, M., Kovalyshyn, V., Ialongo, I., Yashchun,
1309 O., and Romanchuk, Z.: Tracking unaccounted greenhouse gas emissions due to the war in Ukraine since 2022,
1310 Science of The Total Environment, 914, 169879, https://doi.org/10.1016/j.scitotenv.2024.169879, 2024.
1311 Burger, F. A., Terhaar, J., Frolicher, T. L.: Compound marine heatwaves and ocean acidity extremes, Nat. Commun.,
1312 13, 4722, https://doi.org/10.1038/s41467-022-32120-7, 2022.
1313 Burton, C., Lampe, S., Kelley, D. I., Thiery, W., Hantson, S., Christidis, N., Gudmundsson, L., Forrest, M., Burke,
1314 E., Chang, J., Huang, H., Ito, A., Kou-Giesbrecht, S., Lasslop, G., Li, W., Nieradzik, L., Li, F., Chen, Y., Randerson,

https://doi.org/10.5194/essd-2026-287
Preprint. Discussion started: 23 April 2026

J., Reyer, C. P. O., and Mengel, M.: Global burned area increasingly explained by climate change, Nat. Clim. Chang., 14, 1186–1192, https://doi.org/10.1038/s41558-024-02140-w, 2024.

Canadell, J.G., P. M. S. Monteiro, M. H. Costa, L. Cotrim da Cunha, P. M. Cox, A.V. Eliseev, S. Henson, M. Ishii, S. Jaccard, C. Koven, A. Lohila, P. K. Patra, S. Piao, J. Rogelj, S. Syampungani, S. Zaehle, and K. Zickfeld: Global Carbon and other Biogeochemical Cycles and Feedbacks. In Climate Change 2021: The Physical Science Basis. Contribution of Working Group I to the Sixth Assessment Report of the Intergovernmental Panel on Climate Change [Masson-Delmotte, V., P. Zhai, A. Pirani, S.L. Connors, C. Péan, S. Berger, N. Caud, Y. Chen, L. Goldfarb, M.I. Gomis, M. Huang, K. Leitzell, E. Lonnoy, J.B.R. Matthews, T.K. Maycock, T. Waterfield, O. Yelekçi, R. Yu, and B. Zhou (eds.)]. Cambridge University Press, Cambridge, United Kingdom and New York, NY, USA, pp. 673–816, https://doi.org/10.1017/9781009157896.007, 2021.

Cao, J., Wang, H., Wang, B., Zhao, H., Wang, C., and Zhu, X.: Higher sensitivity of Northern Hemisphere monsoon to anthropogenic aerosol than greenhouse gases, Geophys Res. Lett., 49, e2022GL100270. https://doi.org/10.1029/2022GL100270, 2022.

Cazenave, A., Yang, C., Bouih, M., Storto, A., Chen, J., Llovel, W., Von Schuckmann, K., and Leclercq, L.: Evidence of Increased Deep Ocean Warming From a Sea Level Budget Approach, Earth's Future, 14, e2025EF007403, https://doi.org/10.1029/2025EF007403, 2026.

Cattiaux, J., Ribes, A., and Cariou, E.: How Extreme Were Daily Global Temperatures in 2023 and Early 2024?, Geophysical Research Letters, 51, e2024GL110531, https://doi.org/10.1029/2024GL110531, 2024.

Cheng, L., Abraham, J., Hausfather, Z., and Trenberth, K. E.: How fast are the oceans warming?, Science, 363, 128–129, https://doi.org/10.1126/science.aav7619, 2019.

Ceppi, P., Wilson Kemsley, S., Andersen, H., Andrews, T., Kramer, R. J., Nowack, P., Wall, C. J., and Zelinka, M. D.: Emerging low-cloud feedback and adjustment in global satellite observations, Atmos. Chem. Phys., 26, 4153–4171, https://doi.org/10.5194/acp-26-4153-2026, 2026.

Cheng, L., Von Schuckmann, K., Abraham, J. P., Trenberth, K. E., Mann, M. E., Zanna, L., England, M. H., Zika, J. D., Fasullo, J. T., Yu, Y., Pan, Y., Zhu, J., Newsom, E. R., Bronselaer, B., and Lin, X.: Past and future ocean warming, Nat. Rev. Earth. Environ., 3, 776–794, https://doi.org/10.1038/s43017-022-00345-1, 2022.

Cheung, W. W. L., Frölicher, T. L., Lam, V. W., Oyinlola, M. A., Reygondeau, G., Sumaila, U. R., Tai, T. C., Teh, L. C. L., and Wabnitz, C. C. C.: Marine high temperature extremes amplify the impacts of climate change on fish and fisheries, Sci. Adv., 7, 40, https://doi.org/10.1126/sciadv.abh0895, 2021.

Church, J. A., White, N. J., Konikow, L. F., Domingues, C. M., Cogley, J. G., Rignot, E., Gregory, J. M., Van Den Broeke, M. R., Monaghan, A. J., and Velicogna, I.: Revisiting the Earth's sea-level and energy budgets from 1961 to 2008: SEA-LEVEL AND ENERGY BUDGETS, Geophys. Res. Lett., 38, n/a-n/a, https://doi.org/10.1029/2011GL048794, 2011.

Church, J. A., et al., 2011a: Revisiting the Earth's sea-level and energy budgets from 1961 to 2008. Geophys. Res. Lett., 38, L18601.

https://doi.org/10.5194/essd-2026-287
Preprint. Discussion started: 23 April 2026

1350 Church, J. A. and White, N. J.: Sea-Level Rise from the Late 19th to the Early 21st Century, Surv Geophys, 32, 585–
1351 602, https://doi.org/10.1007/s10712-011-9119-1, 2011b.

1352 Church, J.A., P.U. Clark, A. Cazenave, J.M. Gregory, S. Jevrejeva, A. Levermann, M.A. Merrifield, G.A. Milne, R.S.
1353 Nerem, P.D. Nunn, A.J. Payne, W.T. Pfeffer, D. Stammer and A.S. Unnikrishnan, 2013: Sea Level Change. In:
1354 Climate Change 2013: The Physical Science Basis. Contribution of Working Group I to the Fifth Assessment Report
1355 of the Intergovernmental Panel on Climate Change [Stocker, T.F., D. Qin, G.-K. Plattner, M. Tignor, S.K. Allen, J.
1356 Boschung, A. Nauels, Y. Xia, V. Bex and P.M. Midgley (eds.)]. Cambridge University Press, Cambridge, United
1357 Kingdom and New York, NY, USA

1358

1359 Collins M., M. Sutherland, L. Bouwer, S.-M. Cheong, T. Frölicher, H. Jacot Des Combes, M. Koll Roxy, I. Losada,
1360 K. McInnes, B. Ratter, E. Rivera-Arriaga, R.D. Susanto, D. Swingedouw, and L. Tibig, 2019: Extremes, Abrupt
1361 Changes and Managing Risk. In: IPCC Special Report on the Ocean and Cryosphere in a Changing Climate [H.-O.
1362 Pörtner, D.C. Roberts, V. Masson-Delmotte, P. Zhai, M. Tignor, E. Poloczanska, K. Mintenbeck, A. Alegría, M.
1363 Nicolai, A. Okem, J. Petzold, B. Rama, N.M. Weyer (eds.)]. Cambridge University Press, Cambridge, UK and New
1364 York, NY, USA, pp. 589-655. https://doi.org/10.1017/9781009157964.008, 2019.
1365 Collins, M., Knutti, R., Arblaster, J., Dufresne, J.-L., Fichefet, T., Friedlingstein, P., Gao, X., Gutowski, W.J., Johns,
1366 T., Krinner, G., Shongwe, M., Tebaldi, C., Weaver, A.J. & Wehner, M.: Long-term Climate Change: Projections,
1367 Commitments and Irreversibility. In: V.B. Stocker T.F., .D. Qin, G.K. Plattner, M. Tignor, S.K. Allen, J. Boschung,
1368 A. Nauels, Y. Xia & P.M. Midgley (eds.). Climate Change 2013: The Physical Science Basis. Contribution of Working
1369 Group I to the Fifth Assessment Report of the Intergovernmental Panel on Climate Change. Cambridge, United
1370 Kingdom and New York, NY, USA, Cambridge University Press. pp. 1029–1136, 2013.

1371 Crippa, M., Guizzardi, D., Pagani, F., Banja, M., Muntean, M., Schaaf, E., Becker, W., Monforti-Ferrario, F.,
1372 Quadrelli, R., Risquez Martin, A., Taghavi-Moharamli, P., Grassi, G., Rossi, S., Brandao De Melo, J., Oom, D.,
1373 Branco, A., San-Miguel, J., and Vignati, E.: GHG emissions of all world countries, Publications Office of the
1374 European Union, https://doi:10.2760/9816914 [data set], 2025.

1375 Cuesta-Valero, F. J., Beltrami, H., García-García, A., Krinner, G., Langer, M., MacDougall, A., Nitzbon, J., Peng, J.,
1376 von Schuckmann, K., Seneviratne, S., Thiery, W., Vanderkelen, I., Wu, T.: GCOS EHI 1960-2020 Continental Heat
1377 Content (Version 2), World Data Center for Climate (WDCC) at DKRZ,
1378 https://doi.org/10.26050/WDCC/GCOS_EHI_1960-2020_CoHC_v2, 2023.

1379 Cuesta-Valero, F. J., García-García, A., Beltrami, H., García-Pereira, F., González-Rouco, J. F., and Peng, J.: Robust
1380 increase in observed heat storage by the global subsurface, Sci. Adv., 11, eadw9958,
1381 https://doi.org/10.1126/sciadv.adw9958, 2025.

https://doi.org/10.5194/essd-2026-287
Preprint. Discussion started: 23 April 2026

1382 Dangendorf, S., Hay, C., Calafat, F. M., Marcos, M., Piecuch, C. G., Berk, K., and Jensen, J.: Persistent acceleration
1383 in global sea-level rise since the 1960s, Nat. Clim. Chang., 9, 705–710, https://doi.org/10.1038/s41558-019-0531-8,
1384 2019.
1385 Dangendorf, S., Sun, Q., Wahl, T., Thompson, P., Mitrovica, J. X., and Hamlington, B.: Probabilistic reconstruction
1386 of sea-level changes and their causes since 1900, Earth Syst. Sci. Data, 16, 3471–3494, https://doi.org/10.5194/essd-
1387 16-3471-2024, 2024.
1388 Deng, Z., Ciais, P., Tzompa-Sosa, Z. A., Saunois, M., Qiu, C., Tan, C., Sun, T., Ke, P., Cui, Y., Tanaka, K., Lin, X.,
1389 Thompson, R. L., Tian, H., Yao, Y., Huang, Y., Lauerwald, R., Jain, A. K., Xu, X., Bastos, A., Sitch, S., Palmer, P.
1390 I., Lauvaux, T., d'Aspremont, A., Giron, C., Benoit, A., Poulter, B., Chang, J., Petrescu, A. M. R., Davis, S. J., Liu,
1391 Z., Grassi, G., Albergel, C., Tubiello, F. N., Perugini, L., Peters, W., and Chevallier, F.: Comparing national
1392 greenhouse gas budgets reported in UNFCCC inventories against atmospheric inversions, Earth System Science Data,
1393 14, 1639–1675, https://doi.org/10.5194/essd-14-1639-2022, 2022.
1394 Deng, Z., Zhu, B., Davis, S. J., Ciais, P., Guan, D., Gong, P., and Liu, Z.: Global carbon emissions and decarbonization
1395 in 2024, Nat Rev Earth Environ, 6, 231–233, https://doi.org/10.1038/s43017-025-00658-x, 2025.
1396 Denier van der Gon, H., Gauss, M., Granier, C., Arellano, S., Benedictow, A., Darras, S., Dellaert, S., Guevara, M.,
1397 Jalkanen, J.-P., Krueger, K., Kuenen, J., Liaskoni, M., Liousse, C., Markova, J., Prieto Perez, A., Quack, B., Simpson,
1398 D., Sindelarova, K., and Soulie, A.: Documentation of CAMS emission inventory products,
1399 https://doi.org/10.24380/Q2SI-TI6I, 2023.
1400 Dhakal, S., J. C. Minx, F. L. Toth, A. Abdel-Aziz, M. J. Figueroa Meza, K. Hubacek, I. G. C. Jonckheere, Yong-Gun
1401 Kim, G. F. Nemet, S. Pachauri, X. C. Tan, T. Wiedmann: Emissions Trends and Drivers. In IPCC, 2022: Climate
1402 Change 2022: Mitigation of Climate Change. Contribution of Working Group III to the Sixth Assessment Report of
1403 the Intergovernmental Panel on Climate Change [P.R. Shukla, J. Skea, R. Slade, A. Al Khourdajie, R. van Diemen,
1404 D. McCollum, M. Pathak, S. Some, P. Vyas, R. Fradera, M. Belkacemi, A. Hasija, G. Lisboa, S. Luz, J. Malley,
1405 (eds.)]. Cambridge University Press, Cambridge, UK and New York, NY, USA,
1406 https://doi.org/10.1017/9781009157926.004, 2022.
1407 Donlon, C. J., Martin, M., Stark, J., Roberts-Jones, J., Fiedler, E., and Wimmer, W.: The Operational Sea Surface
1408 Temperature and Sea Ice Analysis (OSTIA) system, Rem. Sens. Environ., 116, 140-158,
1409 https://doi.org/10.1016/j.rse.2010.10.017, 2012.
1410 Douville, H., K. Raghavan, J. Renwick, R.P. Allan, P.A. Arias, M. Barlow, R. Cerezo-Mota, A. Cherchi, T.Y. Gan, J.
1411 Gergis, D. Jiang, A. Khan, W. Pokam Mba, D. Rosenfeld, J. Tierney, and O. Zolina: Water Cycle Changes. In Climate
1412 Change 2021: The Physical Science Basis. Contribution of Working Group I to the Sixth Assessment Report of the
1413 Intergovernmental Panel on Climate Change [Masson-Delmotte, V., P. Zhai, A. Pirani, S.L. Connors, C. Péan, S.
1414 Berger, N. Caud, Y. Chen, L. Goldfarb, M.I. Gomis, M. Huang, K. Leitzell, E. Lonnoy, J.B.R. Matthews, T.K.
1415 Maycock, T. Waterfield, O. Yelekçi, R. Yu, and B. Zhou (eds.)]. Cambridge University Press, Cambridge, United
1416 Kingdom and New York, NY, USA, pp. 1055–1210, https://doi.org/10.1017/9781009157896.010, 2021.

https://doi.org/10.5194/essd-2026-287
Preprint. Discussion started: 23 April 2026

1417 Droste, E. S., Adcock, K. E., Ashfold, M. J., Chou, C., Fleming, Z., Fraser, P. J., Gooch, L. J., Hind, A. J., Langenfelds,
1418 R. L., Leedham Elvidge, E. C., Mohd Hanif, N., O'Doherty, S., Oram, D. E., Ou-Yang, C.-F., Panagi, M., Reeves, C.
1419 E., Sturges, W. T., and Laube, J. C.: Trends and emissions of six perfluorocarbons in the Northern Hemisphere and
1420 Southern Hemisphere, Atmos. Chem. Phys., 20, 4787–4807, https://doi.org/10.5194/acp-20-4787-2020, 2020.

1421 Dunn, R. J. H., Alexander, L. V., Donat, M. G., Zhang, X., Bador, M., Herold, N., Lippmann, T., Allan, R., Aguilar,
1422 E., Barry, A. A., Brunet, M., Caesar, J., Chagnaud, G., Cheng, V., Cinco, T., Durre, I., Guzman, R., Htay, T. M., Wan
1423 Ibadullah, W. M., Bin Ibrahim, M. K. I., Khoshkam, M., Kruger, A., Kubota, H., Leng, T. W., Lim, G., Li-Sha, L.,
1424 Marengo, J., Mbatha, S., McGree, S., Menne, M., Milagros Skansi, M., Ngwenya, S., Nkrumah, F., Oonariya, C.,
1425 Pabon-Caicedo, J. D., Panthou, G., Pham, C., Rahimzadeh, F., Ramos, A., Salgado, E., Salinger, J., Sané, Y.,
1426 Sopaheluwakan, A., Srivastava, A., Sun, Y., Timbal, B., Trachow, N., Trewin, B., Schrier, G., Vazquez-Aguirre, J.,
1427 Vasquez, R., Villarroel, C., Vincent, L., Vischel, T., Vose, R., and Bin Hj Yussof, M. N.: Development of an updated
1428 global land in situ-based data set of temperature and precipitation extremes: HadEX3, J. Geophys. Res.-Atmos., 125,
1429 e2019JD032263, https://doi.org/10.1029/2019JD032263, 2020.

1430 Dunn, R. J. H., Donat, M. G., and Alexander, L. V.: Comparing extremes indices in recent observational and reanalysis
1431 products, Front. Clim., 4, 98905, https://doi.org/10.3389/fclim.2022.989505, 2022.

1432 Dunn, R.J.H., Alexander, L., Donat, M., Zhang, X., Bador, M., Herold, N., Lippmann, T., Allan, R.J., Aguilar, E.,
1433 Aziz, A., Brunet, M., Caesar, J., Chagnaud, G., Cheng, V., Cinco, T., Durre, I., de Guzman, R., Htay, T.M., Wan
1434 Ibadullah, W.M., Bin Ibrahim, M.K.I., Khoshkam, M., Kruge, A., Kubota, H., Leng, T.W., Lim, G., Li-Sha, L.,
1435 Marengo, J., Mbatha, S., McGree, S., Menne, M., de los Milagros Skansi, M., Ngwenya, S., Nkrumah, F., Oonariya,
1436 C., Pabon-Caicedo, J.D., Panthou, G., Pham, C., Rahimzadeh, F., Ramos, A., Salgado, E., Salinger, J., Sane, Y.,
1437 Sopaheluwakan, A., Srivastava, A., Sun, Y., Trimbal, B., Trachow, N., Trewin, B., van der Schrier, G., Vazquez-
1438 Aguirre, J., Vasquez, R., Villarroel, C., Vincent, L., Vischel, T., Vose, R., Bin Hj Yussof, and M.N.A.: HadEX3:
1439 Global land-surface climate extremes indices v3.0.4 (1901-2018), NERC EDS Centre for Environmental Data
1440 Analysis [data set], https://dx.doi.org/10.5285/115d5e4ebf7148ec941423ec86fa9f26, 2023.

1441 Dunn, R. J. H., Blannin, J., Gobron, N., Miller, J. B. and Willett, K. M. eds: Global climate [in "State of the Climate
1442 in 2023"]. Bull. Amer. Meteor. Soc., 105, S12-S155, https://doi.org/10.1175/BAMS-D-24-0116.1, 2024.

1443 Dutton, G.S., B. D. Hall, S.A. Montzka, J. D. Nance, S. D. Clingan, K. M. Petersen, Combined Atmospheric
1444 Chloroflurocarbon-12 Dry Air Mole Fractions from the NOAA GML Halocarbons Sampling Network, 1977-2024,
1445 Version: 2024-03-07, https://doi.org/10.15138/PJ63-H440, 2024.

1446 ECCAD: CAMS database version 6.2 (v6.2), https://permalink.aeris-data.fr/CAMS-GLOB-ANT, [data set], accessed
1447 17 March 2026, 2026.

1448 Eyring, V., N. P. Gillett, K.M. Achuta Rao, R. Barimalala, M. Barreiro Parrillo, N. Bellouin, C. Cassou, P. J. Durack,
1449 Y. Kosaka, S. McGregor, S. Min, O. Morgenstern, and Y. Sun: Human Influence on the Climate System. In Climate
1450 Change 2021: The Physical Science Basis. Contribution of Working Group I to the Sixth Assessment Report of the

https://doi.org/10.5194/essd-2026-287
Preprint. Discussion started: 23 April 2026

1451 Intergovernmental Panel on Climate Change[Masson-Delmotte, V., P. Zhai, A. Pirani, S.L. Connors, C. Péan, S.
1452 Berger, N. Caud, Y. Chen, L. Goldfarb, M.I. Gomis, M. Huang, K. Leitzell, E. Lonnoy, J.B.R. Matthews, T.K.
1453 Maycock, T. Waterfield, O. Yelekçi, R. Yu, and B. Zhou (eds.)]. Cambridge University Press, Cambridge, United
1454 Kingdom and New York, NY, USA, pp. 423–552, http://doi:10.1017/9781009157896.005, 2021.

1455 Feron, S., Malhotra, A., Bansal, S., Fluet-Chouinard, E., McNicol, G., Knox, S. H., Delwiche, K. B., Cordero, R. R.,
1456 Ouyang, Z., Zhang, Z., Poulter, B., and Jackson, R. B.: Recent increases in annual, seasonal, and extreme methane
1457 fluxes driven by changes in climate and vegetation in boreal and temperate wetland ecosystems, Global Change
1458 Biology, 30, e17131, https://doi.org/10.1111/gcb.17131, 2024.

1459 FAO: Greenhouse gas emissions from agrifood systems – Global, regional and country trends, Food and Agriculture
1460 Organization of the United Nations, Rome, https://doi.org/10.4060/cd7300en, 2025.

1461 Forster, P. M., Forster, H. I., Evans, M. J., Gidden, M. J., Jones, C. D., Keller, C. A., Lamboll, R. D., Le Quéré, C.,
1462 Rogelj, J., Rosen, D., Schleussner, C. F., Richardson, T. B., Smith, C. J. and Turnock, S. T.: Current and future global
1463 climate impacts resulting from COVID-19, Nature Clim. Chang, 10, 913–919, https://doi.org/10.1038/s41558-020-
1464 0883-0, 2020.

1465 Forster, P., T. Storelvmo, K. Armour, W. Collins, J.-L. Dufresne, D. Frame, D.J. Lunt, T. Mauritsen, M.D. Palmer,
1466 M. Watanabe, M. Wild, and H. Zhang, 2021: The Earth's Energy Budget, Climate Feedbacks, and Climate Sensitivity.
1467 In Climate Change 2021: The Physical Science Basis. Contribution of Working Group I to the Sixth Assessment
1468 Report of the Intergovernmental Panel on Climate Change [Masson-Delmotte, V., P. Zhai, A. Pirani, S.L. Connors,
1469 C. Péan, S. Berger, N. Caud, Y. Chen, L. Goldfarb, M.I. Gomis, M. Huang, K. Leitzell, E. Lonnoy, J.B.R. Matthews,
1470 T.K. Maycock, T. Waterfield, O. Yelekçi, R. Yu, and B. Zhou (eds.)]. Cambridge University Press, Cambridge, United
1471 Kingdom and New York, NY, USA, pp. 923–1054, https://doi.org/10.1017/9781009157896.009, 2021.

1472 Forster, P., Smith, C., Walsh, T., Lamb, W., Lamboll, R., Hauser, M., Ribes, A., Rosen, D., Gillett, N., Palmer, M.,
1473 Rogelj, J., von Schuckmann, K., Seneviratne, S., Trewin, B., Zhang, X., Allen, M., Andrew, R., Birt, A., Borger, A.,
1474 Boyer, T., Broersma, J., Cheng, L., Dentener, F., Friedlingstein, P., Gutiérrez, J., Gütschow, J., Hall, B., Ishii, M.,
1475 Jenkins, S., Lan, X., Lee, J.-Y., Morice, C., Kadow, C., Kennedy, J., Killick, R., Minx, J., Naik, V., Peters, G., Pirani,
1476 A., Pongratz, J., Schleussner, C.-F., Szopa, S., Thorne, P., Rohde, R., Rojas Corradi, M., Schumacher, D., Vose, R.,
1477 Zickfeld, K., Masson-Delmotte, V., and Zhai, P.: Indicators of Global Climate Change 2022: annual update of large-
1478 scale indicators of the state of the climate system and human influence, Earth System Science Data, 15, 2295–2327,
1479 https://doi.org/10.5194/essd-15-2295-2023, 2023.

1480 Forster, P. M., Smith, C., Walsh, T., Lamb, W. F., Lamboll, R., Hall, B., Hauser, M., Ribes, A., Rosen, D., Gillett, N.
1481 P., Palmer, M. D., Rogelj, J., Von Schuckmann, K., Trewin, B., Allen, M., Andrew, R., Betts, R. A., Borger, A.,
1482 Boyer, T., Broersma, J. A., Buontempo, C., Burgess, S., Cagnazzo, C., Cheng, L., Friedlingstein, P., Gettelman, A.,
1483 Gütschow, J., Ishii, M., Jenkins, S., Lan, X., Morice, C., Mühle, J., Kadow, C., Kennedy, J., Killick, R. E., Krummel,
1484 P. B., Minx, J. C., Myhre, G., Naik, V., Peters, G. P., Pirani, A., Pongratz, J., Schleussner, C.-F., Seneviratne, S. I.,

https://doi.org/10.5194/essd-2026-287
Preprint. Discussion started: 23 April 2026

1485 Szopa, S., Thorne, P., Kovilakam, M. V. M., Majamäki, E., Jalkanen, J.-P., Van Marle, M., Hoesly, R. M., Rohde, R.,
1486 Schumacher, D., Van Der Werf, G., Vose, R., Zickfeld, K., Zhang, X., Masson-Delmotte, V., and Zhai, P.: Indicators
1487 of Global Climate Change 2023: annual update of key indicators of the state of the climate system and human
1488 influence, Earth Syst. Sci. Data, 16, 2625–2658, https://doi.org/10.5194/essd-16-2625-2024, 2024.
1489 Forster, P. M., Smith, C., Walsh, T., Lamb, W. F., Lamboll, R., Cassou, C., Hauser, M., Hausfather, Z., Lee, J.-Y.,
1490 Palmer, M. D., von Schuckmann, K., Slangen, A. B. A., Szopa, S., Trewin, B., Yun, J., Gillett, N. P., Jenkins, S.,
1491 Matthews, H. D., Raghavan, K., Ribes, A., Rogelj, J., Rosen, D., Zhang, X., Allen, M., Aleluia Reis, L., Andrew, R.
1492 M., Betts, R. A., Borger, A., Broersma, J. A., Burgess, S. N., Cheng, L., Friedlingstein, P., Domingues, C. M.,
1493 Gambarini, M., Gasser, T., Gütschow, J., Ishii, M., Kadow, C., Kennedy, J., Killick, R. E., Krummel, P. B., Liné, A.,
1494 Monselesan, D. P., Morice, C., Mühle, J., Naik, V., Peters, G. P., Pirani, A., Pongratz, J., Minx, J. C., Rigby, M.,
1495 Rohde, R., Savita, A., Seneviratne, S. I., Thorne, P., Wells, C., Western, L. M., van der Werf, G. R., Wijffels, S. E.,
1496 Masson-Delmotte, V., and Zhai, P.: Indicators of Global Climate Change 2024: annual update of key indicators of the
1497 state of the climate system and human influence, Earth Syst. Sci. Data, 17, 2641–2680, https://doi.org/10.5194/essd-
1498 17-2641-2025, 2025.
1499 Fox-Kemper, B.,Fox-Kemper, B., H. T. Hewitt, C. Xiao, G. Aðalgeirsdóttir, S.S. Drijfhout, T. L. Edwards, N. R.
1500 Golledge, M. Hemer, R. E. Kopp, G. Krinner, A. Mix, D. Notz, S. Nowicki, I. S. Nurhati, L. Ruiz, J.-B. Sallée, A. B.
1501 A. Slangen, and Y. Yu: Ocean, Cryosphere and Sea Level Change. In Climate Change 2021: The Physical Science
1502 Basis. Contribution of Working Group I to the Sixth Assessment Report of the Intergovernmental Panel on Climate
1503 Change [Masson-Delmotte, V., P. Zhai, A. Pirani, S.L. Connors, C. Péan, S. Berger, N. Caud, Y. Chen, L. Goldfarb,
1504 M.I. Gomis, M. Huang, K. Leitzell, E. Lonnoy, J. B. R. Matthews, T. K. Maycock, T. Waterfield, O. Yelekçi, R. Yu,
1505 and B. Zhou (eds.)]. Cambridge University Press, Cambridge, United Kingdom and New York, NY, USA, pp. 1211–
1506 1362, https://doi.org/10.1017/9781009157896.011, 2021.
1507 Francey, R.J., L.P. Steele, R.L. Langenfelds and B.C. Pak, High precision long-term monitoring of radiatively-active
1508 trace gases at surface sites and from ships and aircraft in the Southern Hemisphere atmosphere, J. Atmos. Science, 56,
1509 279-285 https://doi.org/10.1175/1520-0469(1999)056<0279:HPLTMO>2.0.CO;2, 1999.
1510 Frederikse, T., Landerer, F., Caron, L., Adhikari, S., Parkes, D., Humphrey, V. W., Dangendorf, S., Hogarth, P.,
1511 Zanna, L., Cheng, L., and Wu, Y.-H.: The causes of sea-level rise since 1900, Nature, 584, 393–397,
1512 https://doi.org/10.1038/s41586-020-2591-3, 2020.
1513 Friedlingstein, P., O'Sullivan, M., Jones, M. W., Andrew, R. M., Hauck, J., Olsen, A., Peters, G. P., Peters, W.,
1514 Pongratz, J., Sitch, S., Le Quéré, C., Canadell, J. G., Ciais, P., Jackson, R. B., Alin, S., Aragão, L. E. O. C., Arneth,
1515 A., Arora, V., Bates, N. R., Becker, M., Benoit-Cattin, A., Bittig, H. C., Bopp, L., Bultan, S., Chandra, N., Chevallier,
1516 F., Chini, L. P., Evans, W., Florentie, L., Forster, P. M., Gasser, T., Gehlen, M., Gilfillan, D., Gkritzalis, T., Gregor,
1517 L., Gruber, N., Harris, I., Hartung, K., Haverd, V., Houghton, R. A., Ilyina, T., Jain, A. K., Joetzjer, E., Kadono, K.,
1518 Kato, E., Kitidis, V., Korsbakken, J. I., Landschützer, P., Lefèvre, N., Lenton, A., Lienert, S., Liu, Z., Lombardozzi,
1519 D., Marland, G., Metzl, N., Munro, D. R., Nabel, J. E. M. S., Nakaoka, S.-I., Niwa, Y., O'Brien, K., Ono, T., Palmer,

https://doi.org/10.5194/essd-2026-287
Preprint. Discussion started: 23 April 2026

1520 P. I., Pierrot, D., Poulter, B., Resplandy, L., Robertson, E., Rödenbeck, C., Schwinger, J., Séférian, R., Skjelvan, I.,
1521 Smith, A. J. P., Sutton, A. J., Tanhua, T., Tans, P. P., Tian, H., Tilbrook, B., van der Werf, G., Vuichard, N., Walker,
1522 A. P., Wanninkhof, R., Watson, A. J., Willis, D., Wiltshire, A. J., Yuan, W., Yue, X., and Zaehle, S.: Global carbon
1523 budget 2020, Earth Syst. Sci. Data, 12, 3269–3340, https://doi.org/10.5194/essd-12-3269-2020, 2020.

1524 Friedlingstein, P., O'Sullivan, M., Jones, M. W., Andrew, R. M., Bakker, D. C. E., Hauck, J., Landschützer, P., Le
1525 Quéré, C., Li, H., Luijkx, I. T., Peters, G. P., Peters, W., Pongratz, J., Schwingshackl, C., Sitch, S., Canadell, J. G.,
1526 Ciais, P., Aas, K., Alin, S. R., Anthoni, P., Barbero, L., Bates, N. R., Bellouin, N., Benoit-Cattin, A., Berghoff, C. F.,
1527 Bernardello, R., Bopp, L., Brasika, I. B. M., Chamberlain, M. A., Chandra, N., Chevallier, F., Chini, L. P., Collier, N.
1528 O., Colligan, T. H., Cronin, M., Djeutchouang, L., Dou, X., Enright, M. P., Enyo, K., Erb, M., Evans, W., Feely, R.
1529 A., Feng, L., Ford, D. J., Foster, A., Fransner, F., Gasser, T., Gehlen, M., Gkritzalis, T., Goncalves De Souza, J.,
1530 Grassi, G., Gregor, L., Gruber, N., Guenet, B., Gürses, Ö., Harrington, K., Harris, I., Heinke, J., Hurtt, G. C., Iida, Y.,
1531 Ilyina, T., Ito, A., Jacobson, A. R., Jain, A. K., Jarníková, T., Jersild, A., Jiang, F., Jones, S. D., Kato, E., Keeling, R.
1532 F., Klein Goldewijk, K., Knauer, J., Kong, Y., Korsbakken, J. I., Koven, C., Kunimitsu, T., Lan, X., Liu, J., Liu, Z.,
1533 Liu, Z., Lo Monaco, C., Ma, L., Marland, G., McGuire, P. C., McKinley, G. A., Melton, J., Monacci, N., Monier, E.,
1534 Morgan, E. J., Munro, D. R., Müller, J. D., Nakaoka, S.-I., Nayagam, L. R., Niwa, Y., Nutzel, T., Olsen, A., Omar, A.
1535 M., Pan, N., Pandey, S., Pierrot, D., Qin, Z., Regnier, P. A. G., Rehder, G., Resplandy, L., Roobaert, A., Rosan, T.
1536 M., Rödenbeck, C., Schwinger, J., Skjelvan, I., Smallman, T. L., Spada, V., Sreeush, M. G., Sun, Q., Sutton, A. J.,
1537 Sweeney, C., Swingedouw, D., Séférian, R., Takao, S., Tatebe, H., Tian, H., Tian, X., Tilbrook, B., Tsujino, H.,
1538 Tubiello, F., van Ooijen, E., van der Werf, G., van de Velde, S. J., Walker, A., Wanninkhof, R., Yang, X., Yuan, W.,
1539 Yue, X., and Zeng, J.: Global Carbon Budget 2025, Earth Syst. Sci. Data Discuss. [preprint],
1540 https://doi.org/10.5194/essd-2025-659, in review, 2025.

1541 Frölicher, T. L., Fischer, E. M., and Gruber, N.: Marine heatwaves under global warming, Nature, 560, 360-364,
1542 https://doi.org/10.1038/s41586-018-0383-9, 2018.
1543 Frölicher, T. L. and Laufkötter, C.: Emerging risks from marine heatwaves, Nat. Commun., 9, 650,
1544 https://doi.org/10.1038/s41467-018-03163-6, 2018.
1545 Gasser, T., Crepin, L., Quilcaille, Y., Houghton, R. A., Ciais, P., and Obersteiner, M.: Historical CO2 emissions from
1546 land use and land cover change and their uncertainty, Biogeosciences, 17, 4075–4101, https://doi.org/10.5194/bg-17-
1547 4075-2020, 2020.

1548 Gidden, M. J., Gasser, T., Grassi, G., Forsell, N., Janssens, I., Lamb, W. F., Minx, J., Nicholls, Z., Steinhauser, J., and
1549 Riahi, K.: Aligning climate scenarios to emissions inventories shifts global benchmarks, Nature, 624, 102–108,
1550 https://doi.org/10.1038/s41586-023-06724-y, 2023.
1551 Gillett, N.P., Kirchmeier-Young, M., Ribes, A., Shiogama, H., Hegerl, G.C., Knutti, R., Gastineau, G., John, J.G., Li,
1552 L., Nazarenko, L., Rosenbloom, N., Seland, Ø., Wu, T., Yukimoto, S., and Ziehn, T.: Constraining human
1553 contributions to observed warming since the pre-industrial period, Nat. Clim. Chang., 11, 207–212,
1554 https://doi.org/10.1038/s41558-020-00965-9, 2021.

https://doi.org/10.5194/essd-2026-287
Preprint. Discussion started: 23 April 2026

1555 Gleckler, P. J., Durack, P. J., Stouffer, R. J., Johnson, G. C., and Forest, C. E.: Industrial-era global ocean heat uptake
1556 doubles in recent decades, Nat. Clim. Chang., 6, 394–398, https://doi.org/10.1038/nclimate2915, 2016.
1557 Goessling, H. F., Rackow, T., and Jung, T.: Recent global temperature surge intensified by record-low planetary
1558 albedo, Science, 387, 68–73, https://doi.org/10.1126/science.adq7280, 2025.
1559 Grassi, G., Stehfest, E., Rogelj, J., Van Vuuren, D., Cescatti, A., House, J., Nabuurs, G.-J., Rossi, S., Alkama, R.,
1560 Viñas, R. A., Calvin, K., Ceccherini, G., Federici, S., Fujimori, S., Gusti, M., Hasegawa, T., Havlik, P., Humpenöder,
1561 F., Korosuo, A., Perugini, L., Tubiello, F. N., and Popp, A.: Critical adjustment of land mitigation pathways for
1562 assessing countries' climate progress, Nat. Clim. Chang., 11, 425–434, https://doi.org/10.1038/s41558-021-01033-6,
1563 2021.
1564 Grassi, G., Schwingshackl, C., Gasser, T., Houghton, R. A., Sitch, S., Canadell, J. G., Cescatti, A., Ciais, P., Federici,
1565 S., Friedlingstein, P., Kurz, W. A., Sanz Sanchez, M. J., Abad Viñas, R., Alkama, R., Bultan, S., Ceccherini, G., Falk,
1566 S., Kato, E., Kennedy, D., Knauer, J., Korosuo, A., Melo, J., McGrath, M. J., Nabel, J. E. M. S., Poulter, B.,
1567 Romanovskaya, A. A., Rossi, S., Tian, H., Walker, A. P., Yuan, W., Yue, X., and Pongratz, J.: Harmonising the land-
1568 use flux estimates of global models and national inventories for 2000–2020, Earth Syst. Sci. Data, 15, 1093–1114,
1569 https://doi.org/10.5194/essd-15-1093-2023, 2023.
1570 Gregory, C. H., Artana, C., Lama, S., Leon-FonFay, D., Sala, J., Xiao, F., Xu, T., Capotondi, A., Martinez-Villalobos,
1571 C., Holbrook, N. J.: Global Marine Heatwaves Under Different Flavors of ENSO, Geophys. Res. Lett., 51, 20,
1572 e2024GL110399, 2024.
1573 Gruber, N., Boyd, P. W., Frolicher, T. L., and Vogt, M.: Biogeochemical extremes and compound events in the ocean,
1574 nature, 600, 395-407, https://doi.org/10.1038/s41586-021-03981-7, 2021.
1575 Guinaldo, T., Cassou, C., Sallée, J.-B., and Liné, A.: Internal variability effect doped by climate change drove the
1576 2023 marine heat extreme in the North Atlantic, Commun Earth Environ, 6, 291, https://doi.org/10.1038/s43247-025-
1577 02197-1, 2025.
1578 Gulev, S. K., P. W. Thorne, J. Ahn, F. J. Dentener, C. M. Domingues, S. Gerland, D. Gong, D. S. Kaufman, H. C.
1579 Nnamchi, J. Quaas, J.A. Rivera, S. Sathyendranath, S.L. Smith, B. Trewin, K. von Schuckmann, and R. S. Vose:
1580 Changing State of the Climate System. In Climate Change 2021: The Physical Science Basis. Contribution of Working
1581 Group I to the Sixth Assessment Report of the Intergovernmental Panel on Climate Change[Masson-Delmotte, V., P.
1582 Zhai, A. Pirani, S.L. Connors, C. Péan, S. Berger, N. Caud, Y. Chen, L. Goldfarb, M.I. Gomis, M. Huang, K. Leitzell,
1583 E. Lonnoy, J.B.R. Matthews, T.K. Maycock, T. Waterfield, O. Yelekçi, R. Yu, and B. Zhou (eds.)]. Cambridge
1584 University Press, Cambridge, United Kingdom and New York, NY, USA, pp. 287–422,
1585 https://doi.org/10.1017/9781009157896.004, 2021.
1586 Gupta, A. K., Mittal, T., Fauria, K. E., Bennartz, R., and Kok, J. F.: The January 2022 Hunga eruption cooled the
1587 southern hemisphere in 2022 and 2023, Commun Earth Environ, 6, 240, https://doi.org/10.1038/s43247-025-02181-
1588 9, 2025.

https://doi.org/10.5194/essd-2026-287
Preprint. Discussion started: 23 April 2026

1589 Gütschow, J., Busch, D., and Pflüger, M.: The PRIMAP-hist national historical emissions time series (1750-2024)
1590 v2.7, Zenodo [data set], https://doi.org/10.5281/zenodo.17090760, 2025.

1591 Hardy, A., Palmer, P. I., and Oakes, G.: Satellite data reveal how Sudd wetland dynamics are linked with globally-
1592 significant methane emissions, Environ. Res. Lett., 18, 074044, https://doi.org/10.1088/1748-9326/ace272, 2023.
1593 Hay, C. C., Morrow, E., Kopp, R. E., and Mitrovica, J. X.: Probabilistic reanalysis of twentieth-century sea-level rise,
1594 Nature, 517, 481–484, https://doi.org/10.1038/nature14093, 2015.
1595 Hakuba, M. Z., Frederikse, T., and Landerer, F. W.: Earth's energy imbalance from the ocean perspective (2005–
1596 2019), Geophys Res Lett, 48, e2021GL093624, https://doi.org/10.1029/2021GL093624, 2021.

1597 Hansen, J. E., Sato, M., Simons, L., Nazarenko, L. S., Sangha, I., Kharecha, P., Zachos, J. C., von Schuckmann, K.,
1598 Loeb, N. G., Osman, M. B., Jin, Q., Tselioudis, G., Jeong, E., Lacis, A., Ruedy, R., Russell, G., Cao, J., and Li, J.:
1599 Global warming in the pipeline, Oxford Open Climate Change, 3, kgad008, https://doi.org/10.1093/oxfclm/kgad008,
1600 2023.

1601 Hansis, E., Davis, S. J., and Pongratz, J.: Relevance of methodological choices for accounting of land use change
1602 carbon fluxes, Global Biogeochem. Cy., 29, 1230–1246, https://doi.org/10.1002/2014GB004997, 2015.

1603 Haustein, K., Allen, M. R., Forster, P. M., Otto, F. E. L., Mitchell, D. M., Matthews, H. D., and Frame, D. J.: A real-
1604 time Global Warming Index, Sci Rep, 7, 15417, https://doi.org/10.1038/s41598-017-14828-5, 2017.

1605 Harris, I., Osborn, T. J., Jones, P., and Lister, D.: Version 4 of the CRU TS monthly high-resolution gridded
1606 multivariate climate dataset, Scientific data, 7, 109, https://doi.org/10.1038/s41597-020-045303, 2020

1607 Hersbach, H., Bell, B., Berrisford, P., Hirahara, S., Horányi, A., Muñoz-Sabater, J., Nicolas, J., Peubey, C., Radu, R.,
1608 Schepers, D., Simmons, A., Soci, C., Abdalla, S., Abellan, X., Balsamo, G., Bechtold, P., Biavati, G., Bidlot, J.,
1609 Bonavita, M., De Chiara, G., Dahlgren, P., Dee, D., Diamantakis, M., Dragani, R., Flemming, J., Forbes, R., Fuentes,
1610 M., Geer, A., Haimberger, L., Healy, S., Hogan, R. J., Hólm, E., Janisková, M., Keeley, S., Laloyaux, P., Lopez, P.,
1611 Lupu, C., Radnoti, G., de Rosnay, P., Rozum, I., Vamborg, F., Villaume, S., and Thépaut, J.-N.: The ERA5 global
1612 reanalysis, Q. J. R. Meteorol. Soc., 146, 1999–2049, https://doi.org/10.1002/qj.3803, 2020.

1613 Hodnebrog, Ø., Aamaas, B., Fuglestvedt, J. S., Marston, G., Myhre, G., Nielsen, C. J., Sandstad, M., Shine, K. P., and
1614 Wallington, T. J.: Updated Global Warming Potentials and Radiative Efficiencies of Halocarbons and Other Weak
1615 Atmospheric Absorbers, Rev. Geophys., 58, e2019RG000691, https://doi.org/10.1029/2019RG000691, 2020.

1616 Hodnebrog, Ø., Myhre, G., Jouan, C., Andrews, T., Forster, P. M., Jia, H., Loeb, N. G., Olivié, D. J. L., Paynter, D.,
1617 Quaas, J., Raghuraman, S. P., and Schulz, M.: Recent reductions in aerosol emissions have increased Earth's energy
1618 imbalance, Communications Earth & Environment, 5, 166, https://doi.org/10.1038/s43247-024-01324-8, 2024.
1619 Hoesly, R., Smith, S. J., Ahsan, H., Prime, N., O'Rourke, P., Crippa, M., Klimont, Z., Guizzardi, D., Feng, L., Harkins,
1620 C., MCDONALD, B., and Wang, S.: CEDS v_2025_03_18 Aggregate Data (v_2025_03_18),
1621 https://doi.org/10.5281/ZENODO.15059443, 2025.

https://doi.org/10.5194/essd-2026-287
Preprint. Discussion started: 23 April 2026

1622 Hoesly, R. M., Smith, S. J., Feng, L., Klimont, Z., Janssens-Maenhout, G., Pitkanen, T., Seibert, J. J., Vu, L., Andres,
1623 R. J., Bolt, R. M., Bond, T. C., Dawidowski, L., Kholod, N., Kurokawa, J.-I., Li, M., Liu, L., Lu, Z., Moura, M. C. P.,
1624 O'Rourke, P. R., and Zhang, Q.: Historical (1750–2014) anthropogenic emissions of reactive gases and aerosols from
1625 the Community Emissions Data System (CEDS), Geosci. Model. Dev., 11, 369–408, https://doi.org/10.5194/gmd-11-
1626 369-2018, 2018.

1627 Hoesly, R., Smith, S. J., Ahsan, H., Prime, N., O'Rourke, P., Crippa, M., Klimont, Z., Guizzardi, D., Feng, L., Harkins,
1628 C., MCDONALD, B., and Wang, S.: CEDS v_2025_03_18 Aggregate Data, Zenodo [data set],
1629 https://doi.org/10.5281/zenodo.15059443, 2025.

1630 Houghton, R. A., and Nassikas, A. A.: Global and regional fluxes of carbon from land use and land cover change
1631 1850–2015, Global Biogeochem. Cy., 31, 456– 472, https://doi.org/10.1002/2016GB005546, 2017.

1632 Houghton, R. A. and Castanho, A.: Annual emissions of carbon from land use, land-use change, and forestry from
1633 1850 to 2020, Earth System Science Data, 15, 2025–2054, https://doi.org/10.5194/essd-15-2025-2023, 2023.

1634 Hu, L.: A Global Assessment of Coastal Marine Heatwaves and Their Relation With Coastal Urban Thermal Changes,
1635 Geophys. Res. Lett., 48, 9, https://doi.org/10.1029/2021GL093260, 2021.
1636 Hu, Y., Yue, X., Tian, C., Zhou, H., Fu, W., Zhao, X., Zhao, Y., and Chen, Y.: Identifying the main drivers of the
1637 spatiotemporal variations in wetland methane emissions during 2001–2020, Frontiers in Environmental Science, 11,
1638 https://doi.org/10.3389/fenvs.2023.1275742, 2023.

1639 Huang, B., Liu, C., Banzon, V., Freeman, E., Graham, G., Hankins, B., Smith, T., and Zhang, H.-M.: Daily Optimum
1640 Interpolation Sea Surface Temperature (DOISST) Version 2.1, J. Clim., 34, 8, https://doi.org/10.1175/JCLI-D-21-
1641 0001.1, 2021.
1642 Huang, B., Yin, X., Boyer, T., Liu, C., Menne, M., Rao, Y. D., Smith, T., Vose, R., and Zhang, H.-M.: Extended
1643 Reconstructed Sea Surface Temperature, Version 6 (ERSSTv6). Part I: An Artificial Neural Network Approach,
1644 Journal of Climate, 38, 1105–1121, https://doi.org/10.1175/JCLI-D-23-0707.1, 2025.
1645 Hughes, T. P., Barnes, M. L., Bellwood, D. R., Cinner, J. E., Cumming, G. S., Jackson, J. B. C., Kleypas, J., van de
1646 Leemput, I. A., Lough, J. M., Morrison, T. H., Palumbi, S. R., van Nes, E. H., and Scheffer, M.: Coral reefs in the
1647 Anthropocene, Nature, 546, 82-90, https://doi.org/10.1038/nature22901, 2017.
1648 Hubert et al., TOAR-II past and present free tropospheric ozone using satellite observations, submitted to Phil. Trans.
1649 Royal Society A, 2026.
1650 IATA, Global Outlook for Air Transport, https://www.iata.org/en/iata-repository/publications/economic-
1651 reports/global-outlook-for-air-transport-december-2025/, accessed 14 April 2026, 2025.

1652 IEA: CO2 Emissions in 2023. https://www.iea.org/reports/co2-emissions-in-2023, accessed 20.04.2024, 2024.

https://doi.org/10.5194/essd-2026-287
Preprint. Discussion started: 23 April 2026

IPCC: Sixty-second Session of the IPCC (IPCC-62), Fifteenth Session of the IPCC Working Group I (WGI-15), Thirteenth Session of the IPCC Working Group II (WGII-13), and Fifteenth Session of the IPCC Working Group III (WGIII-15), https://www.ipcc.ch/meeting-doc/ipcc-62/, accessed 20 April 2025, 2025.

IPCC: Climate Change 2013: The Physical Science Basis. Contribution of Working Group I to the Fifth Assessment Report of the Intergovernmental Panel on Climate Change [Stocker, T.F., D. Qin, G.-K. Plattner, M. Tignor, S.K. Allen, J. Boschung, A. Nauels, Y. Xia, V. Bex and P.M. Midgley (eds.)]. Cambridge University Press, Cambridge, United Kingdom and New York, NY, USA, 1535 pp, https://doi:10.1017/CBO9781107415324, 2013.

IPCC: Summary for Policymakers. In: Global Warming of 1.5°C. An IPCC Special Report on the impacts of global warming of 1.5°C above pre-industrial levels and related global greenhouse gas emission pathways, in the context of strengthening the global response to the threat of climate change, sustainable development, and efforts to eradicate poverty [Masson-Delmotte, V., P. Zhai, H.-O. Pörtner, D. Roberts, J. Skea, P.R. Shukla, A. Pirani, W. Moufouma-Okia, C. Péan, R. Pidcock, S. Connors, J.B.R. Matthews, Y. Chen, X. Zhou, M.I. Gomis, E. Lonnoy, T. Maycock, M. Tignor, and T. Waterfield (eds.)]. Cambridge University Press, Cambridge, UK and New York, NY, USA, pp. 3-24, https://doi.org/10.1017/9781009157940.001, 2018.

IPCC: Climate Change 2021: The Physical Science Basis. Contribution of Working Group I to the Sixth Assessment Report of the Intergovernmental Panel on Climate Change, Cambridge University Press, Cambridge, United Kingdom and New York, NY, USA, https://doi.org/10.1017/9781009157896, 2021a.

IPCC: Summary for Policymakers, in: Climate Change 2021: The Physical Science Basis. Contribution of Working Group I to the Sixth Assessment Report of the Intergovernmental Panel on Climate Change, edited by: Masson-Delmotte, V., Zhai, P., Pirani, A., Connors, S. L., Péan, C., Berger, S., Caud, N., Chen, Y., Goldfarb, L., Gomis, M. I., Huang, M., Leitzell, K., Lonnoy, E., Matthews, J. B. R., Maycock, T. K., Waterfield, T., Yelekçi, O., Yu, R., and Zhou, B., Cambridge University Press, Cambridge, United Kingdom and New York, NY, USA, pp.3–32 https://doi.org/10.1017/9781009157896.001, 2021b.

IPCC: Climate Change 2022: Impacts, Adaptation, and Vulnerability. Contribution of Working Group II to the Sixth Assessment Report of the Intergovernmental Panel on Climate Change [H.-O. Pörtner, D.C. Roberts, M. Tignor, E.S. Poloczanska, K. Mintenbeck, A. Alegría, M. Craig, S. Langsdorf, S. Löschke, V. Möller, A. Okem, B. Rama (eds.)]. Cambridge University Press. Cambridge University Press, Cambridge, UK and New York, NY, USA, 3056 pp., https://doi:10.1017/9781009325844, 2022.

IPCC, 2023: Climate Change 2023: Synthesis Report. Contribution of Working Groups I, II and III to the Sixth Assessment Report of the Intergovernmental Panel on Climate Change [Core Writing Team, H. Lee and J. Romero (eds.)]. IPCC, Geneva, Switzerland., Intergovernmental Panel on Climate Change (IPCC), https://doi.org/10.59327/IPCC/AR6-9789291691647, 2023a.

https://doi.org/10.5194/essd-2026-287
Preprint. Discussion started: 23 April 2026

1686 IPCC, 2023: Climate Change 2023: Summary for Policy Makers. Contribution of Working Groups I, II and III to the
1687 Sixth Assessment Report of the Intergovernmental Panel on Climate Change [Core Writing Team, H. Lee and J.
1688 Romero (eds.)]. IPCC, Geneva, Switzerland., Intergovernmental Panel on Climate Change (IPCC),
1689 https://doi.org/10.59327/IPCC/AR6-9789291691647, 2023b.

1690 Iturbide, M., Fernández, J., Gutiérrez, J. M., Pirani, A., Huard, D., Al Khourdajie, A., Baño-Medina, J., Bedia, J.,
1691 Casanueva, A., Cimadevilla, E., Cofiño, A. S., De Felice, M., Diez-Sierra, J., García-Díez, M., Goldie, J., Herrera, D.
1692 A., Herrera, S., Manzanas, R., Milovac, J., Radhakrishnan, A., San-Martín, D., Spinuso, A., Thyng, K. M., Trenham,
1693 C., and Yelekçi, Ö.: Implementation of FAIR principles in the IPCC: the WGI AR6 Atlas repository, Sci Data, 9, 629,
1694 https://doi.org/10.1038/s41597-022-01739-y, 2022.

1695 Janardanan, R., Maksyutov, S., Wang, F., Nayagam, L., Sahu, S. K., Mangaraj, P., Saunois, M., Lan, X., and
1696 Matsunaga, T.: Country-level methane emissions and their sectoral trends during 2009–2020 estimated by high-
1697 resolution inversion of GOSAT and surface observations, Environ. Res. Lett., 19, 034007,
1698 https://doi.org/10.1088/1748-9326/ad2436, 2024.

1699 Jenkins, S., Povey, A., Gettelman, A., Grainger, R., Stier, P., and Allen, M.: Is Anthropogenic Global Warming
1700 Accelerating?, Journal of Climate, 35, 7873–7890, https://doi.org/10.1175/JCLI-D-22-0081.1, 2022.
1701 Jenkins, S., Smith, C., Allen, M., and Grainger, R.: Tonga eruption increases chance of temporary surface temperature
1702 anomaly above 1.5 °C, Nature Clim. Chang., 13, 127–129, https://doi.org/10.1038/s41558-022-01568-2, 2023.

1703 Kirchengast, G., Gorfer, M., Mayer, M., Steiner, A. K., and Haimberger, L.: GCOS EHI 1960-2020 Atmospheric Heat
1704 Content, https://doi.org/10.26050/WDCC/GCOS_EHI_1960-2020_AHC, 2022.

1705 Kramer, R. J., He, H., Soden, B. J., Oreopoulos, L., Myhre, G., Forster, P. M., and Smith, C. J., Observational evidence
1706 of increasing global radiative forcing, Geophys. Res. Lett., 48, e2020GL091585,
1707 https://doi.org/10.1029/2020GL091585, 2021.

1708 Lamb, W. F., Andrew, R. M., Jones, M., Nicholls, Z., Peters, G. P., Smith, C., Saunois, M., Grassi, G., Pongratz, J.,
1709 Smith, S. J., Tubiello, F. N., Crippa, M., Gidden, M., Friedlingstein, P., Minx, J., and Forster, P. M.: Differences in
1710 anthropogenic greenhouse gas emissions estimates explained, Earth Syst. Sci. Data, 18, 2549–2572,
1711 https://doi.org/10.5194/essd-18-2549-2026, 2026.
1712 Lamboll, R. D., Jones, C. D., Skeie, R. B., Fiedler, S., Samset, B. H., Gillett, N. P., Rogelj, J., and Forster, P. M.:
1713 Modifying emissions scenario projections to account for the effects of COVID-19: protocol for CovidMIP,
1714 Geoscientific Model Development, 14, 3683–3695, https://doi.org/10.5194/gmd-14-3683-2021, 2021.

1715 Lamboll, R. D. and Rogelj, J.: Code for estimation of remaining carbon budget in IPCC AR6 WGI, Zenodo [code],
1716 https://doi.org/10.5281/zenodo.6373365, 2022.

1717 Lamboll, R. and Rogelj, J.: Carbon Budget Calculator, 2025, Github [code],
1718 https://github.com/Rlamboll/AR6CarbonBudgetCalc/tree/v1.0.1, last access: 25 April 2025, 2025.

https://doi.org/10.5194/essd-2026-287
Preprint. Discussion started: 23 April 2026

1719 Lamboll, R. D., Nicholls, Z. R. J., Smith, C. J., Kikstra, J. S., Byers, E., and Rogelj, J.: Assessing the size and
1720 uncertainty of remaining carbon budgets, Nature Climate Change, 13, 1360–1367, https://doi.org/10.1038/s41558-
1721 023-01848-5, 2023.
1722 Lan, X., Tans, P. and Thoning, K.W.: Trends in globally-averaged CO_2 determined from NOAA Global Monitoring
1723 Laboratory measurements, Version Monday, 14-Apr-2025 09:08:57 MDT https://doi.org/10.15138/9N0H-ZH07,
1724 2025.
1725 Lan, X., Thoning, K. W., and Dlugokencky, E.J.: Trends in globally-averaged CH4 N2O, and SF6 determined from
1726 NOAA Global Monitoring Laboratory measurements, Version 2023-04, https://doi.org/10.15138/P8XG-AA10,
1727 2023b.
1728 Laube, J., Newland, M., Hogan, C., Brenninkmeijer, A.M., Fraser, P.J., Martinerie, P., Oram, D.E., Reeves, C.E.,
1729 Röckmann, T., Schwander, J., Witrant, E., Sturges, W.T.: Newly detected ozone-depleting substances in the
1730 atmosphere. Nature Geosci., 7, 266–269, https://doi.org/10.1038/ngeo2109, 2014.
1731 Leach, N. J., Jenkins, S., Nicholls, Z., Smith, C. J., Lynch, J., Cain, M., Walsh, T., Wu, B., Tsutsui, J., and Allen, M.
1732 R.: FaIRv2.0.0: a generalized impulse response model for climate uncertainty and future scenario exploration, Geosci.
1733 Model Dev., 14, 3007–3036, https://doi.org/10.5194/gmd-14-3007-2021, 2021.
1734 Lee, J.-Y., J. Marotzke, G. Bala, L. Cao, S. Corti, J.P. Dunne, F. Engelbrecht, E. Fischer, J.C. Fyfe, C. Jones, A.
1735 Maycock, J. Mutemi, O. Ndiaye, S. Panickal, and T. Zhou: Future Global Climate: Scenario-Based Projections and
1736 Near-Term Information. In Climate Change 2021: The Physical Science Basis. Contribution of Working Group I to
1737 the Sixth Assessment Report of the Intergovernmental Panel on Climate Change[Masson-Delmotte, V., P. Zhai, A.
1738 Pirani, S.L. Connors, C. Péan, S. Berger, N. Caud, Y. Chen, L. Goldfarb, M.I. Gomis, M. Huang, K. Leitzell, E.
1739 Lonnoy, J.B.R. Matthews, T.K. Maycock, T. Waterfield, O. Yelekçi, R. Yu, and B. Zhou (eds.)]. Cambridge
1740 University Press, Cambridge, United Kingdom and New York, NY, USA, pp. 553–
1741 672,https://doi.org/10.1017/9781009157896.006, 2021.
1742 Lee, H., K. Calvin, D. Dasgupta, G. Krinner, A. Mukherji, P. Thorne, C. Trisos, J. Romero, P. Aldunce, K. Barrett,
1743 G. Blanco, W.W.L. Cheung, S.L. Connors, F. Denton, A. Diongue-Niang, D. Dodman, M. Garschagen, O. Geden, B.
1744 Hayward, C. Jones, F. Jotzo, T. Krug, R. Lasco, J.-Y. Lee, V. Masson-Delmotte, M. Meinshausen, K. Mintenbeck, A.
1745 Mokssit, F.E.L. Otto, M. Pathak, A. Pirani, E. Poloczanska, H.-O. Pörtner, A. Revi, D.C. Roberts, J. Roy, A.C. Ruane,
1746 J. Skea, P.R. Shukla, R. Slade, A. Slangen, Y. Sokona, A.A. Sörensson, M. Tignor, D. van Vuuren, Y.-M. Wei, H.
1747 Winkler, P. Zhai, and Z. Zommers: Synthesis Report of the IPCC Sixth Assessment Report (AR6): Summary for
1748 Policymakers. Intergovernmental Panel on Climate Change [accepted], available at
1749 https://www.ipcc.ch/report/ar6/syr/, 2023.
1750 Le Grix, N., Zscheischler, J., Laufkötter, C., Rousseaux, C. S., and Frölicher, T. L.: Compound high-temperature and
1751 low-chlorophyll extremes in the ocean over the satellite period, BG, 18, 6, https://doi.org/10.5194/bg-18-2119-2021,
1752 2021.

https://doi.org/10.5194/essd-2026-287
Preprint. Discussion started: 23 April 2026

1753 Li, C., Burger, F. A., Raible, C. C., and Frölicher, T. L.: Observed Regional Impacts of Marine Heatwaves on Sea-Air
1754 CO2 Exchange, Geophys. Res. Lett., 51, 24, https://doi.org/10.1029/2024GL110379, 2024.
1755 Liu, G., Heron, S. F., Eakin, C. M., Muller-Karger, F. E., Vega-Rodriguez, M., Guild, L. S., De La Cour, J. L., Geiger,
1756 E. F., Skirving, W. J., Burgess, T. F. R., Strong, A. E., Harris, A., Maturi, E., Ignatov, A., Sapper, J., Li, J., Lynds, S.:
1757 Reef-Scale Thermal Stress Monitoring of Coral Ecosystems: New 5-km Global Products, from NOAA Coral Reef
1758 Watch, remote sensing, 6(11), https://doi.org/10.3390/rs61111579, 2014.
1759 Liu, Z., Deng, Z., Davis, S. J., and Ciais, P.: Global carbon emissions in 2023, Nature Reviews Earth & Environment,
1760 5, 253–254, https://doi.org/10.1038/s43017-024-00532-2, 2024.

1761 Loeb, N. G., Johnson, G. C., Thorsen, T. J., Lyman, J. M., Rose, F. G., Kato, S.: Satellite and ocean data reveal marked
1762 increase in Earth's heating rate. Geophys. Res. Lett., 48, e2021GL093047, https://doi.org/10.1029/2021GL093047,
1763 2021.

1764 Loeb, N. G., Ham, S.-H., Allan, R. P., Thorsen, T. J., Meyssignac, B., Kato, S., Johnson, G. C., and Lyman, J. M.:
1765 Observational Assessment of Changes in Earth's Energy Imbalance Since 2000, Surv Geophys, 45, 1757–1783,
1766 https://doi.org/10.1007/s10712-024-09838-8, 2024.

1767 Mauritsen, T., Tsushima, Y., Meyssignac, B., Loeb, N. G., Hakuba, M., Pilewskie, P., Cole, J., Suzuki, K., Ackerman,
1768 T. P., Allan, R. P., Andrews, T., Bender, F. A. -M., Bloch-Johnson, J., Bodas-Salcedo, A., Brookshaw, A., Ceppi, P.,
1769 Clerbaux, N., Dessler, A. E., Donohoe, A., Dufresne, J., Eyring, V., Findell, K. L., Gettelman, A., Gristey, J. J.,
1770 Hawkins, E., Heimbach, P., Hewitt, H. T., Jeevanjee, N., Jones, C., Kang, S. M., Kato, S., Kay, J. E., Klein, S. A.,
1771 Knutti, R., Kramer, R., Lee, J., McCoy, D. T., Medeiros, B., Megner, L., Modak, A., Ogura, T., Palmer, M. D., Paynter,
1772 D., Quaas, J., Ramanathan, V., Ringer, M., Von Schuckmann, K., Sherwood, S., Stevens, B., Tan, I., Tselioudis, G.,
1773 Sutton, R., Voigt, A., Watanabe, M., Webb, M. J., Wild, M., and Zelinka, M. D.: Earth's Energy Imbalance More
1774 Than Doubled in Recent Decades, AGU Advances, 6, e2024AV001636, https://doi.org/10.1029/2024AV001636,
1775 2025.

1776 van Marle, M. J. E., Kloster, S., Magi, B. I., Marlon, J. R., Daniau, A.-L., Field, R. D., Arneth, A., Forrest, M.,
1777 Hantson, S., Kehrwald, N. M., Knorr, W., Lasslop, G., Li, F., Mangeon, S., Yue, C., Kaiser, J. W., and van der Werf,
1778 G. R.: Historic global biomass burning emissions for CMIP6 (BB4CMIP) based on merging satellite observations
1779 with proxies and fire models (1750–2015), Geosci. Model Dev., 10, 3329–3357, https://doi.org/10.5194/gmd-10-
1780 3329-2017, 2017.

1781 Melo, J., Rossi, S., Achard, F., Alkama, R., Canadell, J. G., Friedlingstein, P., Gibbs, D., Harris, N., Heinrich, V.,
1782 O'Sullivan, M., Peters, G., Pongratz, J., Rose, M., Roman-Cuesta, R., Sanz Sanchez, M. J., Schwingshackl, C., Sitch,
1783 S., and Grassi, G.: The LULUCF data hub: translating global land use emissions estimates into the national GHG
1784 inventory framework (Version 3.0, 2025 NGHGI release) (3.0), Zenodo [data set],
1785 https://doi.org/10.5281/zenodo.17153438, 2025.

https://doi.org/10.5194/essd-2026-287
Preprint. Discussion started: 23 April 2026

1786 Menne, M. J., Williams, C. N., Gleason, B. E., Rennie, J. J., and Lawrimore, J. H.: The global historical climatology
1787 network monthly temperature dataset, version 4, J. Climate, 31, 9835-9854, https://doi.org/10.1175/JCLI-D-18-
1788 0094.1, 2018.

1789 Merchant, C. J., Allan, R.P., Embury, O.: Quantifying the acceleration of multidecadal global sea surface warming
1790 driven by Earth's energy imbalance, Environ. Res. Lett., 20, 024037, https://doi.org/10.1088/1748-9326/adaa8a, 2025.

1791 Minière, A., von Schuckmann, K., Sallée, J.-B., and Vogt, L.: Robust acceleration of Earth system heating observed
1792 over the past six decades, Scientific Reports, 13, 22975, https://doi.org/10.1038/s41598-023-49353-1, 2023.

1793 Minobe, S., Behrens, E., Findell, K. L., Loeb, N. G., Meyssignac, B., and Sutton, R.: Global and regional drivers for
1794 exceptional climate extremes in 2023-2024: beyond the new normal, npj Clim Atmos Sci, 8, 138,
1795 https://doi.org/10.1038/s41612-025-00996-z, 2025.

1796 Minx, J. C., Lamb, W. F., Andrew, R. M., Canadell, J. G., Crippa, M., Döbbeling, N., Forster, P. M., Guizzardi, D.,
1797 Olivier, J., Peters, G. P., Pongratz, J., Reisinger, A., Rigby, M., Saunois, M., Smith, S. J., Solazzo, E., and Tian, H.:
1798 A comprehensive and synthetic dataset for global, regional, and national greenhouse gas emissions by sector 1970–
1799 2018 with an extension to 2019, Earth Syst. Sci. Data, 13, 5213–5252, https://doi.org/10.5194/essd-13-5213-2021,
1800 2021.

1801 Mu, D., Huang, R., Yin, P., Yan, H., and Xu, T.: Reconstructing sea level rise from global 945 tide gauges since 1900,
1802 Earth Syst. Sci. Data, 17, 5507–5528, https://doi.org/10.5194/essd-17-5507-2025, 2025.

1803 Müller, J. D., Gruber, N., Schneuwly, A., Bakker, D. C. E., Gehlen, M., Gregor, L., Hauck, J., Landschuetzer, P., and
1804 McKinley G. A.: Unexpected decline in the ocean carbon sink under record-high sea surface temperatures in 2023,
1805 Nat. Clim. Chang., 15, 978-985, https://doi.org/10.1038/s41558-025-02380-4, 2025.

1806 NASA: Satellite sea level observations, [data set], https://sealevel.nasa.gov/understanding-sea-level/key-
1807 indicators/global-mean-sea-level/, accessed 19 February 2025, 2025.

1808 Myhre, G., Hodnebrog, Ø., Loeb, N., and Forster, P. M.: Observed trend in Earth energy imbalance may provide a
1809 constraint for low climate sensitivity models, Science, 388, 1210–1213, https://doi.org/10.1126/science.adt0647,
1810 2025.

1811 Nickolay A. Krotkov, Lok N. Lamsal, Sergey V. Marchenko, Edward A. Celarier, Eric J.Bucsela, William H. Swartz,
1812 Joanna Joiner and the OMI core team, OMI/Aura NO2 Cloud-Screened Total and Tropospheric Column L3 Global
1813 Gridded 0.25 degree x 0.25 degree V3, NASA Goddard Space Flight Center, Goddard Earth Sciences Data and
1814 Information Services Center (GES DISC), Accessed: [Data Access 22 April 2024],
1815 https://doi.org/10.5067/Aura/OMI/DATA3007, 2019. Nisbet, E. G., Manning, M. R., Dlugokencky, E. J., Michel, S.
1816 E., Lan, X., Roeckmann, T., Gon, H. A. D. V. D., Palmer, P., Oh, Y., Fisher, R., Lowry, D., France, J. L., and White,
1817 J. W. C.: Atmospheric methane: Comparison between methane's record in 2006-2022 and during glacial terminations,
1818 Preprints, https://doi.org/10.22541/essoar.167689502.25042797/v1, 2023.

https://doi.org/10.5194/essd-2026-287
Preprint. Discussion started: 23 April 2026

1819 Nitzbon, J., Krinner, G., Langer, M.: GCOS EHI 1960-2020 Permafrost Heat Content, World Data Center for Climate
1820 (WDCC) at DKRZ, https://doi.org/10.26050/WDCC/GCOS_EHI_1960-2020_PHC, 2022.
1821 NOAA: Global sea level timeseries,
1822 https://www.star.nesdis.noaa.gov/socd/lsa/SeaLevelRise/LSA_SLR_timeseries.php , [data set], accessed 19 February
1823 2025, 2025.
1824 Oliveira, A.P.; Gil Martins, P. Global Shifts in Fire Regimes Under Climate Change: Patterns, Drivers, and Ecological
1825 Implications Across Biomes. Forests, 17, 104. https://doi.org/10.3390/f17010104, 2026.
1826 Oliver, E. C. J., Donat, M. G., Burrows, M. T., Moore, P. J., Smale, D. A., Alexander, L. V., Benthuysen, J. A., Feng,
1827 M., Sen Gupta, A., Hobday, A. J., Holbrook, N. J., Perkins-Kirkpatrick, S. E., Scannell, H. A., Straub, S. C., and
1828 Wernberg, T.: Longer and more frequent marine heatwaves over the past century, Nat. Commun., 9, 1324,
1829 https://doi.org/10.1038/s41467-018-03732-9, 2018.
1830 Palmer, M. D. and McNeall, D. J.: Internal variability of Earth's energy budget simulated by CMIP5 climate models,
1831 Environ. Res. Lett., 9, 034016, https://doi.org/10.1088/1748-9326/9/3/034016, 2014.
1832 Palmer, M. D., Domingues, C. M., Slangen, A. B. A., and Boeira Dias, F.: An ensemble approach to quantify global
1833 mean sea-level rise over the 20th century from tide gauge reconstructions, Environ. Res. Lett., 16, 044043,
1834 https://doi.org/10.1088/1748-9326/abdaec, 2021.
1835 Pan, Y., Cheng, L., Abraham, J., Trenberth, K. E., Reagan, J., Du, J., Wang, Z., Storto, A., Von Schuckmann, K., Zhu,
1836 Y., Mann, M. E., Zhu, J., Wang, F., Yu, F., Locarnini, R., Fasullo, J., Huang, B., Graham, G., Yin, X., Gouretski, V.,
1837 Zheng, F., Li, Y., Zhang, B., Wan, L., Chen, X., Wang, D., Feng, L., Song, X., Liu, Y., Reseghetti, F., Simoncelli, S.,
1838 Chen, G., Zhang, R., Mishonov, A., Wei, W., Tan, Z., Li, G., Cao, L., Chen, L., Yuan, H., Lyu, K., Sulaiman, A.,
1839 Mayer, M., Wang, H., Ma, Z., Bao, S., Yan, H., Liu, Z., Yang, C., Liu, X., Hausfather, Z., Gues, F., Song, X., Zhang,
1840 M., and Chen, L.: Ocean Heat Content Sets Another Record in 2025, Adv. Atmos. Sci.,
1841 https://doi.org/10.1007/s00376-026-5876-0, 2026.
1842 Peng, S., Lin, X., Thompson, R. L., Xi, Y., Liu, G., Hauglustaine, D., Lan, X., Poulter, B., Ramonet, M., Saunois, M.,
1843 Yin, Y., Zhang, Z., Zheng, B., and Ciais, P.: Wetland emission and atmospheric sink changes explain methane growth
1844 in 2020, Nature, 612, 477–482, https://doi.org/10.1038/s41586-022-05447-w, 2022.
1845 Pelz, S., Ganti, G., Lamboll, R., Grant, L., Smith, C., Pachauri, S., Rogelj, J., Riahi, K., Thiery, W., and Gidden, M.
1846 J.: Using net-zero carbon debt to track climate overshoot responsibility, Proc. Natl. Acad. Sci. U.S.A., 122,
1847 e2409316122, https://doi.org/10.1073/pnas.2409316122, 2025.
1848 Pirani, A., Alegria, A., Khourdajie, A. A., Gunawan, W., Gutiérrez, J. M., Holsman, K., Huard, D., Juckes, M.,
1849 Kawamiya, M., Klutse, N., Krey, V., Matthews, R., Milward, A., Pascoe, C., Van Der Shrier, G., Spinuso, A.,
1850 Stockhause, M., and Xiaoshi Xing: The implementation of FAIR data principles in the IPCC AR6 assessment process,
1851 https://doi.org/10.5281/ZENODO.6504469, 2022.

https://doi.org/10.5194/essd-2026-287
Preprint. Discussion started: 23 April 2026

1852 Pongratz, J., Schwingshackl, C., Bultan, S., Obermeier, W., Havermann, F., and Guo, S.: Land Use Effects on Climate:
1853 Current State, Recent Progress, and Emerging Topics, Curr. Clim. Change Rep., 7, 99–120,
1854 https://doi.org/10.1007/s40641-021-00178-y, 2021.

1855 Prinn, R. G., Weiss, R. F., Arduini, J., Arnold, T., DeWitt, H. L., Fraser, P. J., Ganesan, A. L., Gasore, J., Harth, C.
1856 M., Hermansen, O., Kim, J., Krummel, P. B., Li, S., Loh, Z. M., Lunder, C. R., Maione, M., Manning, A. J., Miller,
1857 B. R., Mitrevski, B., Mühle, J., O'Doherty, S., Park, S., Reimann, S., Rigby, M., Saito, T., Salameh, P. K., Schmidt,
1858 R., Simmonds, P. G., Steele, L. P., Vollmer, M. K., Wang, R. H., Yao, B., Yokouchi, Y., Young, D., and Zhou, L.:
1859 History of chemically and radiatively important atmospheric gases from the Advanced Global Atmospheric Gases
1860 Experiment (AGAGE), Earth Syst. Sci. Data, 10, 985–1018, https://doi.org/10.5194/essd-10-985-2018, 2018.

1861 Prinn, R., Weiss, R., Arduini, J., Choi, H., Engel, A., Fraser, P., Ganesan, A., Harth, C., Hermansen, O., Kim, J.,
1862 Krummel, P., Loh, Z., Lunder, C., Maione, M., Manning, A., Mitrevski, B., Mühle, J., O'Doherty, S., Park, S., Pitt,
1863 J., Reimann, S., Rigby, M., Saito, T., Salameh, P., Schmidt, R., Simmonds, P., Stanley, K., Stavert, A., Steele, P.,
1864 Vollmer, M., Wagenhäuser, T., Wang, H., Wenger, A., Western, L., Yao, B., Young, D., Zhou, L., and Zhu, L.: The
1865 dataset of in-situ measurements of chemically and radiatively important atmospheric gases from the Advanced Global
1866 Atmospheric Gas Experiment (AGAGE) and affiliated stations (20251230), https://doi.org/10.60718/2ZET-CN22,
1867 2025.

1868 Purich, A. and Doddridge, E. W.: Record low Antarctic sea ice coverage indicates a new sea ice state, Commun Earth
1869 Environ, 4, 314, https://doi.org/10.1038/s43247-023-00961-9, 2023.
1870 Quaas, J., Jia, H., Smith, C., Albright, A. L., Aas, W., Bellouin, N., Boucher, O., Doutriaux-Boucher, M., Forster, P.
1871 M., Grosvenor, D., Jenkins, S., Klimont, Z., Loeb, N. G., Ma, X., Naik, V., Paulot, F., Stier, P., Wild, M., Myhre, G.,
1872 and Schulz, M.: Robust evidence for reversal of the trend in aerosol effective climate forcing, Atmos. Chem. Phys.,
1873 22, 12221–12239, https://doi.org/10.5194/acp-22-12221-2022, 2022.

1874 Qin, Z., Zhu, Y., Canadell, J. G., Chen, M., Li, T., Mishra, U., and Yuan, W.: Global spatially explicit carbon emissions
1875 from land-use change over the past six decades (1961–2020), One Earth, 7, 835–847,
1876 https://doi.org/10.1016/j.oneear.2024.04.002, 2024.
1877 Raghuraman, S.P., Paynter, D. and Ramaswamy, V.: Anthropogenic forcing and response yield observed positive
1878 trend in Earth's energy imbalance, Nat. Commun. 12, 4577, https://doi.org/10.1038/s41467-021-24544-4, 2021.

1879 Raghuraman, S. P., Soden, B., Clement, A., Vecchi, G., Menemenlis, S., and Yang, W.: The 2023 global warming
1880 spike was driven by the El Niño–Southern Oscillation, Atmos. Chem. Phys., 24, 11275–11283,
1881 https://doi.org/10.5194/acp-24-11275-2024, 2024.
1882 Ribes, A., Qasmi, S., and Gillett, N. P.: Making climate projections conditional on historical observations, Sci. Adv.,
1883 7, eabc0671, https://doi.org/10.1126/sciadv.abc0671, 2021.

1884 Rhein, M., S.R. Rintoul, S. Aoki, E. Campos, D. Chambers, R.A. Feely, S. Gulev, G.C. Johnson, S.A. Josey, A.
1885 Kostianoy, C. Mauritzen, D. Roemmich, L.D. Talley and F. Wang, 2013: Observations: Ocean. In: Climate Change
1886 2013: The Physical Science Basis. Contribution of Working Group I to the Fifth Assessment Report of the

https://doi.org/10.5194/essd-2026-287
Preprint. Discussion started: 23 April 2026

1887 Intergovernmental Panel on Climate Change [Stocker, T.F., D. Qin, G.-K. Plattner, M. Tignor, S.K. Allen, J.
1888 Boschung, A. Nauels, Y. Xia, V. Bex and P.M. Midgley (eds.)]. Cambridge University Press, Cambridge, United
1889 Kingdom and New York, NY, USA.

1890 Ribes, A., Tessiot, O., Forster, P. M., Gillett, N. P., Masson-Delmotte, V., Rogelj, J., Vautard, R., and Walsh, T.:
1891 Towards annual updating of forced warming to date and constrained climate projections, Nat Commun, 16, 9214,
1892 https://doi.org/10.1038/s41467-025-63026-9, 2025.

1893 Rogelj, J., D. Shindell, K. Jiang, S. Fifita, P. Forster, V. Ginzburg, C. Handa, H. Kheshgi, S. Kobayashi, E. Kriegler,
1894 L. Mundaca, R. Séférian, and M. V. Vilariño: Mitigation Pathways Compatible with 1.5°C in the Context of
1895 Sustainable Development. In: Global Warming of 1.5°C. An IPCC Special Report on the impacts of global warming
1896 of 1.5°C above pre-industrial levels and related global greenhouse gas emission pathways, in the context of
1897 strengthening the global response to the threat of climate change, sustainable development, and efforts to eradicate
1898 poverty [Masson-Delmotte, V., P. Zhai, H.-O. Pörtner, D. Roberts, J. Skea, P.R. Shukla, A. Pirani, W. Moufouma-
1899 Okia, C. Péan, R. Pidcock, S. Connors, J. B. R. Matthews, Y. Chen, X. Zhou, M. I. Gomis, E. Lonnoy, T. Maycock,
1900 M. Tignor, and T. Waterfield (eds.)]. Cambridge University Press, Cambridge, UK and New York, NY, USA, pp. 93-
1901 174, https://doi.org/10.1017/9781009157940.004, 2018.

1902 Rogelj, J., Forster, P. M., Kriegler, E., Smith, C. J., and Séférian, R.: Estimating and tracking the remaining carbon
1903 budget for stringent climate targets, Nature, 571, 335–342, https://doi.org/10.1038/s41586-019-1368-z, 2019.

1904 Rogelj, J., Lamboll, R.D.: Substantial reductions in non-CO2 greenhouse gas emissions reductions implied by IPCC
1905 estimates of the remaining carbon budget. Communications Earth Environ 5, 35. https://doi.org/10.1038/s43247-023-
1906 01168-8, 2024.

1907 Rogelj, J., Rao, S., McCollum, D. L., Pachauri, S., Klimont, Z., Krey, V., and Riahi, K: Air-pollution emission ranges
1908 consistent with the representative concentration pathways, Nature Clim. Chang., 4 (6), 446–450,
1909 https://doi.org/10.1038/nclimate2178, 2014.

1910 Rohde, R., Muller, R., Jacobsen, R., Perlmutter, S., Rosenfeld, A. et al.: Berkeley Earth Temperature Averaging
1911 Process, Geoinfor. Geostat.: An Overview 1:2., http://dx.doi.org/10.4172/gigs.1000103, 2013.

1912 Saunois, M., Stavert, A. R., Poulter, B., Bousquet, P., Canadell, J. G., Jackson, R. B., Raymond, P. A., Dlugokencky,
1913 E. J., Houweling, S., Patra, P. K., Ciais, P., Arora, V. K., Bastviken, D., Bergamaschi, P., Blake, D. R., Brailsford, G.,
1914 Bruhwiler, L., Carlson, K. M., Carrol, M., Castaldi, S., Chandra, N., Crevoisier, C., Crill, P. M., Covey, K., Curry, C.
1915 L., Etiope, G., Frankenberg, C., Gedney, N., Hegglin, M. I., Höglund-Isaksson, L., Hugelius, G., Ishizawa, M., Ito,
1916 A., Janssens-Maenhout, G., Jensen, K. M., Joos, F., Kleinen, T., Krummel, P. B., Langenfelds, R. L., Laruelle, G. G.,
1917 Liu, L., Machida, T., Maksyutov, S., McDonald, K. C., McNorton, J., Miller, P. A., Melton, J. R., Morino, I., Müller,
1918 J., Murguia-Flores, F., Naik, V., Niwa, Y., Noce, S., O'Doherty, S., Parker, R. J., Peng, C., Peng, S., Peters, G. P.,
1919 Prigent, C., Prinn, R., Ramonet, M., Regnier, P., Riley, W. J., Rosentreter, J. A., Segers, A., Simpson, I. J., Shi, H.,
1920 Smith, S. J., Steele, L. P., Thornton, B. F., Tian, H., Tohjima, Y., Tubiello, F. N., Tsuruta, A., Viovy, N., Voulgarakis,

https://doi.org/10.5194/essd-2026-287
Preprint. Discussion started: 23 April 2026

A., Weber, T. S., Van Weele, M., Van Der Werf, G. R., Weiss, R. F., Worthy, D., Wunch, D., Yin, Y., Yoshida, Y., Zhang, W., Zhang, Z., Zhao, Y., Zheng, B., Zhu, Q., Zhu, Q., and Zhuang, Q.: The Global Methane Budget 2000–2017, Earth Syst. Sci. Data, 12, 1561–1623, https://doi.org/10.5194/essd-12-1561-2020, 2020.

Sato, K., Sato, K., Savita, A., Schweiger, A., Shepherd, A., Seneviratne, S. I., Simons, L., Slater, D. A., Slater, T., Steiner, A. K., Suga, T., Szekely, T., Thiery, W., Timmermans, M.-L., Vanderkelen, I., Wjiffels, S. E., Wu, T., and Zemp, M.: GCOS EHI 1960-2020 Earth Heat Inventory Ocean Heat Content (Version 2), https://doi.org/10.26050/WDCC/GCOS_EHI_1960-2020_OHC_v2, 2023b.

Sawyer, V., Levy, R.C., Mattoo, S., Shi, Y.R., Kim, M., Remer, L.A. and Cureton G.: An updated VIIRS dark target aerosol product for continuity with MODIS: assessing regional aerosol trends. Front. Environ. Sci. 13:1602145. https://doi: 10.3389/fenvs.2025.1602145, 2025.

Scarpelli, T. R., Jacob, D. J., Grossman, S., Lu, X., Qu, Z., Sulprizio, M. P., Zhang, Y., Reuland, F., Gordon, D., and Worden, J. R.: Updated Global Fuel Exploitation Inventory (GFEI) for methane emissions from the oil, gas, and coal sectors: evaluation with inversions of atmospheric methane observations, Atmos. Chem. Phys., 22, 3235–3249, https://doi.org/10.5194/acp-22-3235-2022, 2022.

Schamm, K., Ziese, M., Becker A., Finger, P., Meyer-Christoffer, A., Schneider, U., Schroder, M., and Stender, P.: Global gridded precipitation over land: a description of the new GPCC First Guess Daily product, Earth Syst. Sci. Data, 6, 49-60. https://doi.org/10.5194/essd-6-49-2014, 2014.

Schmidt, G.: Climate models can't explain 2023's huge heat anomaly — we could be in uncharted territory, Nature, 627, 467–467, https://doi.org/10.1038/d41586-024-00816-z, 2024.

von Schuckmann, K., Cheng, L., Palmer, M. D., Hansen, J., Tassone, C., Aich, V., Adusumilli, S., Beltrami, H., Boyer, T., Cuesta-Valero, F. J., Desbruyères, D., Domingues, C., García-García, A., Gentine, P., Gilson, J., Gorfer, M., Haimberger, L., Ishii, M., Johnson, G. C., Killick, R., King, B. A., Kirchengast, G., Kolodziejczyk, N., Lyman, J., Marzeion, B., Mayer, M., Monier, M., Monselesan, D. P., Purkey, S., Roemmich, D., Schweiger, A., Seneviratne, S. I., Shepherd, A., Slater, D. A., Steiner, A. K., Straneo, F., Timmermans, M.-L., and Wijffels, S. E.: Heat stored in the Earth system: where does the energy go?, Earth Syst. Sci. Data, 12, 2013–2041, https://doi.org/10.5194/essd-12-2013-2020, 2020.

von Schuckmann, K., Minière, A., Gues, F., Cuesta-Valero, F. J., Kirchengast, G., Adusumilli, S., Straneo, F., Ablain, M., Allan, R. P., Barker, P. M., Beltrami, H., Blazquez, A., Boyer, T., Cheng, L., Church, J., Desbruyeres, D., Dolman, H., Domingues, C. M., García-García, A., Giglio, D., Gilson, J. E., Gorfer, M., Haimberger, L., Hakuba, M. Z., Hendricks, S., Hosoda, S., Johnson, G. C., Killick, R., King, B., Kolodziejczyk, N., Korosov, A., Krinner, G., Kuusela, M., Landerer, F. W., Langer, M., Lavergne, T., Lawrence, I., Li, Y., Lyman, J., Marti, F., Marzeion, B., Mayer, M., MacDougall, A. H., McDougall, T., Monselesan, D. P., Nitzbon, J., Otosaka, I., Peng, J., Purkey, S., Roemmich, D., Sato, K., Sato, K., Savita, A., Schweiger, A., Shepherd, A., Seneviratne, S. I., Simons, L., Slater, D. A., Slater, T., Steiner, A. K., Suga, T., Szekely, T., Thiery, W., Timmermans, M.-L., Vanderkelen, I., Wjiffels, S. E., Wu, T., and

https://doi.org/10.5194/essd-2026-287
Preprint. Discussion started: 23 April 2026

1955 Zemp, M.: Heat stored in the Earth system 1960–2020: where does the energy go?, Earth System Science Data, 15,
1956 1675–1709, https://doi.org/10.5194/essd-15-1675-2023, 2023a.

1957 Schoeberl, M. R., Wang, Y., Taha, G., Zawada, D. J., Ueyama, R., and Dessler, A.: Evolution of the Climate Forcing
1958 During the Two Years After the Hunga Tonga-Hunga Ha'apai Eruption, JGR Atmospheres, 129, e2024JD041296,
1959 https://doi.org/10.1029/2024JD041296, 2024.

1960 Schwingshackl, C., Obermeier, W. A., Bultan, S., Grassi, G., Canadell, J. G., Friedlingstein, P., Gasser, T., Houghton,
1961 R. A., Kurz, W. A., Sitch, S., and Pongratz, J.: Differences in land-based mitigation estimates reconciled by separating
1962 natural and land-use CO2 fluxes at the country level, One Earth, 5, 1367–1376,
1963 https://doi.org/10.1016/j.oneear.2022.11.009, 2022.

1964 Seneviratne, S.I., X. Zhang, M. Adnan, W. Badi, C. Dereczynski, A. Di Luca, S. Ghosh, I. Iskandar, J. Kossin, S.
1965 Lewis, F. Otto, I. Pinto, M. Satoh, S. M. Vicente-Serrano, M. Wehner, and B. Zhou: Weather and Climate Extreme
1966 Events in a Changing Climate. In Climate Change 2021: The Physical Science Basis. Contribution of Working Group
1967 I to the Sixth Assessment Report of the Intergovernmental Panel on Climate Change [Masson-Delmotte, V., P. Zhai,
1968 A. Pirani, S.L. Connors, C. Péan, S. Berger, N. Caud, Y. Chen, L. Goldfarb, M.I. Gomis, M. Huang, K. Leitzell, E.
1969 Lonnoy, J.B.R. Matthews, T.K. Maycock, T. Waterfield, O. Yelekçi, R. Yu, and B. Zhou (eds.)]. Cambridge
1970 University Press, Cambridge, United Kingdom and New York, NY, USA, pp. 1513–1766,
1971 doi:10.1017/9781009157896.013.1513–1766, https://doi.org/10.1017/9781009157896.013, 2021.

1972 Seo, K.-W., Ryu, D., Jeon, T., Youm, K., Kim, J.-S., Oh, E. H., Chen, J., Famiglietti, J. S., and Wilson, C. R.: Abrupt
1973 sea level rise and Earth's gradual pole shift reveal permanent hydrological regime changes in the 21st century, Science,
1974 387, 1408–1413, https://doi.org/10.1126/science.adq6529, 2025.

1975 Sherwin, E. D., Rutherford, J. S., Zhang, Z., Chen, Y., Wetherley, E. B., Yakovlev, P. V., Berman, E. S. F., Jones, B.
1976 B., Cusworth, D. H., Thorpe, A. K., Ayasse, A. K., Duren, R. M., and Brandt, A. R.: US oil and gas system emissions
1977 from nearly one million aerial site measurements, Nature, 627, 328–334, https://doi.org/10.1038/s41586-024-07117-
1978 5, 2024.

1979 Simmonds, P. G., Rigby, M., McCulloch, A., O'Doherty, S., Young, D., Mühle, J., Krummel, P. B., Steele, P., Fraser,
1980 P. J., Manning, A. J., Weiss, R. F., Salameh, P. K., Harth, C. M., Wang, R. H. J., and Prinn, R. G.: Changing trends
1981 and emissions of hydrochlorofluorocarbons (HCFCs) and their hydrofluorocarbon (HFCs) replacements, Atmos.
1982 Chem. Phys., 17, 4641–4655, https://doi.org/10.5194/acp-17-4641-2017, 2017.

1983 Sippel, S., Zscheischler, J., Heimann, M., Otto, F. E. L., Peters, J., and Mahecha, M. D.: Quantifying changes in
1984 climate variability and extremes: Pitfalls and their overcoming, Geophys. .Res. Lett., 42, 9990–9998,
1985 https://doi.org/10.1002/2015GL066307, 2015.

1986 Smale, D. A., Wernberg, T., Oliver, E. C. J., Thomsen, M., Harvey, B. P., Straub, S. C., Burrows, M. T., Alexander,
1987 L. V., Benthuysen, J. A., Donat, M. G., Feng, M., Hobday, A. J., Holbrook, N. J., Perkins-Kirkpatrick, S. E., Scannell,

https://doi.org/10.5194/essd-2026-287
Preprint. Discussion started: 23 April 2026

H. A., Sen Gupta, A., Payne, B. L., and Moore, P. J.: Marine heatwaves threaten global biodiversity and the provision of ecosystem services, Nat. Clim. Chang., 9, 306-312, https://doi.org/10.1038/s41558-019-0412-1, 2019.

Smith, C., Walsh, T., Gillett, N., Hauser, M., Krummel, P., Lamb, W., Lamboll, R., Mühle, J., Palmer, M., Ribes, A., Schumacher, D., Seneviratne, S., Slangen, A., Trewin, B., von Schuckmann, K., and Forster, P.: Indicators of Global Climate Change 2025 [Data set and software], https://doi.org/10.5281/ZENODO.7883757, 2026a.

Smith, C., Walsh, T., Gillett, N., Hall, B., Hauser, M., Krummel, P., Lamb, W., Lamboll, R., X., Muhle, J., Palmer, M., Ribes, A., Seneviratne, S., Trewin, B., von Schuckmann, K., and Forster, P.: Data repository for Indicators of Global Climate Change, Github [code], https://github.com/ClimateIndicator/data/tree/v2026.04.14, last access: 14 April 2026, 2026b.

Smith, C., Nicholls, Z. R. J., Armour, K., Collins, W., Forster, P., Meinshausen, M., Palmer, M. D., and Watanabe, M.: The Earth's Energy Budget, Climate Feedbacks, and Climate Sensitivity Supplementary Material, in: Climate Change 2021: The Physical Science Basis. Contribution of Working Group I to the Sixth Assessment Report of the Intergovernmental Panel on Climate Change, edited by: Masson-Delmotte, V., Zhai, P., Pirani, A., Connors, S. L., Péan, C., Berger, S., Caud, N., Chen, Y., Goldfarb, L., Gomis, M. I., Huang, M., Leitzell, K., Lonnoy, E., Matthews, J. B. R., Maycock, T. K., Waterfield, T., Yelekçi, O., Yu, R., and Zhou, B., 2021.

Smith, C., Forster, P., Palmer, M., Collins, B., Leach, N., Watanabe, M., Berger, S., Hall, B., Zelinka, M., Lunt, D., Cain, M., Harris, G., and Ringer, M.: IPCC WGI AR6 Chapter 7 (v.1.0). Zenodo. https://doi.org/10.5281/zenodo.5211358, 2021.

Smith, C., Cummins, D. P., Fredriksen, H.-B., Nicholls, Z., Meinshausen, M., Allen, M., Jenkins, S., Leach, N., Mathison, C., and Partanen, A.-I.: fair-calibrate v1.4.1: calibration, constraining, and validation of the FaIR simple climate model for reliable future climate projections, Geosci. Model Dev., 17, 8569–8592, https://doi.org/10.5194/gmd-17-8569-2024, 2024.

Smith, K. E., Burrows, M. T., Hobday, A. J., Sen Gupta, A., Moore, P. J., Thomsen, M., Wernberg, T., and Smale, D. A.: Socioeconomic impacts of marine heatwaves: Global issues and opportunities, Science, 374, 6566, https://doi.org/10.1126/science.abj3593, 2021.

Smith, K. E., Burrows, M. T., Hobday, A. J., King, N. G., Moore, P. J., Sen Gupta, A., Thomsen, M. S., Wernberg, T., and Smale, D. A.: Biological Impacts of Marine Heatwaves, Annu. Rev. Mar. Sci., 15:119-145, https://doi.org/10.1146/annurev-marine-032122-121437, 2023.

Smith, S. J., van Aardenne, J., Klimont, Z., Andres, R. J., Volke, A., and Delgado Arias, S.: Anthropogenic sulfur dioxide emissions: 1850–2005, Atmos. Chem. and Phys., 11, 1101–1116, https://doi.org/10.5194/acp-11-1101-2011, 2011.

Song, C., Ponder, D., Peng, W., and Ren, Z. J.: Discrepancies in national inventories reveal a large emissions gap in the wastewater sector, Nat. Clim. Chang., 16, 313–321, https://doi.org/10.1038/s41558-025-02540-6, 2026.

https://doi.org/10.5194/essd-2026-287
Preprint. Discussion started: 23 April 2026

Soulie, A., C. Granier, S. Darras, N. Zilbermann, T. Doumbia, M. Guevara, J.-P. Jalkanen, S. Keita, C. Liousse, M. Crippa, D. Guizzardi, R. Hoesly, S. J. Smith: Global Anthropogenic Emissions (CAMS-GLOB-ANT) for the Copernicus Atmosphere Monitoring Service Simulations of Air Quality Forecasts and Reanalyses Earth Syst. Sci. Data, https://doi.org/10.5194/essd-16-2261-2024, 2023.

Storto, A. and Yang, C.: Acceleration of the ocean warming from 1961 to 2022 unveiled by large-ensemble reanalyses, Nature Communications, 15, 545, https://doi.org/10.1038/s41467-024-44749-7, 2024.

Su, J. et al: Precipitation observing network gaps limit climate change impact assessment. Nature, https://doi.org/10.1038/s41586-026-10300-5, 2026.

Szopa, S., Cooper, O. R., Collins, W. J., Fiore, A.M., Lee, J., Lin, M.,Naik, V., Turnock, S. T., West, J.J. Tropospheric Ozone Assessment Report Phase-II: Ozone interactions with climate change: drivers and long-term trends, in revision for Phil. Trans. Royal Society A., 2026.

Szopa, S., V. Naik, B. Adhikary, P. Artaxo, T. Berntsen, W.D. Collins, S. Fuzzi, L. Gallardo, A. Kiendler-Scharr, Z. Klimont, H. Liao, N. Unger, and P. Zanis: Short-Lived Climate Forcers. In Climate Change 2021: The Physical Science Basis. Contribution of Working Group I to the Sixth Assessment Report of the Intergovernmental Panel on Climate Change [Masson-Delmotte, V., P. Zhai, A. Pirani, S.L. Connors, C. Péan, S. Berger, N. Caud, Y. Chen, L. Goldfarb, M.I. Gomis, M. Huang, K. Leitzell, E. Lonnoy, J.B.R. Matthews, T.K. Maycock, T. Waterfield, O. Yelekçi, R. Yu, and B. Zhou (eds.)]. Cambridge University Press, Cambridge, United Kingdom and New York, NY, USA, pp. 817–922, https://doi:10.1017/9781009157896.008, 2021.

Terhaar, J., Burger, F.A., Vogt, L. et al.: Record sea surface temperature jump in 2023–2024 unlikely but not unexpected, Nature 639, 942–946, https://doi.org/10.1038/s41586-025-08674-z, 2025.

Thorne, P. W., Nicklas, J. M., Kennedy, J. J., Calvert, B., Fox-Kemper, B., Richardson, M. T., Simmons, A., Hawkins, E., Rhode, R., Cowtan, K., Abram, N. J., Andersson, A., Noone, S., Marbaix, P., Lenssen, N., Olonscheck, D., Walsh, T., Outten, S., Bethke, I., Samset, B. H., Smith, C., Pirani, A., Fuglestvedt, J., Rajamani, L., Betts, R. A., Kent, E. C., Trewin, B., Morice, C., Osborn, T., Burgess, S. N., Geden, O., Parnell, A., Forster, P. M., Hewitt, C., Hausfather, Z., Masson-Delmotte, V., Marotzke, J., Gillett, N., Seneviratne, S. I., Schmidt, G. A., Chan, D., Brönnimann, S., Reisinger, A., Menne, M., Rojas Corradi, M., Kadow, C., Huybers, P., Stephenson, D. B., Wallis, E., Rogelj, J., Schurer, A., McKinnon, K., Zhai, P., Driouech, F., Moufouma Okia, W., Vazifehkhah, S., Szopa, S., Merchant, C. J., Hirahara, S., Ishii, M., Engelbrecht, F. A., Li, Q., Lee, J.-Y., Cannon, A. J., Cassou, C., Von Schuckmann, K., Delju, A. H., and Murtagh, E.: How well can we quantify when 1.5 °C of global warming has been exceeded?, https://doi.org/10.5194/essd-2025-825, 28 January 2026.

Tibrewal, K., Ciais, P., Saunois, M., Martinez, A., Lin, X., Thanwerdas, J., Deng, Z., Chevallier, F., Giron, C., Albergel, C., Tanaka, K., Patra, P., Tsuruta, A., Zheng, B., Belikov, D., Niwa, Y., Janardanan, R., Maksyutov, S., Segers, A., Tzompa-Sosa, Z. A., Bousquet, P., and Sciare, J.: Assessment of methane emissions from oil, gas and coal sectors across inventories and atmospheric inversions, Communications Earth & Environment, 5, 26, https://doi.org/10.1038/s43247-023-01190-w, 2024.

https://doi.org/10.5194/essd-2026-287
Preprint. Discussion started: 23 April 2026

2056 Trewin, B.: Assessing Internal Variability of Global Mean Surface Temperature From Observational Data and
2057 Implications for Reaching Key Thresholds, JGR Atmospheres, 127, e2022JD036747,
2058 https://doi.org/10.1029/2022JD036747, 2022.
2059 Tsuchida, K., Kosaka, Y., and Minobe, S.: Multi-year La Niña–El Niño transition influenced Earth's extreme energy
2060 uptake in 2022–2023, Nat. Geosci., https://doi.org/10.1038/s41561-026-01921-6, 2026.
2061 UNEP: Emissions Gap Report 2025: Off Target - Continued Collective inaction puts Global Temperature Goal at
2062 Risk, United Nations Environment Programme, https://doi.org/10.59117/20.500.11822/48854, 2025.
2063 United Nations Environment Programme: Global Environment Outlook 7: A future we choose – Why investing in
2064 Earth now can lead to a trillion-dollar benefit for all. Nairobi. https://wedocs.unep.org/handle/20.500.11822/49014,
2065 accessed 14 April 2026, 2025.
2066 Vakilifard, N., Williams, R. G., Holden, P. B., Turner, K., Edwards, N. R., and Beerling, D. J.: Impact of negative and
2067 positive CO_2 emissions on global warming metrics using an ensemble of Earth system model simulations,
2068 Biogeosciences, 19, 4249–4265, https://doi.org/10.5194/bg-19-4249-2022, 2022.
2069 Vanderkelen, I. and Thiery, W.: GCOS EHI 1960-2020 Inland Water Heat Content,
2070 https://doi.org/10.26050/WDCC/GCOS_EHI_1960-2020_IWHC, 2022.
2071 Vimont, I. J, B. D. Hall, G. Dutton, S. A. Montzka, J. Mühle, M. Crotwell, K. Petersen, S. Clingan, and D. Nance, [in
2072 "State of the Climate in 2022"]. Bull. Amer. Meteor. Soc., 104 , 9, S76–S78, https://doi.org/10.1175/BAMS-D-23-
2073 0090.1., 2022.
2074 Vollmer, M. K., Young, D., Trudinger, C. M., Mühle, J., Henne, S., Rigby, M., Park, S., Li, S., Guillevic, M.,
2075 Mitrevski, B., Harth, C. M., Miller, B. R., Reimann, S., Yao, B., Steele, L. P., Wyss, S. A., Lunder, C. R., Arduini, J.,
2076 McCulloch, A., Wu, S., Rhee, T. S., Wang, R. H. J., Salameh, P. K., Hermansen, O., Hill, M., Langenfelds, R. L., Ivy,
2077 D., O'Doherty, S., Krummel, P. B., Maione, M., Etheridge, D. M., Zhou, L., Fraser, P. J., Prinn, R. G., Weiss, R. F.,
2078 and Simmonds, P. G.: Atmospheric histories and emissions of chlorofluorocarbons CFC-13 (CClF3), ΣCFC-114
2079 (C2Cl2F4), and CFC-115 (C2ClF5), Atmos. Chem. Phys., 18, 979–1002, https://doi.org/10.5194/acp-18-979-2018,
2080 2018.
2081 Wang, J., Church, J. A., Zhang, X., and Chen, X.: Improved Sea Level Reconstruction from 1900 to 2019, Journal of
2082 Climate, 37, 6453–6474, https://doi.org/10.1175/JCLI-D-23-0410.1, 2024.
2083 Watson-Parris, D., Christensen, M. W., Laurenson, A., Clewley, D., Gryspeerdt, E., and Stier, P.: Shipping regulations
2084 lead to large reduction in cloud perturbations, Proc. Natl. Acad. Sci. U.S.A., 119, e2206885119,
2085 https://doi.org/10.1073/pnas.2206885119, 2022.
2086 WCRP Global Sea Level Budget Group: Global sea-level budget 1993–present, Earth Syst. Sci. Data, 10, 1551–1590,
2087 https://doi.org/10.5194/essd-10-1551-2018, 2018.
2088 Wernberg, T., Thomsen, M. S., Burrows, M. T., Filbee-Dexter, K., Hobday, A. J., Holbrook, N. J., Montie, S., Moore,
2089 P. J., Oliver, E. C. J., Sen Gupta, A., Smale, D. A., and Smith, K.: Marine heatwaves as hot spots of climate change

https://doi.org/10.5194/essd-2026-287
Preprint. Discussion started: 23 April 2026

2090 and impacts on biodiversity and ecosystem services, Nat. Rev. Biodivers., 1, 461-479, https://doi.org/10.1038/s44358-
2091 025-00058-5, 2025.
2092 Western, L. M., Vollmer, M. K., Krummel, P. B., Adcock, K. E., Fraser, P. J., Harth, C. M., Langenfelds, R. L.,
2093 Montzka, S. A., Mühle, J., O'Doherty, S., Oram, D. E., Reimann, S., Rigby, M., Vimont, I., Weiss, R. F., Young, D.,
2094 and Laube, J. C.: Global increase of ozone-depleting chlorofluorocarbons from 2010 to 2020, Nat. Geosci., 16, 309–
2095 313, https://doi.org/10.1038/s41561-023-01147-w, 2023.
2096 Western, L. M., Daniel, J. S., Vollmer, M. K., Clingan, S., Crotwell, M., Fraser, P. J., Ganesan, A. L., Hall, B., Harth,
2097 C. M., Krummel, P. B., Mühle, J., O'Doherty, S., Salameh, P. K., Stanley, K. M., Reimann, S., Vimont, I., Young,
2098 D., Rigby, M., Weiss, R. F., Prinn, R. G., and Montzka, S. A.: A decrease in radiative forcing and equivalent effective
2099 chlorine from hydrochlorofluorocarbons, Nat. Clim. Chang., 14, 805–807, https://doi.org/10.1038/s41558-024-02038-
2100 7, 2024.
2101 Western, L. M., Rigby, M., Mühle, J., Krummel, P. B., Lunder, C. R., O'Doherty, S., Reimann, S., Vollmer, M. K.,
2102 Young, D., Adam, B., Fraser, P. J., Ganesan, A. L., Harth, C. M., Hermansen, O., Kim, J., Langenfelds, R. L., Loh,
2103 Z. M., Mitrevski, B., Pitt, J. R., Salameh, P. K., Schmidt, R., Stanley, K., Stavert, A. R., Wang, H.-J., Weiss, R. F.,
2104 and Prinn, R. G.: Global emissions and abundances of chemically and radiatively important trace gases from the
2105 AGAGE network, Earth Syst. Sci. Data, 17, 6557–6582, https://doi.org/10.5194/essd-17-6557-2025, 2025.
2106 Western, L. M., Rigby, M., Mühle, J., Krummel, P. B., Lunder, C. R., O'Doherty, S., Reimann, S., Vollmer, M. K.,
2107 Adam, B., Fraser, P. J., Ganesan, A. L., Harth, C. M., Hermansen, O., Kim, J., Langenfelds, R. L., Loh, Z. M.,
2108 Mitrevski, B., Pitt, J. R., Salameh, P. K., Schmidt, R., Stanley, K., Stavert, A. R., Wang, H.-J. (Ray), Young, D.,
2109 Weiss, R. F., and Prinn, R. G.: Global Emissions and Abundances of Chemically and Radiatively Important Trace
2110 Gases from the AGAGE Network (20260305), https://doi.org/10.5281/ZENODO.18878005, 2026.
2111 van der Werf, G. R., Randerson, J. T., Giglio, L., van Leeuwen, T. T., Chen, Y., Rogers, B. M., Mu, M., van Marle,
2112 M. J. E., Morton, D. C., Collatz, G. J., Yokelson, R. J., and Kasibhatla, P. S.: Global fire emissions estimates during
2113 1997–2016, Earth System Science Data, 9, 697–720, https://doi.org/10.5194/essd-9-697-2017, 2017.
2114 van der Werf, G.R., Randerson, J.T., van Wees, D. et al. Landscape fire emissions from the 5th version of the Global
2115 Fire Emissions Database (GFED5). Sci Data 12, 1870, https://doi-org.insu.bib.cnrs.fr/10.1038/s41597-025-06127-w,
2116 2025.
2117 Wild, M., Gilgen, H., Roesch, A., Ohmura, A., Long, C. N., Dutton, E. G., Forgan, B., Kallis, A., Russak, V., and
2118 Tsvetkov, A.: From Dimming to Brightening: Decadal Changes in Solar Radiation at Earth's Surface, Science, 308,
2119 847–850, https://doi.org/10.1126/science.1103215, 2005.
2120 WMO: State of the Global Climate 2025, World Meteorological Organization, Geneva, Switzerland,
2121 https://doi.org/10.59327/WMO/S/CRI/SOC/1, 2025.
2122 Xu, Q., Wei, S., Li, Z., and Li, Q.: A New Evaluation of Observed Changes in Diurnal Temperature Range,
2123 Geophysical Research Letters, 52, e2024GL113406, https://doi.org/10.1029/2024GL113406, 2025.

https://doi.org/10.5194/essd-2026-287
Preprint. Discussion started: 23 April 2026

2124 Yate, T. A. and Ren, G.: An overview of observed changes in precipitation totals and extremes over global land, with
2125 a focus on Africa. Earth-Science Reviews, 262, 105063. https://doi.org/10.1016/j.earscirev.2025.105063, 2025.
2126 Zickfeld, K., Azevedo, D., Mathesius, S., and Matthews, H. D.: Asymmetry in the climate–carbon cycle response to
2127 positive and negative CO2 emissions, Nat. Clim. Chang., 11, 613–617, https://doi.org/10.1038/s41558-021-01061-2,
2128 2021.
2129 Zhang, J., Kinnison, D., Zhu, Y., Wang, X., Tilmes, S., Dube, K., and Randel, W.: Chemistry Contribution to
2130 Stratospheric Ozone Depletion After the Unprecedented Water-Rich Hunga Tonga Eruption, Geophysical Research
2131 Letters, 51, e2023GL105762, https://doi.org/10.1029/2023GL105762, 2024a.
2132 Zhang, W., Zhou, T., and Wu, P.: Anthropogenic amplification of precipitation variability over the past century,
2133 Science, 385, 427–432, https://doi.org/10.1126/science.adp0212, 2024b.
2134 Zhang, Z., Poulter, B., Melton, J. R., Riley, W. J., Allen, G. H., Beerling, D. J., Bousquet, P., Canadell, J. G., Fluet-
2135 Chouinard, E., Ciais, P., Gedney, N., Hopcroft, P. O., Ito, A., Jackson, R. B., Jain, A. K., Jensen, K., Joos, F., Kleinen,
2136 T., Knox, S. H., Li, T., Li, X., Liu, X., McDonald, K., McNicol, G., Miller, P. A., Müller, J., Patra, P. K., Peng, C.,
2137 Peng, S., Qin, Z., Riggs, R. M., Saunois, M., Sun, Q., Tian, H., Xu, X., Yao, Y., Xi, Y., Zhang, W., Zhu, Q., Zhu, Q.,
2138 and Zhuang, Q.: Ensemble estimates of global wetland methane emissions over 2000–2020, Biogeosciences, 22, 305–
2139 321, https://doi.org/10.5194/bg-22-305-2025, 2025
2140 Zhu, Y., Mann, G., Newman, P. A., and Randel, W.: The Hunga Volcanic Eruption Atmospheric Impacts Report,
2141 edited by: Zhu, Y., Mann, G., Newman, P. A., and Randel, W., Forschungzentrum Jülich,
2142 https://doi.org/10.34734/FZJ-2025-05237, 2025.